

VASA VASORUM IN HYPERGLYCEMIC ACCELERATED ATHEROSCLEROSIS

HYPERGLYCEMIA PROMOTES ACCELERATED ATHEROSCLEROSIS AND
ABERRANT VASA VASORUM NEOVASCULARIZATION

By HEIDI STOUTE, BSc

A Thesis Submitted to the School of Graduate Studies in Partial Fulfilment of the
Requirements for the Degree Master of Science

McMaster University MASTER OF SCIENCE (2015) Hamilton, Ontario (Medical Sciences)

TITLE: Hyperglycemia Promotes Accelerated Atherosclerosis and Aberrant Vasa Vasorum Neovascularization AUTHOR: Heidi Stoute, BSc (University of Waterloo) SUPERVISOR: Dr. G.H. Werstuck NUMBER OF PAGES: xx, 138

LAY ABSTRACT

People with diabetes have elevated glucose levels that affect the vessels that distribute blood in our body. This puts them at higher risk of developing cardiovascular disease and having heart attacks and strokes. One set of vessels, known as the vasa vasorum, delivers blood to the walls of larger vessels. The primary goals of this study are 1) to determine if diabetes affects the vasa vasorum and, 2) to determine if changes to the vasa vasorum increase a person's risk of developing cardiovascular disease. The results of this study show that diabetes in mice decreases the number of vasa vasorum vessels. The decrease in vasa vasorum blood vessels appears to influence the larger blood vessels they supply which promotes an environment that is more prone to cardiovascular disease. This information could be used in the future to develop drugs that target the vasa vasorum and possibly decrease cardiovascular events.

ABSTRACT

Individuals with diabetes mellitus often develop complications that traditionally have been separated into microvascular pathologies, such as retinopathy, nephropathy and neuropathy, or macrovascular pathologies, including cardiovascular disease. Increasing evidence suggests that these micro- and macro-vascular complications may be linked. Our objective is to determine if direct effects of hyperglycemia on a microvascular bed that supplies cells in large arteries, the vasa vasorum, promotes diabetes-associated accelerated atherosclerosis.

Normoglycemic apolipoprotein-E deficient (ApoE^{-/-}) mice showed continuous atherosclerosis progression throughout the study that was directly correlated to increased vasa vasorum density with time. Hyperglycemic ApoE^{-/-} Ins2^{+/*Akita*} mice and streptozotocin-injected (STZ) ApoE^{-/-} mice also demonstrated progressive plaque growth over time, but had accelerated atherosclerosis at 15 weeks of age compared to normoglycemic controls. The increased atherosclerosis in hyperglycemic mice correlated with impaired angiogenesis at 10 and 15 weeks of age. These mice showed increased expression for a marker of hypoxia in the atherosclerotic lesions yet decreased expression of vascular endothelial growth factor (VEGF), suggesting disruption of hypoxia-mediated angiogenesis. Cell culture experiments suggested that alternative splicing of an antiangiogenic form of VEGF in macrophages as well as post-translational

modifications of macrophages and smooth muscle cells may contribute to reduced VEGF expression and decreased vasa vasorum neovascularization. After 25 weeks of age, vasa vasorum expansion plateaued in normoglycemic mice but continued to increase in hyperglycemic ApoE^{-/-} STZ-injected mice. The increase in vasa vasorum neovascularization correlates to increases in plasma cholesterol.

We have shown that hyperglycemia alters the microvascular structure of the vasa vasorum in two distinct mouse models of diabetes. Initially, elevations in glucose correlate to a significant reduction in lesion vascularization that results in increased lesional hypoxia that may promote the development and progression of atherosclerosis. At later time points there appears to be a burst of neovascularization that correlate with increases in cholesterol.

ACKNOWLEDGEMENTS

I would like to acknowledge the numerous individuals who have assisted me and contributed to this project. I would like to start by thanking my supervisor, Dr. Geoff Werstuck, without whom this project would not have been possible. He was an excellent mentor who taught me a tremendous amount about research and atherosclerosis, and provided many opportunities to expand my knowledge. I truly appreciate all of his guidance and constant support throughout my time in his lab.

Dr. Peter Shi, Daniel Venegas-Pino and Cameron McAlpine were essential members of this project as they taught me various skills and procedures utilized in the lab and assisted me with technical advice. Other members of the Werstuck lab that I would like to thank include former graduate students, Dan Beriault, Melec Zeadin and Christina Petlura as well as current graduate student, Vi Dang. The Werstuck lab members were a friendly, encouraging and knowledgeable group that promoted a positive work environment. I would also like to acknowledge undergraduate members Emma Butcher and Aric Huang for their hard work assisting me in various aspects of this project.

I am grateful for the assistance and guidance I was provided from individuals outside of the Werstuck lab, namely Linda May and Dr. Vidhya Nair. They were invaluable in providing technical knowledge and expertise and I appreciate all of their help and time.

I would also like to thank my committee members, Dr. Thomas Hawke and Dr. Jon Schertzer, for their insights and advice as this was important in guiding my project forward. I also appreciate the opportunity to use a microscope and get trained by members in Dr. Hawke's lab. This project would not be complete without their assistance in imaging and analysis.

Lastly I would like to acknowledge my parents, David and Gillian Stoute as well as Jacob Vincent for their overwhelming love and support. This project was completed with a great deal of encouragement and motivation from them.

TABLE OF CONTENTS

1.0 INTRODUCTION	1
1.1 DIABETES MELLITUS	1
1.1.1 Definition, Classification and Clinical Diagnosis	1
1.1.2 Prevalence	2
1.2 VASCULAR PATHOLOGIES OF DIABETES	3
1.2.1 Macro- and Microvascular Complications	3
1.2.2 Role for both vascular beds in disease pathology	4
1.2.3 Potential unified mechanisms for Vascular Dysfunction	5
1.2.4 Glycemic control and vascular complications	10
1.3 MACRO- AND MICROVASCULAR DISEASE MECHANISMS	11
1.3.1 Atherosclerosis	12
1.3.2 Atherosclerosis and Diabetes	17
1.3.3 Hypoxia-mediated Angiogenesis	17
1.3.4 Regulatory Mechanisms of Hypoxia	18
1.3.5 Vascular Endothelial Growth Factor Physiology	23
1.4 DISRUPTION OF ANGIOGENESIS IN DIABETES	24
1.4.1 Angiogenic Paradox	24
1.4.2 Methylglyoxal modification	25
1.4.3 Vascular Endothelial Growth Factor Resistance	26
1.4.4 Vascular Endothelial Growth Factor mRNA splicing	26
1.4.5 Enhanced Angiogenesis	27
1.5 VASA VASORUM	28
1.5.1 Structure and Function	28
1.5.2 Vasa Vasorum Neovascularization and Atherosclerosis	29
1.5.3 Vasa Vasorum Neovascularization and Diabetes	34
2.0 RATIONALE, HYPOTHESIS AND RESEARCH OBJECTIVES	36
2.1 RATIONALE	36
2.2 HYPOTHESIS	37
2.3 RESEARCH OBJECTIVES	37

3.0 METHODOLOGY	38
3.1 ANIMAL MODELS	38
3.1.1 Animals and diets	38
3.1.2 Female STZ-injected ApoE ^{-/-} mice	38
3.1.3 Female ApoE ^{-/-} Ins2 ^{+Akita} mice	39
3.2 PLASMA ANALYSIS	39
3.3 TISSUE COLLECTION AND PROCESSING	39
3.3.1 Mouse samples	39
3.3.2 Human Samples	40
3.4 HISTOLOGY AND IMMUNOFLUORESCENCE	41
3.5 AORTIC LESION ANALYSIS	41
3.6 VASA VASORUM QUANTIFICATION	42
3.7 ANALYSIS OF HYPOXIA AND ANGIOGENESIS	43
3.8 CELL CULTURE PROCEDURES	44
3.8.1 Cell Survival	45
3.8.2 Western blot analysis	45
3.8.3 Real-time Polymerase Chain Reaction (PCR)	45
3.8.4 Enzyme-linked Immunosorbent Assay (ELISA)	48
3.9 STATISTICS	48
4.0 RESULTS	49
4.1 METABOLIC CHARACTERISTICS AND TISSUE WEIGHTS OF FEMALE APOE ^{-/-} STZ-INJECTED MICE	49
4.2 ATHEROSCLEROTIC PLAQUE SIZES INCREASE IN FEMALE APOE ^{-/-} STZ-INJECTED MICE FROM 25 TO 40 WEEKS OF AGE	55

4.3 THE AORTIC LUMINAL AREA DOES NOT CHANGE WITH INCREASES IN ATHEROSCLEROSIS	61
4.4 FEMALE APOE ^{-/-} STZ-INJECTED MICE HAVE IMPAIRED ANGIOGENESIS FOLLOWED BY ENHANCED NEOVASCULARIZATION	64
4.5 METABOLIC CHARACTERISTICS OF FEMALE APOE ^{-/-} INS2 ^{+/AKITA} MICE	70
4.6 FEMALE APOE ^{-/-} INS2 ^{+/AKITA} MICE HAVE LARGER LESIONS AT 15 WEEKS OF AGE	73
4.7 FEMALE APOE ^{-/-} INS2 ^{+/AKITA} MICE HAVE IMPAIRED NEOVASCULARIZATION AT 10 WEEKS OF AGE AND ENHANCED NEOVASCULARIZATION AT 15 WEEKS OF AGE AT THE AORTIC SINUS	76
4.8 FEMALE APOE ^{-/-} INS2 ^{+/AKITA} MICE HAVE INCREASED HYPOXIA AND INSUFFICIENT ANGIOGENESIS	79
4.8.1 Increased Hypoxia	79
4.8.2 Insufficient Angiogenesis	79
4.9 EXPRESSION OF ANTI-ANGIOGENIC VEGF-A ₁₆₅ B MRNA IS ENHANCED IN THP-1 MACROPHAGES TREATED WITH GLUCOSE	89
4.9.1 Cell Survival	89
4.9.2 HIF-1 α Stabilization	89
4.9.3 mRNA Expression	94
4.10 SECRETED VEGF-A LEVELS ARE DECREASED IN THP-1 MACROPHAGES AND HASMC TREATED WITH GLUCOSE	100
4.11 VASA VASORUM IN HUMAN CORONARY ARTERIES	104
5.0 DISCUSSION	110

5.1 VASA VASORUM NEOVASCULARIZATION IN APOE ^{-/-} STZ-INJECTED MICE	110
5.2 HYPERGLYCEMIA IN APOE ^{-/-} INS2 ^{+/AKITA} MICE IS ASSOCIATED WITH ACCELERATED ATHEROSCLEROSIS, INCREASED HYPOXIA AND ABERRANT ANGIOGENESIS OF THE VASA VASORUM	111
5.3 POST-TRANSLATIONAL MODIFICATIONS AND ALTERNATIVE SPLICING MAY BE RESPONSIBLE FOR ACUTE CHANGES SEEN IN GLUCOSE-TREATED MACROPHAGES	113
5.4 HUMAN CORONARY ARTERIES REQUIRE FURTHER INVESTIGATION	117
5.5 FUTURE DIRECTIONS	118
5.5.1 Chromatin Immunoprecipitation (ChIP) assay	118
5.5.2 Explore molecular mechanisms of diabetes-associated aberrant angiogenesis	119
5.5.3 Explore effects of cholesterol on vasa vasorum angiogenesis	120
5.6 LIMITATIONS	121
6.0 CONCLUSIONS	123
7.0 REFERENCES	125

LIST OF FIGURES

Figure 1- Potential Unified Molecular Mechanisms of Diabetes Pathogenesis

Figure 2- Progression of Atherosclerosis

Figure 3- HIF-1 α regulation

Figure 4- Vasa Vasorum and Atherosclerosis

Figure 5- Metabolic profile of ApoE^{-/-} and ApoE^{-/-} STZ-injected mice

Figure 6- Tissue weights of ApoE^{-/-} and ApoE^{-/-}STZ-injected mice

Figure 7- Atherosclerotic lesions volume from 5 to 40 weeks in female ApoE^{-/-} and ApoE^{-/-} STZ-injected mice

Figure 8- Atherosclerotic lesions in female ApoE^{-/-} and ApoE^{-/-} STZ-injected mice

Figure 9- Lumen size in female ApoE^{-/-} and ApoE^{-/-} STZ-injected mice

Figure 10- Vasa vasorum density in female ApoE^{-/-} and ApoE^{-/-} STZ-injected mice

Figure 11- Vasa vasorum density at the aortic sinus

Figure 12- Atherosclerotic lesions in female ApoE^{-/-} and ApoE^{-/-} Ins2^{+/Akita} mice

Figure 13- Vasa vasorum neovascularization in female ApoE^{-/-} and ApoE^{-/-} Ins2^{+/Akita} mice

Figure 14- HIF-1 α levels in female ApoE^{-/-} and ApoE^{-/-} Ins2^{+/Akita} mice

Figure 15- Angiogenesis in female ApoE^{-/-} and ApoE^{-/-} Ins2^{+/Akita} mice

Figure 16- Number of vasa vasorum per plaque area in 15 week old female ApoE^{-/-} and ApoE^{-/-} Ins2^{+/Akita} mice

Figure 17- Receptor for VEGF-A in female ApoE^{-/-} and ApoE^{-/-} Ins2^{+/*Akita*} mice

Figure 18- Cell viability in THP-1 macrophages and HASMCs

Figure 19- HIF-1 α stability in THP-1 macrophages and HASMCs

Figure 20- Expression of VEGF-A, VEGF-A_{165a} and VEGF-A_{165b} in THP-1 macrophages

Figure 21- Expression of VEGF-A, VEGF-A_{165a} and VEGF-A_{165b} in HASMCs

Figure 22- Secretion of VEGF-A in THP-1 macrophages and HASMCs

Figure 23- Vasa vasorum in diabetic, prediabetic and non-diabetic human coronary arteries

Figure 24- Vasa vasorum density relative to HbA1C levels

LIST OF TABLES

Table 1- Primers Utilized for PCR

Table 2- Metabolic characteristics of Female ApoE^{-/-} Ins2^{+/*Akita*} mice

LIST OF ABBREVIATIONS AND SYMBOLS

2hPG	2-hour Plasma glucose
AGEs	Advanced glycation end-products
ANOVA	Analysis of variance
ApoE ^{-/-}	Apolipoprotein-E deficient
Arf1	ADP-ribosylation factor 1
ARNT	Aryl hydrocarbon nuclear translocator
CAD	Coronary artery disease
CBP	CREB-binding protein
cDNA	Complementary deoxyribonucleic acid
CH1	Cysteine/histidine rich region
CVD	Cardiovascular Disease
DAMPs	Damage-associated molecular patterns
DAPI	4',6-diamidino-2-phenylindole
DFO	Deferoxamine
DM	Diabetes Mellitus
DNA	Deoxyribonucleic acid
eIF4G	Eukaryotic translation initiation factor 4 gamma
ELISA	Enzyme-linked immunosorbent assay
eNOS	Endothelial nitric oxide synthase
EPCs	Endothelial progenitor cells

EPO	Erythropoietin
ER	Endoplasmic Reticulum
ETC	Electron transport chain
FADH ₂	Flavin adenine dinucleotide hydroquinone
FBG	Fasting blood glucose
FFA	Free fatty acids
FGF	Fibroblast growth factor
FIH-1	Factor inhibiting hypoxia-inducible factor-1
FPG	Fasting plasma glucose
GAIT	Gamma interferon-activated inhibitor of translation
GAPDH	Glyceraldehyde 3-phosphate dehydrogenase
GDM	Gestational Diabetes Mellitus
GLO1	Glyoxalase 1
H & E	Hematoxylin and Eosin
HASMCs	Human aortic smooth muscle cells
HbA1C	Hemoglobin A1C
HeLa cells	Henrietta Lacks cells
HG	High glucose
HIF	Hypoxia-inducible factor
HPR	Horseradish-peroxidase
HREs	Hypoxic response elements
ICAM-1	Intercellular adhesion molecule-1

IDF	International Diabetes Federation
IFG	Impaired fasting glucose
IgG	Immunoglobulin G
IGT	Impaired glucose tolerance
Ins2 ^{+Akita}	Heterozygous Insulin 2 mutation
IR	Insulin resistance
JNK	c-Jun N-terminal kinase
LDL	Low density lipoprotein
LDLR ^{-/-}	Low density lipoprotein receptor deficient
LG	Low glucose
MAPK	Mitogen-activated protein kinase
MI	Myocardial Infarction
miRNA	Micro ribonucleic acid
MMPs	Matrix metalloproteinases
mRNA	Messenger ribonucleic acid
NADH	Nicotinamide adenine dinucleotide
NADPH	Nicotinamide adenine dinucleotide phosphate
NFκB	Nuclear factor Kappa B
NO	Nitric oxide
Nrp	Neuropilin
O ₂	Dioxide molecule
O ₂ ⁻	Superoxide

ODDD	Oxygen-dependent degradation domain
OGTT	Oral glucose tolerance test
ONOO ⁻	Peroxynitrite
PAD	Peripheral artery disease
PAMPs	Pathogen-associated molecular patterns
PARP	Poly (ADP-ribose) polymerase
PBS	Phosphate buffered saline
PCR	Polymerase chain reaction
PHD	Prolyl hydroxylase domain-containing
PKC	Protein kinase C
PIGF	Placenta growth factor
PMA	Phorbol 12-myristate 13-acetate
PtdIns2(4,5)P ₂	Phosphatidylinositol 4,5-bisphosphate
RAGE	Receptor for advanced glycation end-products
RNA	Ribonucleic acid
ROS	Reactive oxygen species
SC35	Splicing factor, arginine/serine-rich 2
SDS-PAGE	Sodium dodecyl sulfate polyacrylamide gel electrophoresis
SEM	Standard error of the mean
Sfrp5	Secreted frizzled-related protein 5
SOD	Superoxide dismutase
STZ	Streptozotocin

T1DM	Type 1 Diabetes Mellitus
T2DM	Type 2 Diabetes Mellitus
TCA	Tricarboxylic acid
THP-1	Human Leukemic monocyte
UTR	Untranslated region
VCAM-1	Vascular cell adhesion molecule-1
VEGF	Vascular endothelial growth factor
VEGFR	Vascular endothelial growth factor receptor
VHL	von Hippel Lindau tumour suppressor protein
VSMC	Vascular smooth muscle cell
vWF	von Willebrand Factor
Wnt5a	Wingless-type MMTV integration site family, member 5A

DECLARATION OF ACADEMIC ACHIEVEMENT

This study has shown that two mouse models of diabetes have had initial decreases in vasa vasorum density and insufficient angiogenesis that correlates with accelerated atherosclerosis. The impaired vasa vasorum neovascularization appears to be associated with disruption of hypoxia-mediated angiogenesis and the mechanism(s) behind this are still being explored. Long-term hyperglycemia demonstrated increases in vasa vasorum microvessels in one mouse model that correlated with cholesterol levels and resembles the trends observed in diabetic retinopathy.

Experiments conducted in this thesis were completed by Heidi Stoute with some assistance. Kaley Veerman and Daniel Venegas-Pino previously collected information on the ApoE^{-/-} STZ-injected mouse model from 5 to 20 weeks of age that assisted with analysis of trends over time. Dr. Peter Shi breed, monitored and handled the mice utilized in this study. Emma Butcher assisted with staining and analysis of human coronary arteries as well as analysis of mouse necrotic cores. Aric Huang assisted with PCR preparation and analysis.

1.0 INTRODUCTION

1.1 DIABETES MELLITUS

1.1.1 Definition, Classification and Clinical Diagnosis

The metabolic disorder diabetes mellitus (DM), also commonly referred to as diabetes, is characterized as defective insulin secretion and/or impaired insulin sensitivity that results in chronic hyperglycemia^{1, 2}. DM leads to metabolic disturbances in carbohydrates, lipids and proteins, and can cause damage and dysfunction in various organs¹.

There are two main classifications of DM based on etiology². Type 1 DM (T1DM) is a result of destruction of pancreatic beta cells either from an autoimmune disorder or unknown cause and accounts for 5-10% of people diagnosed with DM³. Approximately 90-95% of individuals with diabetes are diagnosed with Type 2 DM (T2DM), which involves peripheral insulin resistance that may or may not be accompanied with insulin deficiency. A less common type of diabetes is gestational DM (GDM), which is diagnosed when a women first experiences glucose intolerance during pregnancy. There are other types of diabetes, but these are much less prevalent and may result from genetic mutations, complications from other diseases or in response to certain drugs^{2, 3}.

The criteria for diagnosing DM are a fasting plasma glucose (FPG) ≥ 7.0 mM, a causal plasma glucose test that can be taken regardless of the patient's last meal ≥ 11.1 , mM, or a 2-hour plasma glucose (2hPG) in a 75g oral glucose

tolerance test (OGTT) ≥ 11.1 mM². Another test that can be used in conjunction with the previous tests is the hemoglobin A1C (HbA1C) test that defines A1C levels $\geq 6.5\%$ to be classified as diabetic and provides a measurement of chronic elevated glucose levels⁴. Individuals who have elevated glucose levels, but are not high enough to be classified as diabetic have what is termed “prediabetes” and are classified as having impaired fasting glucose (IFG), which is a FPG of 5.6-6.9 mM, and/or impaired glucose tolerance (IGT), which is a 2hPG in a OGTT of 7.8-11 mM³. It is important to identify people with prediabetes as they are at an increased risk of developing diabetes as well as cardiovascular disease (CVD).

1.1.2 Prevalence

Since 2000, the International Diabetes Federation (IDF) has made annual predictions on increasing diabetes prevalence⁵. In 2013, the IDF gathered information from 217 countries and territories and estimated that 1 in 12 people currently have diabetes. This organization also predicted that the world incidence of diabetes would increase by 55% in adults by 2035. Factors such as an aging population and a country’s income level influence the predicted prevalence. In every geographic location, the prevalence of diabetes increases with age and is predicted to have the greatest increase in 60 to 79 year olds. Low-income countries, such as those in Africa, currently have the lowest prevalence of diabetes, but are predicted to have the largest increases in the next 20 years at

109%. These estimates may be conservative due to the number of undiagnosed diabetics⁶. Reports from 2014 indicate that approximately half of the individuals worldwide with DM do not know that they have the disease⁷.

With increasing prevalence of diabetes, there will be a greater burden on the health care industry to allocate resources to this population and encourage preventative strategies⁵. New or more effective treatments that target the potentially life-threatening cardiovascular complications of diabetes may alleviate some of this problem.

1.2 VASCULAR PATHOLOGIES OF DIABETES

1.2.1 Macro- and Microvascular Complications

Chronic complications of DM are associated with vascular pathologies that are often separated into pathologies arising from the macrovasculature and microvasculature^{8,9}. Macrovascular complications result from structural and functional changes to the endothelium and smooth muscle cells of large blood vessels leading to the accelerated development and progression of atherosclerosis¹⁰. Atherosclerosis contributes to CVD, which is the leading cause of mortality in the diabetic population¹¹. The mortality rate for people with DM from CVD is up to 75% and represents a 2-to 4-fold increase in risk of dying from a myocardial infarction (MI) or stroke compared to the rest of the population^{12,13}. Microvascular complications are a major cause of morbidity in DM and often result from changes in angiogenesis leading to dysfunction of organs near these

vascular beds¹⁴. Microangiopathies can include retinopathy, neuropathy and nephropathy^{8, 11}. These comorbidities are among the leading causes of adult blindness, lower limb amputation and renal failure¹⁵.

1.2.2 Role for both vascular beds in disease pathology

While disorders of the micro- and macrovasculature have been traditionally seen as independent consequences of DM, there is increasing evidence that dysfunction of these vascular beds may be linked. Patients with DM who have microvascular complications, such as retinopathy or nephropathy, are at increased risk for systematic vascular complications such as CVD compared to individuals with DM that do not have microvascular complications^{11, 16-19}. One hypothesis for these findings is that these vascular beds are a continuum so dysfunction of the microvessels may lead to changes in resistance and blood flow reserve that cause upstream effects on the macrovasculature^{20, 21}. The information collected from these studies indicate that the presence of microvascular disease may be able to predict macrovascular outcomes and suggests that the potential for similar molecular pathways that may promote these vascular diseases.

While there is an abundance of research on the established link between diabetes and CVD; it is still unclear how accelerated atherosclerosis and microangiopathies occur on a molecular and cellular level¹⁵.

1.2.3 Potential unified mechanisms for Vascular Dysfunction

The mechanism by which diabetes may promote atherosclerosis and microangiopathies may be related to one or more common pathways²²⁻²⁴. Since both macrovascular and microvascular blood vessels are exposed to the chronic metabolic anomalies of hyperglycemic and insulin deficiency/resistance that cause structural and functional changes to the endothelium, it is possible that common pathways may exert these effects on both vascular beds^{10, 22}.

Hyperglycemia can cause a decrease in nitric oxide (NO) bioavailability and synthesis, and an increase in reactive oxygen species (ROS) resulting in a molecular imbalance that alters vascular function¹⁰. Enhanced glycolysis can promote the accumulation of electron donors (NADH & FADH₂) from the tricarboxylic acid (TCA) cycle^{23, 24}. These electron donors increase the voltage gradient in the mitochondria until it reaches a critical threshold. When this threshold is reached, electron transfer to complex III in the electron transport chain (ETC) is blocked and backs up electrons in coenzyme Q, which then donates some electrons to dioxygen (O₂) to produce superoxide (O₂⁻). Superoxide inhibits glyceraldehyde 3-phosphate dehydrogenase (GAPDH), an enzyme in the glycolytic pathway, by activating poly (ADP-ribose) polymerase (PARP) in the nucleus. PARP attaches polymers of ADP-ribose to GAPDH that has translocated to the nucleus resulting in inhibited activity of GAPDH and a buildup of glycolytic intermediates. The superoxide molecule is also able to reduce NO bioavailability by converting NO to peroxynitrite (ONOO⁻) and

participate in substrate nitration¹⁰. The activity of endothelial NO synthase (eNOS) and antioxidant enzymes is reduced by substrate nitration and contributes to metabolic imbalances of NO and ROS²⁵.

A buildup of glycolytic intermediates, such as glucose, fructose-6-phosphate and glyceraldehyde-3 phosphate, activate mechanisms that contribute to vascular pathologies through five pathways (Figure 1), namely, 1) the polyol pathway, 2) increased advanced glycation end-products (AGEs), 3) increased expression of the receptor for AGEs (RAGE), 4) protein kinase C (PKC) activation and 5) the hexosamine pathway^{10, 15, 23, 24}. These pathways increase the production of ROS, decrease antioxidant enzyme activity and/or alter protein expression. The increases in ROS may explain why clinical trials testing antioxidant therapies have shown little or no cardiovascular benefit²⁶. Normally, antioxidants neutralize ROS molecules on a one-to-one basis, but the continuous and excessive production of ROS in addition to inactivation of key enzymes such as eNOS and prostacyclin synthase, may make this therapy ineffective²⁴. New studies are investigating the effect of novel antioxidant molecules, such as superoxide dismutase (SOD)/catalase mimetics, which are not inhibited by ROS²⁷.

In hyperglycemic conditions, ROS and protein modifications have various effects on vascular endothelial cells including blood flow abnormalities, pro-inflammatory gene expression, dysregulation of coagulation factors, platelet activation, increased cellular permeability, changes in angiogenesis, extracellular

matrix expansion, cell growth and apoptosis^{10, 22-24}. In microvascular cells there is increased thickening of the vascular basement membrane, disrupted gap junction intercellular communication and increased vascular permeability²⁸. Prolonged exposure to hyperglycemia can induce apoptosis in endothelial cells and pericytes leading to hypoxia and subsequent stimulation of angiogenesis. Endothelial dysfunction in the macrovasculature is likely activated through the same pathways and is accompanied by increased lipid accumulation in the artery walls, vascular smooth muscle cell proliferation and migration, and eventually apoptosis^{10, 13, 15}.

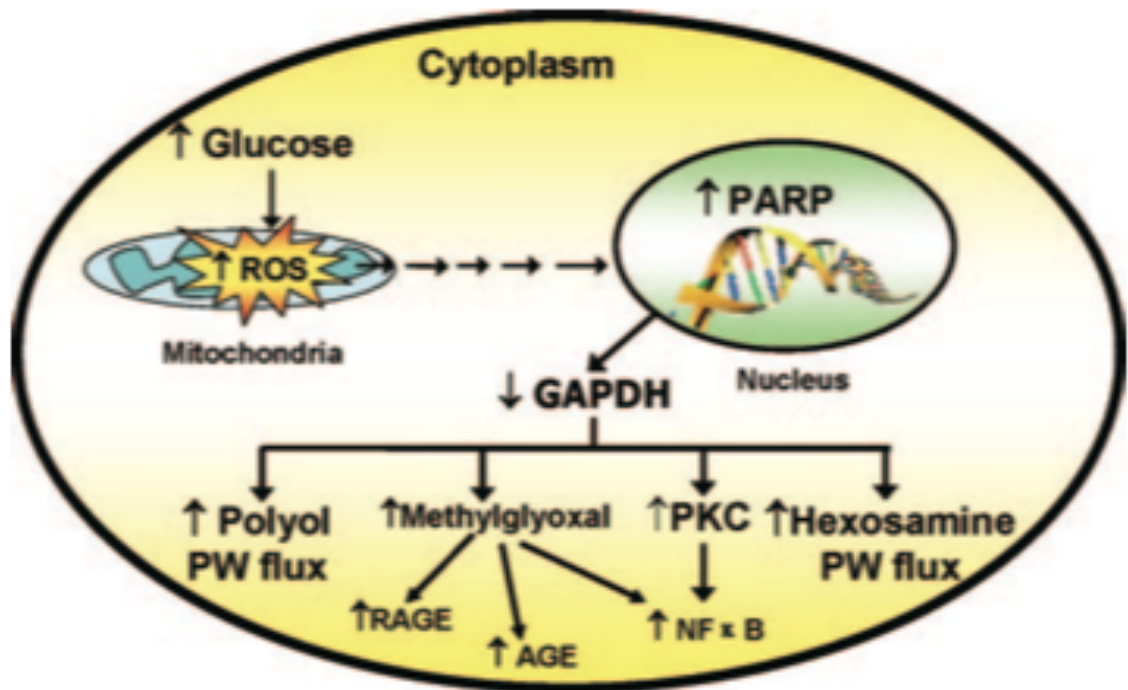
Some studies have also looked at the influence of insulin resistance (IR), which can occur in both Type 1 and Type 2 DM, on the number of cardiovascular events in the absence of hyperglycemia²⁴. These studies have consistently shown that adipocytes affected by IR have an increased release of free fatty acids (FFA) from triglycerides and subsequent increases in FFA oxidation that promotes overproduction of superoxide in the ETC^{23, 24}. The increased amount of ROS results in activation of the five pathways (described above) and promotion of atherogenesis. In addition to these pathways, insulin resistance may alter microRNA (miRNA) levels that are responsible for endothelial homeostasis, vascular repair and angiogenesis¹⁰.

Figure 1- Potential Unified Molecular Mechanisms of Diabetes Pathogenesis

Increased glucose from hyperglycemia increases ROS production in the mitochondria, which subsequently increases activity of PARP in the nucleus.

Activated PARP can modify and inhibit the activity of GAPDH causing a buildup of glycolytic intermediates that can be shunted into other metabolic pathways.

Increased flux through pathways upstream of GAPDH such as the polyol pathway, increased AGEs, increased expression of RAGE, PKC activation and the hexosamine pathway are believed to contribute to vascular dysfunction.



Adapted from F. Giacco and M. Brownlee (2010)²⁴

1.2.4 Glycemic control and vascular complications

Therapeutic interventions aimed at improving vascular outcomes often involve normalizing glucose levels through pharmacological medications and/or lifestyle modifications^{29, 30}. Lowering FPG below 7.0mM is associated with a significant reduction in microvascular disorders such as retinopathy, neuropathy and nephropathy³¹⁻³³. The relationship between glucose normalization and macrovascular disease does not appear to be as clear since CVD outcomes often appear to not improve with glycemic control. Research from the ACCORD study even saw increases in mortality with intensive glucose control treatments³¹.

One explanation for why normalizing glucose levels may not be beneficial for macrovascular complications is that individuals may still have IR. Research may also need to address IR and its ability to independently activate the same pathological mechanisms as chronic hyperglycemia²⁴. There appears to be non-resistant insulin signaling pathways, such as the mitogen-activated protein kinase (MAPK) cascade, that are amplified with increases in insulin. Studies have shown that this can cause increases in inflammatory markers, enhanced expression of adhesion molecules, vascular smooth muscle cell (VSMC) proliferation and migration, and formation of prothrombotic factors that contribute to the progression of atherosclerosis and CVD^{34, 35}.

Other studies have shown that early glucose normalization of hyperglycemia may improve CVD prognosis, while delaying such treatments until years later causes no beneficial results^{10, 29}. The reason early interventions may be

beneficial is that superoxide has had less time to buildup and cause excessive oxidative stress on endothelial cells²³. With time, however, superoxide production can promote post-translational modifications of histones that result in chromatin remodeling and epigenetic changes²⁴. These changes can alter gene expression even after glucose normalization and has been shown to upregulate PKC β and a pro-oxidant enzyme, NADPH oxidase^{36, 37}. Researchers have termed this ability of the artery wall to remember hyperglycemic stresses, “hyperglycemic memory.” This demonstrates the increasingly complex relationship between atherosclerosis and hyperglycemia.

1.3 MACRO- AND MICROVASCULAR DISEASE MECHANISMS

While both macrovascular and microvascular diseases may be influenced by the different molecular pathways that were previously described, the ways by which they respond to signals from these pathways differ. These pathways promote atherogenesis in large arteries while they promote aberrant angiogenesis in smaller blood vessels²⁰.

The structure and function of the vessels appears to play a role in the different regulatory mechanisms of these vascular beds³⁸. The macrovascular system is composed of large muscular arteries, including the aorta, coronary arteries and carotid arteries. The walls of large arteries consist of three distinct layers called the tunica intima, tunica media and tunica adventitia or more simply intima, media and adventitia³⁹. The intimal layer, which is the closest layer to the

vessel lumen, consists of a layer of endothelial cells and subendothelial connective tissue, and is typically separated from the media by an internal elastic lamina⁴⁰. The middle layer of the artery is the media and contains layers of VSMCs that are surrounded by elastic fibers³⁹. The outer layer, the adventitia, is separated from the media by an external elastic lamina and is mainly composed of connective tissue including collagen and elastin, adipocytes and fibroblasts⁴¹. Autonomic nerves, lymphatic vessels and blood vessels known as the vasa vasorum also permeate the adventitia of large arteries. The major function of macrovascular arteries is to deliver blood to peripheral tissues and organs and to withstand changes in pressure during each heart contraction³⁸.

The microvascular circulation consists of smaller blood vessels including arterioles, capillaries and venules³⁸. Some of the larger arterioles and venules also have the three distinct layers of the intima, media and adventitia. As the blood vessels continue to get progressively smaller the arterioles, capillaries and venules may only consist of endothelial cells, a basement membrane and may be stabilized by pericytes^{42, 43}. Vessels of the microvasculature are required to regulate nutrient delivery, blood pressure, organ perfusion, vasomotion, and must be able to respond to metabolic demands of local tissues³⁸.

1.3.1 Atherosclerosis

As mentioned previously, atherosclerosis is a major underlying cause of CVD, which includes coronary artery disease (CAD), cerebrovascular disease

and peripheral artery disease (PAD) ¹¹. Atherosclerosis is typically characterized as an inflammatory disease of large muscular arteries that results in lipid accumulation in the artery walls (Figure 2)⁴⁴.

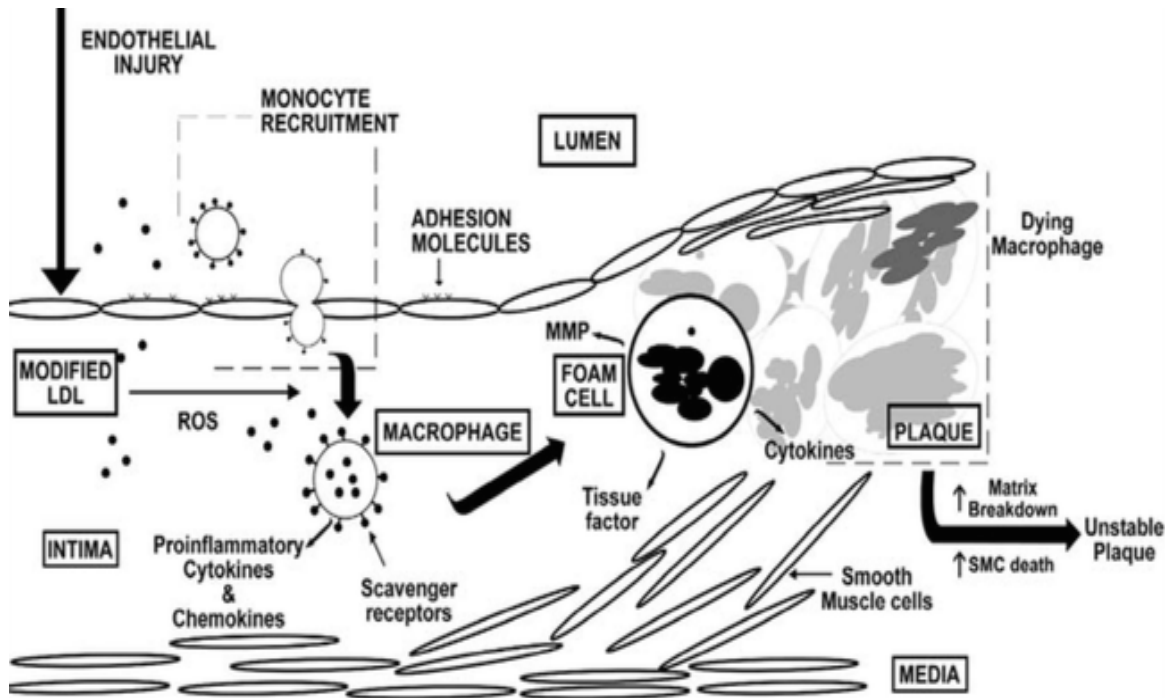
The process of atherosclerosis is influenced by genetic, environmental and metabolic factors, but is thought to be triggered as a response to endothelial injury in areas of disrupted flow⁴⁴⁻⁴⁶. The injury causes endothelial dysfunction and a variety of compensatory events. Monocytes and T cells are recruited to the vessel wall due to increased secretion of cytokines and growth factors, as well as enhanced expression of vascular adhesion molecules, such as vascular cell adhesion molecule-1 (VCAM-1), intercellular adhesion molecule-1 (ICAM-1), P-selectin and E-selectin, on the endothelial cell surface^{44, 45}. The endothelium also becomes more permeable to infiltration of lipoproteins, monocytes and T-cells into the intima. Once in the subendothelial portion of the intima, low-density lipoproteins (LDL) molecules can become modified through oxidation and retained in the vessel wall. Monocytes differentiate into macrophages and are activated by cytokines, pathogen-associated molecular patterns (PAMPs) and damage-associated molecular patterns (DAMPs). The activated macrophages express scavenger receptors that can attach to and engulf the LDL and oxidized LDL particles. Lipid engorged macrophages are called foam cells. As foam cells accumulate in the vessel wall, a fatty streak is formed. Fatty streaks are not considered pathological atherosclerosis, but if the process is not resolved through

efflux of macrophage foam cells out of the vessel wall or alleviation of vessel wall perturbation, then the lesion may become more advanced⁴⁴.

Lesion development progresses as cytokines are secreted from foam cells and T cells to promote VSMC proliferation and migration from the medial layer to the intima⁴⁴. VSMC are also able to take up some of the LDL particles and secrete elastin, collagen and proteoglycans that stabilize the vessel wall by forming a fibrous cap. As the lesion continues to become more advanced, activated endothelial cells and macrophages as well as the accumulating foam cells are able to secrete inflammatory cytokines that attract more monocytes to the vessel wall and secrete proteolytic enzymes⁴⁵. These enzymes include matrix metalloproteinases (MMPs) and cathepsins that can degrade the fibrous cap causing the plaque to become less stable and more prone to rupture. Increasing amounts of intracellular cholesterol are cytotoxic to foam cells and VSMCs that are taking in these particles⁴⁷. This may cause these cells to undergo apoptosis and begin to form a necrotic core that can also contribute to plaque instability^{44, 45, 47}. While the plaque may begin to intrude into the lumen, it is usually plaque rupture and not vessel occlusion that triggers CVD events such as MI or stroke. When the plaque ruptures, circulatory proteins are exposed to the prothrombotic factors in the vessel wall and the coagulation cascade is triggered to form a thrombus. If an artery is occluded by the thrombus or an embolism, then this may block blood flow to the tissue and cause cell death.

Figure 2- Progression of Atherosclerosis

Atherosclerosis is triggered by endothelial injury causing the cells to become more permeable to LDL particles that can be modified and retained in the intima. Endothelial dysfunction increases secretion of cytokines and expression of adhesion molecules to recruit monocytes to the vessel wall that can then transmigrate into the intimal layer. Monocytes differentiate into macrophages that express scavenger receptors that can take up the modified LDL particles and become foam cells. VSMCs from the media proliferate and migrate into the intimal layer to help stabilize the plaque by forming a fibrous cap. Secretion of MMPs from foam cells contributes to unstable plaques since there is degradation of the fibrous cap. Atherosclerotic plaques may also become unstable from increased apoptosis of macrophages and VSMCs causing formation of a necrotic core. If the plaque ruptures, then a thrombus is formed and a cardiovascular event may occur.



Adapted from A. D'Souza et al. (2009) ²²

1.3.2 Atherosclerosis and Diabetes

Diabetes is a major risk factor for CVD as diabetes is associated with accelerated atherosclerosis^{10, 48, 49}. Hyperglycemia promotes endothelial injury by reducing NO bioavailability that may prevent vessel injury and cause local vasodilation as well as by increasing ROS production that can activate endothelial cells. This imbalance of endothelial function is associated with increases in inflammation, nuclear factor κ B (NF κ B) activation and recruitment of immune cells that promote accelerated plaque growth. The atherosclerotic plaques also have increased VSMC death and secretion of MMPs that contribute to degradation of the fibrous cap and an unstable plaque that is more predisposed to rupture²².

In addition to these findings, recent research has suggested that the microvasculature may play a role in promoting diabetes-accelerated atherosclerosis, specifically through changes in angiogenesis of the vasa vasorum^{8, 50}.

1.3.3 Hypoxia-mediated Angiogenesis

The role of the microvasculature is to regulate blood pressure, vasomotion and provide tissues with nutrients and oxygen to meet metabolic demands of the tissue³⁸. If there is insufficient oxygen to meet the metabolic tissue needs then additional blood vessels must develop and remodel via one of three mechanisms. New blood vessel formation from de novo endothelial cell production is called

vasculogenesis⁵¹. While vasculogenesis is mainly thought to occur during embryogenesis, it has been observed that tumour growth, trauma and endometriosis may stimulate circulating endothelial progenitor cells (EPCs) to form into mature endothelial cells^{52, 53}. Arteriogenesis is the remodeling of an existing artery in order to increase lumen diameter while sprouting of new blood vessels from preexisting blood vessels is known as angiogenesis^{51, 54}. When there is insufficient oxygen in a local area, hypoxia-mediated angiogenesis occurs in order to link vascular oxygen supply to metabolic demands. In DM, however, there appears to be disruption in one or more pathways that link hypoxia and angiogenesis, and this contributes to microvascular disease pathology⁵⁵.

1.3.4 Regulatory Mechanisms of Hypoxia

Under normal physiological conditions, adaptive responses to meet metabolic demands caused by hypoxia and ischemia are mediated by hypoxia-inducible factor (HIF), a α,β -heterodimeric transcription factor (Figure 3)^{56, 57}. HIF- β exists in a variety of isoforms including HIF-1 β , which is a constitutive nuclear protein also referred to as aryl hydrocarbon nuclear translocator (ARNT). HIF- α is regulated by hypoxia and found in 3 isoforms; HIF-1 α , HIF-2 α and HIF-3 α . HIF-1 α and HIF-2 α appear to be the most closely related of the 3 isoforms as they are both degraded by the same mechanism, and are able to interact with HIF-1 β and bind to hypoxia response elements (HREs) on DNA. HIF-3 α , on the other hand,

appears to have an influence in the negative regulation of this response^{56, 58}. HIF-1 α is expressed ubiquitously and found in the cytoplasm where it can be stabilized in hypoxic conditions and translocated to the nucleus^{57, 59}. HIF-2 α , on the other hand, appears to be present during embryonic development, but is restricted to certain organs during adulthood^{58, 60}. The presence of HIF-2 α has been seen in the heart, brain, pancreas, liver, kidney and intestines of rats exposed to hypoxia⁶¹.

Under normoxic conditions, two prolyl residues (P402 and P564 in humans) in the oxygen-dependent degradation domain (ODDD) of HIF-1 α undergo posttranslational hydroxylation by HIF hydroxylases⁵⁶⁻⁵⁹. Prolyl hydroxylase domain-containing (PHD 1-3) enzymes are members of the Fe(II)- and 2-oxoglutarate-dependent oxygenases superfamily that act as HIF hydroxylases and use dioxygen as a cosubstrate⁵⁷. PHD2 appears to have the highest activity with HIF-1 α and is located predominantly in the cytoplasm along with PHD3, whereas PHD1 is primarily in the nucleus⁵⁶⁻⁵⁸. The von Hippel Lindau tumour suppressor protein (VHL) E3 ubiquitin ligase complex then targets the hydroxylated HIF-1 α for ubiquitination and proteasomal destruction.

Along with oxidative modification of the ODDD, there is an asparaginyl residue (N803) in the C-terminal transactivation domain that can be hydroxylated by factor inhibiting HIF-1 (FIH-1)^{56, 57}. This HIF hydroxylase uses dioxygen as a cosubstrate to attach a hydroxyl group to the asparaginyl residue that blocks binding of cofactor p300 to HIF-1 α resulting in no transcription. Studies have

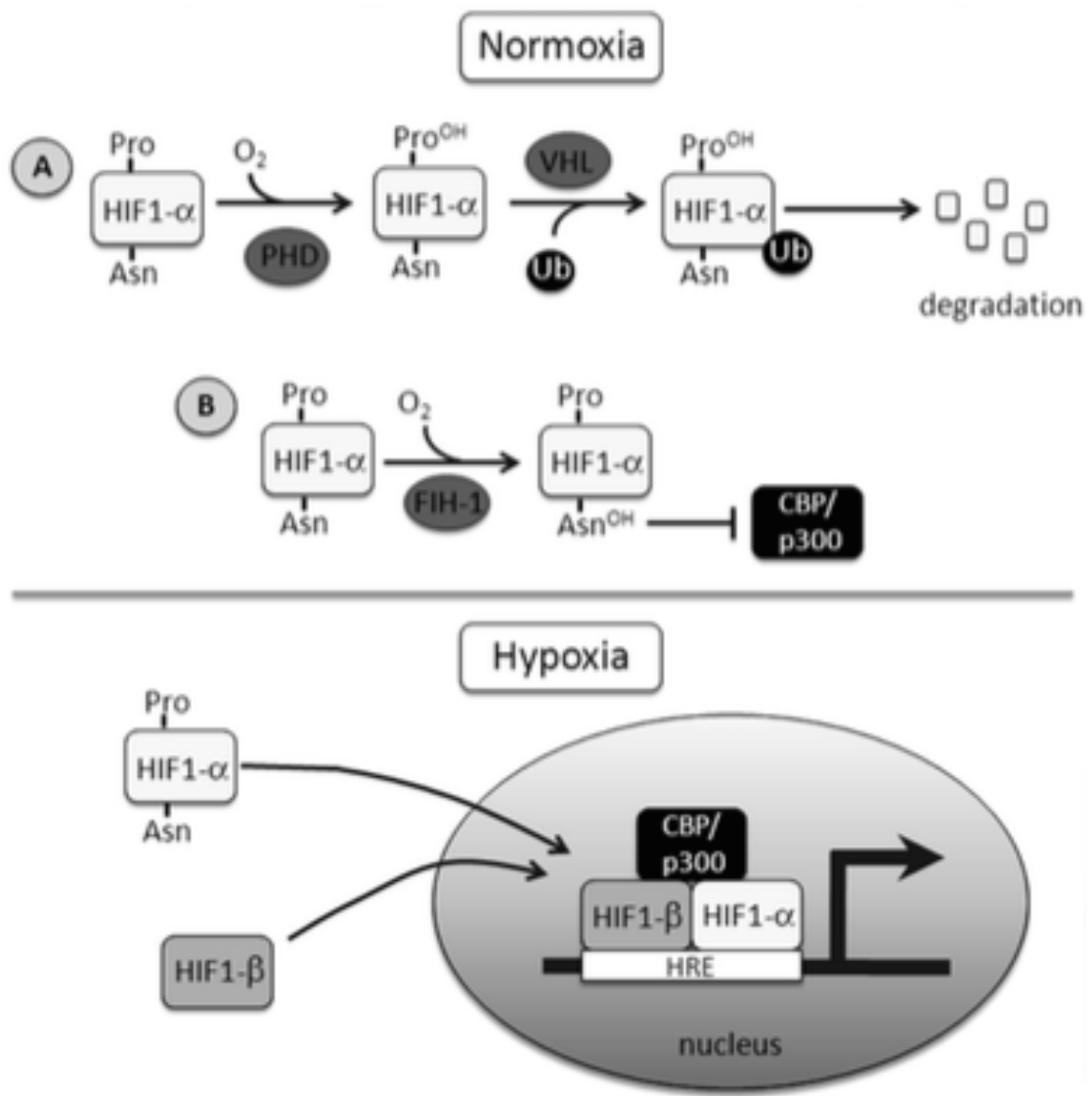
shown that both FIH-1 and the PHD enzymes have similar kinetics and binding affinities for oxygen making them effective at sensing oxygen under physiological conditions⁶⁰.

Under hypoxic conditions, HIF hydroxylase activity is suppressed by the lack of oxygen as a cosubstrate resulting in HIF-1 α stabilization^{56, 57}. HIF-1 α is able to translocate to the nucleus where it forms a heterodimer with HIF-1 β . Binding of cofactors such as p300 and CBP to HIF-1 α/β allows the HIF complex to interact with HREs and induce the transcription of vascular endothelial growth factor (VEGF), erythropoietin (EPO), transferrin and other factors⁶².

It is important to note that normoxia and hypoxia are relative terms and should be defined during each study⁵⁸. Physiological levels of oxygen in the body range from about 14% O₂ (100 mmHg) in arterial blood to about 6% O₂ (40 mmHg) in venous blood with the partial pressure of oxygen varying between organs and even within a tissue. In cell culture experiments, however, normoxic conditions are often cells left in 95% air and 5% carbon dioxide meaning that the cells are exposed to high concentrations of oxygen at about 20% O₂. There is also a range of levels at which HIF-1 α may be stabilized and considered hypoxic. HeLa cells exposed to oxygen concentrations less than 6% have shown dramatic increases in HIF-1 α levels with optimal increases at 0.5% O₂⁶³.

Figure 3- HIF-1 α regulation

Under normoxic conditions (top), HIF-1 α can be modified by **A.** PHD enzymes that attach hydroxyl groups to prolyl residues. The VHL complex can then target the HIF-1 α molecule for ubiquitination and subsequent degradation by proteasomes. HIF-1 α can also be modified by **B.** FIH-1 that attaches a hydroxyl group to an asparaginyl residue that blocks HIF-1 α interaction with cofactors, CBP and p300, to inhibit transcription. Under hypoxic conditions (bottom), the HIF hydroxylases can no longer use oxygen as a cosubstrate to modify HIF-1 α . HIF-1 α and HIF-1 β can then form a heterodimer and bind with cofactors that interact with HREs on promoter regions of DNA to promote transcription.



Adapted from L.A. Shimoda and S.S. Laurie (2013)⁶⁰

1.3.5 Vascular Endothelial Growth Factor Physiology

VEGF is a key protein for oxygen homeostasis as it regulates angiogenesis by stimulating endothelial cell proliferation, permeability, migration and survival, as well as vasodilation through NO production^{64, 65}. There are six proteins encoded by the VEGF gene family including VEGF A, B, C, D, E and placenta growth factor (PlGF) as well as different possible isoforms of each protein⁶⁶. VEGF-A is the most abundant and regulates endothelial and vascular function⁶⁴. VEGF-B appears to be involved in coronary artery development while VEGF-C and -D are considered lymphangiogenic cytokines that, under appropriate conditions, may be able to increase vascular permeability and angiogenesis^{67, 68}. VEGF-E is a related viral protein and PlGF is often expressed in cases of pathological angiogenesis^{69, 70}. Each of these VEGF family proteins can interact with three VEGF receptors (VEGFR), namely, VEGFR-1 (flt-1), VEGFR-2 (kdr/flk-1), and VEGFR-3 (flt-4), and each receptor possess tyrosine kinase activity^{65, 66}. Neuropilin-1 (Nrp-1) and -2 (Nrp-2) are two additional non-kinase receptors that have been shown to bind with VEGF proteins⁶⁹.

Since VEGF-A appears to play the most prominent role in angiogenesis, research has focused primarily on this VEGF family gene protein⁶⁹. Human VEGF-A isoforms consist of 121, 145, 165, 189 and 209 amino acids that are caused by alternative splicing after transcription. VEGF-A₁₆₅ is the most highly expressed isoform of VEGF-A in most tissues as well as under pathological conditions. Variations in the splicing of VEGF-A₁₆₅ at exon 8 cause two isoforms

to be produced; a proangiogenic form, VEGF-A_{165a}, and an antiangiogenic form, VEGF-A_{165b}^{71, 72}. VEGF-A₁₆₅ exerts most of its effects through VEGFR-2, but can also bind to VEGFR-1 although its function is not as clear. One hypothesis is that VEGFR-1 may modulate VEGFR-2 function by acting as a decoy^{65, 73}. Other studies have seen that VEGFR-1 may be able to induce formation of MMPs and growth factors and may also play a role in haematopoiesis.

1.4 DISRUPTION OF ANGIOGENESIS IN DIABETES

1.4.1 Angiogenic Paradox

Aberrant angiogenesis of microvascular beds results in a variety of DM pathologies. Diabetic retinopathy and nephropathy involve enhanced angiogenesis while impaired wound healing, impaired collateral vessel formation and transplant rejection are characteristics of deficient angiogenesis⁵⁵. These differences in angiogenesis are referred to as the “angiogenic paradox”^{55, 65}. Diabetic neuropathies are the result of reduced blood flow and may improve with increased angiogenesis⁵⁵. Pharmacological therapies are exploring proangiogenic factors that may be able to improve diabetic microvasculature complications, but it is unknown if these treatments can target certain tissues to avoid potentially exacerbating retinopathies and nephropathies.

1.4.2 Methylglyoxal modification

The regulation of oxygen homeostasis is disrupted in DM and appears to have an effect on VEGF transcription⁷⁴. The mitochondrial ETC appears to overproduce superoxide in hyperglycemic conditions that leads to the generation of intracellular hydroxyl radicals²²⁻²⁴. As mentioned previously, these free radicals assist in the formation of accumulating glycolytic metabolites in the cell that cause a large portion of diabetic complications. Methylglyoxal is one of the glycolytic metabolites produced by high glucose conditions and is a substrate for the enzyme glyoxalase 1 (GLO1). Hyperglycemia has also been shown to increase free iron, which can catalyze the formation of ROS and lead to excess methylglyoxal accumulation^{74, 75}. Methylglyoxal has been observed to react with arginine and lysine residues and change protein expression⁷⁵.

The coactivator p300 has a cysteine/histidine rich (CH1) region that binds to HIF-1 α ⁷⁴. The CH1 region has a specific arginine residue (R354) that may be covalently modified by high-glucose induced methylglyoxal resulting in decreased binding of p300 to HIF-1 α and impaired transcription of VEGF. HIF-1 α may also be modified to form HIF-1 α -methylglyoxal adducts, which decreases HIF-1 α stability and impairs heterodimerization of HIF-1 α to HIF-1 β ⁷⁶. This impairment leads to decreases in DNA binding even when the HIF-1 α to p300 binding is not impaired.

Overexpression of the rate-limiting enzyme of methylglyoxal catabolism, GLO1, has been shown to prevent methylglyoxal modification of p300 and

reverse the decreased interaction of HIF-1 α with p300⁷⁴. These findings may suggest a novel therapeutic approach to increasing angiogenesis. The iron chelator, deferoxamine (DFO), has also shown promising results by increasing HIF-1 α stability and transactivation^{56, 57, 74, 77}. DFO may normalize the association between HIF-1 α and p300, by decreasing ROS generation and subsequent methylglyoxal modification. In diabetic mice, administration of DFO has been shown to improve wound healing⁷⁴.

1.4.3 Vascular Endothelial Growth Factor Resistance

Generation of ROS from high glucose concentrations may also influence the VEGFR availability/activities^{12, 78}. In DM, generation of ROS promotes ligand- and intrinsic kinase-independent VEGFR2 phosphorylation in the Golgi compartment, which leads to less availability of VEGFR2 at the cell surface^{12, 78}. In diabetic mouse models, endothelial cell responses to exogenous VEGF were inhibited due to the reduced VEGFR2 receptors¹². There were no apparent changes in transcript abundance, suggesting that hyperglycemia can cause “VEGF resistance” and influence angiogenesis due to oxidative stress.

1.4.4 Vascular Endothelial Growth Factor mRNA splicing

A study published in 2014 examined why diabetic patients with PAD experience limb ischemia and potentially limb amputation from impaired angiogenesis while having increased levels of circulating VEGF-A⁷².

Researchers found that levels of antiangiogenic VEGF-A_{165b} were elevated in patients with PAD while proangiogenic VEGF-A_{165a} levels were decreased. Using a murine model of hind limb ischemia, researchers found that an increased level of a pro-inflammatory protein, Wnt5a, was associated with impaired limb revascularization^{71, 72}. These researchers also observed impaired angiogenesis in mice lacking Sfrp5, an anti-inflammatory protein that can inhibit Wnt5a signaling. When neutralizing antibodies for VEGF-A_{165b} were given to the mice lacking Sfrp5, limb revascularization was rescued. Next researchers utilized macrophages to further explore the mechanism by which Wnt5a may promote the formation of VEGF-A_{165b}. Results showed that Wnt5a signaled the c-Jun N-terminal kinase (JNK) pathway through the Ror2 receptor and this lead to upregulation of the splicing factor SC35. SC35 is able to splice VEGF-A₁₆₅ mRNA and promote the production of VEGF-A_{165b} isoform instead of the angiogenic form, VEGF-A_{165a}.

While methylglyoxal modification, VEGF resistance and alternative splicing of VEGF-A mRNA all present valid mechanisms by which hyperglycemia may influence diabetic microangiopathies, other mechanisms may influence post-translational modification of VEGF-A that have yet to be researched⁷⁹⁻⁸¹.

1.4.5 Enhanced Angiogenesis

Excess angiogenesis may be the result of upregulation of fibroblast growth factor (FGF), integrins and fibronectin, protein modification by AGE glycosylation,

sorbitol accumulation and/or metabolic abnormalities such as increased lipolysis and ketone formation^{55, 82-85}. These processes are able to stimulate proliferation and migration of endothelial cells, increase tissue hypoxia to stimulate angiogenesis, and/or alter expression of basement membrane-degrading MMPs. Some studies have also attributed excessive angiogenesis in the retina and kidney to increases in VEGF concentrations⁸⁶⁻⁸⁹. The potential increases in VEGF in some tissues beds and decreases in others demonstrate the perplexing and complex nature of angiogenic paradox.

Some researchers have suggested that hypercholesterolemia may trigger the angiogenic phenotype^{90, 91}. Animals, such as pigs and mice, put on diets to induce hypercholesterolemia have demonstrated increased adventitial vasa vasorum density^{92, 93}. Elevated cholesterol levels may be able to activate growth factor receptors or increase inflammatory markers that may contribute to enhance angiogenesis⁹⁰⁻⁹². Lowering cholesterol with the use of statins has also been associated with less adventitial angiogenesis, although it is unclear whether this is a result of lipid lowering or an effect of the drug^{90, 93}.

1.5 VASA VASORUM

1.5.1 Structure and Function

The vasa vasorum is a microvascular network that originates from various arteries including the coronary, brachiocephalic and intercostal arteries⁹⁴. The vasa vasorum consists of arterioles, capillaries and venules. It functions to

supply oxygen and nutrients to large muscular arteries and is located primarily in the outer layer of the arterial wall, the tunica adventitia. This vascular network can also be found in tunica intima (inner layer of the arterial wall) and tunica media (middle layer of the arterial wall) in humans and large mammals.

Mice have significantly thinner arterial walls, but still have the presence of the vasa vasorum to assist with nutrient and oxygen diffusion⁹⁵. A key difference of the vasa vasorum from humans is that mice have no or few vessels in the media even with plaque growth. The murine vasa vasorum does expand during plaque formation thereby making the mouse model useful for studying vasa vasorum neovascularization⁹⁴.

The influence of vasa vasorum dysfunction on large blood vessel structure and function has been examined extensively over the past few decades due to its role in vessel wall maintenance⁹⁶. It is important to note that some researchers choose to separate physiological and pathological vasa vasorum neovascularization by terming vessels in the lesion area the vasa plaquorum⁹⁷.

1.5.2 Vasa Vasorum Neovascularization and Atherosclerosis

The connection between vasa vasorum neovascularization and the progression of atherosclerosis was examined by Barger in 1984⁹⁸. In this study, human coronary arteries were examined and it was found that the adventitial vasa vasorum extended into the media and intima layers of diseased human vessels. Later studies examined apolipoprotein-E deficient (ApoE^{-/-}) mice and

determined that there is a correlation between atherosclerotic plaque growth and vasa vasorum neovascularization^{95, 99}. Plaque size was reduced in mice after inhibition of angiogenesis and this may mean the vasa vasorum neovascularization is required to sustain plaque size⁹⁹⁻¹⁰¹.

Vasa vasorum neovascularization appears to be initiated by hypoxia and/or inflammatory cells^{56, 102}. Normally the vasa vasorum is present in arteries that have a wall thickness of 150 μm or greater¹⁰³. As atherosclerotic plaque grows, the distance between the lumen and tissue increases, forming a hypoxic environment. This stimulates HIFs to begin angiogenesis through the synthesis and release of VEGF⁵⁶. VEGF expression may also be triggered by proteases released by inflammatory cells¹⁰².

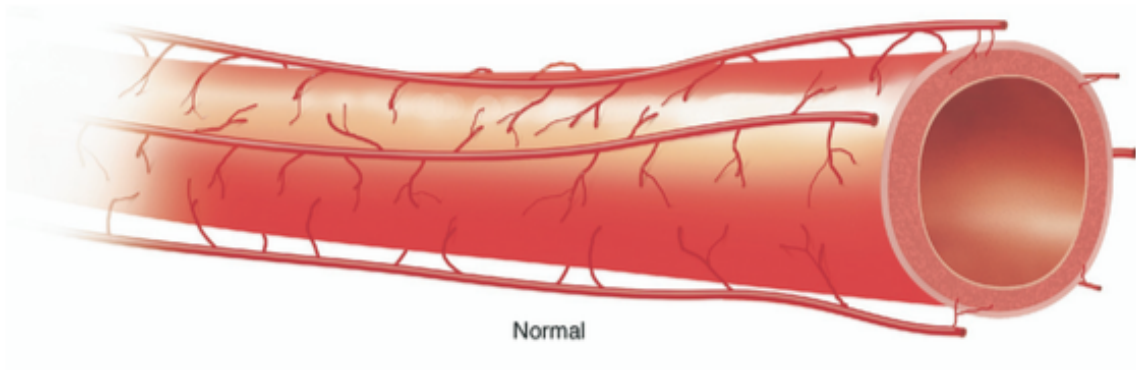
The role of vasa vasorum neovascularization as it applies to the development of atherosclerosis is still unknown. Initially, neovascularization may lead to plaque stability due to the increase in oxygen and nutrients reaching the lesion as well increased area for cholesterol efflux from the tissue^{102, 104}. Impaired angiogenesis may promote endothelial dysfunction as levels of VEGF are typically reduced and do not provide a signal for endothelial cell survival. The atherosclerotic lesions also become more hypoxic and studies have shown that macrophages colocalize to these areas^{102, 105}. This can result in increased cell death that contributes to larger necrotic cores and unstable plaques.

There appears to be a balance to the amount of angiogenesis that is beneficial as increasing hypoxia and inflammation may trigger pathological

neovascularization^{22, 102, 106}. The vasa vasorum expansion may allow for increased infiltration of monocytes, T cells and LDL molecules that are then retained in the vessel wall¹⁰⁷. Enhanced angiogenesis may also result in immature microvessels that are leaky and lead to intraplaque hemorrhage that weaken the plaque^{90, 107, 108}. Studies using non-invasive imaging such as contrast-enhanced ultrasound, nuclear imaging and magnetic resonance imaging are even looking to see if increases vasa vasorum microvessels can predict plaque vulnerability¹⁰⁹.

Figure 4- Vasa Vasorum and Atherosclerosis

The microvascular network of the vasa vasorum (top) can supply oxygen and nutrients to the walls of large muscular arteries. There is a correlation between atherosclerosis growth and vasa vasorum neovascularization (bottom) in non-diabetic models.



Normal



Atherosclerosis

Adapted from B. Doyle and N. Caplice (2007) ¹⁰⁶

1.5.3 Vasa Vasorum Neovascularization and Diabetes

In 2013, Veerman et al. demonstrated hyperglycemic ApoE^{-/-} mice had impaired neovascularization of the vasa vasorum, compared to normoglycemic controls, even though these mice had accelerated atherosclerosis⁸. Until this time, there was limited known research on the effects of DM on vasa vasorum expansion.

The mice were made hyperglycemic with streptozotocin (STZ) injections and a subgroup was given slow-release insulin pellets. At 15 weeks of age, the hyperglycemic mice had a larger lesion volume and necrotic content, but fewer vasa vasorum vessels at the aortic sinus compared to normoglycemic. The STZ mice injected with insulin had less plaque formation than the hyperglycemic mice and appeared to have more vasa vasorum density, but did not show significance. The levels of HIF1 α proteins, endoglin, VEGF-A and its receptor, VEGFR-2, were analyzed. While the hyperglycemic mice had increased staining of HIF-1 α and endoglin, there was decreased staining of VEGF-A and VEGFR2. This suggests that while the lesions are hypoxic, there is impaired angiogenesis.

Later that same year, a study was released that used contrast-enhanced ultrasound imaging to examine the vasa vasorum density in the carotid arteries of patients with T2DM with and without retinopathies¹⁰. They found that individuals with DM had an increased vasa vasorum signal than healthy controls. In addition, the individuals with T2DM with retinopathies had an increased signal compared to those who have T2DM without retinopathy. More research is

needed, however, to i) reproduce and confirm these findings, ii) examine the vasa vasorum in other arteries and iii) to improve this ultrasound method since criticisms were raised in this study about the influence of pseudo-enhancement on the findings¹¹¹.

2.0 RATIONALE, HYPOTHESIS AND RESEARCH OBJECTIVES

2.1 RATIONALE

While macrovascular and microvascular complications of DM were traditionally categorized as distinct pathological consequences of the disease, increasing research suggests that these vascular beds are more closely related^{11, 16-21}. Studies have shown that a common molecular pathway may trigger vascular abnormalities in response to conditions of chronic hyperglycemia^{10, 15, 22-24}. In addition to this mechanism, it has been hypothesized that the microvasculature may have direct effects on cardiovascular outcomes specifically through changes in vasa vasorum angiogenesis^{8, 20, 21, 110, 111}. While research has shown that increases in atherosclerosis correlate to increases in vasa vasorum neovascularization in non-diabetic models, there is limited research showing the effects of hyperglycemia on this microvascular bed. Previous research from our lab, demonstrated that chemically induced hyperglycemic mice had impaired neovascularization at the aortic sinus that correlated to increases in atherosclerosis at 15 weeks of age⁸. These mice showed increased levels of hypoxia in the atherosclerotic plaques yet decreased levels of angiogenesis that were normalized with treatment of insulin. While there appears to be impairment in hypoxia-mediated angiogenesis of the vasa vasorum, the molecular mechanism for this is still unknown. Long-term effects of hyperglycemia on the vasa vasorum have also been yet to be determined.

2.2 HYPOTHESIS

We hypothesize that hyperglycemia has disruptive effects on the vasa vasorum that contribute to the accelerated development and progression of atherosclerosis seen in DM. We believe that the macrovascular complications seen in DM are a result of microvascular dysfunction.

2.3 RESEARCH OBJECTIVES

Utilizing two mouse models of diabetes, cell culture experiments and samples of human coronary arteries, our research objectives are:

1. To assess the long-term effects of chronic hyperglycemia on neovascularization of the vasa vasorum in a chemically induced mouse model of diabetes and correlate this information to atherosclerosis progression.
2. To examine a genetically-induced diabetic mouse model, quantify the effects of hyperglycemia on the vasa vasorum density and correlate this data to the progression of atherosclerosis.
3. To investigate the molecular mechanisms by which hyperglycemia may impair angiogenesis.
4. To examine vasa vasorum density in coronary artery samples from humans with and without diabetes.

3.0 METHODOLOGY

3.1 ANIMAL MODELS

3.1.1 Animals and diets

Female ApoE^{-/-} mice (C57BL/6J genetic background) were purchased from Jackson Laboratory. Male ApoE^{+/+} Ins2^{+/*Akita*} mice were also purchased from Jackson Laboratory and bred to produce ApoE^{-/-} Ins2^{+/*Akita*} mice as previously described¹¹². All mice were maintained on a standard chow diet (2018 Teklad Global 18% protein rodent diet) purchased from Harlan Laboratories and had free access to water. All animal procedures were approved by the McMaster Animal Research Ethics Board.

3.1.2 Female STZ-injected ApoE^{-/-} mice

Female ApoE^{-/-} mice were randomized into two treatment groups at five weeks of age. Over the course of three weeks, one treatment group (n=75) was administered two rounds of low-dose STZ injections (40 mg/kg) to induce hyperglycemia. The second treatment group (n= 54) was used as a control and given two sets of citrate buffer injections over the same time period. Body weight and FBG levels were measured at 4, 8, 12, 16, 20, 25, 30, 35 and 40 weeks of age or until harvested. Mice were sacrificed at 25, 30 or 40 weeks of age (n=7-9 per group), and plasma and tissue samples were collected. The mice were

flushed with 1xPBS before perfusion fixation with 10% neutral buffered formalin.

Liver and adipose weights were also measured post-mortem.

3.1.3 Female ApoE^{-/-} Ins2^{+Akita} mice

Female ApoE^{-/-} mice and ApoE^{-/-} Ins2^{+Akita} mice were harvested at 5, 10 or 15 weeks of age (n=7-10 per group) with fasting blood glucose (FBG) and body weight being measured just prior to sacrifice. Blood was collected for plasma analysis before mice were flushed with 1xPBS and perfusion-fixed with 10% neutral buffered formalin. Various tissue samples were then collected.

3.2 PLASMA ANALYSIS

FBG levels were determined in hyperglycemic and normoglycemic mice using a glucometer (LifeScan). Fasting plasma triglyceride and total cholesterol were measured in female STZ-injected ApoE^{-/-} and ApoE^{-/-} mice at 25, 30 and 40 weeks of age using colourimetric assays (Thermo Scientific).

3.3 TISSUE COLLECTION AND PROCESSING

3.3.1 Mouse samples

The tissue collection procedure for all groups (ApoE^{-/-}, ApoE^{-/-} Ins2^{+Akita} and ApoE^{-/-} STZ-injected mice) was the same. Blood and liver samples were collected and stored in a -80°C freezer. Mesenteric adipose tissue was collected and weighed. Various other tissues were harvested and preserved at room

temperature in neutral buffered 10% formalin solution (Sigma-Aldrich) including the heart, aorta, small intestine, spleen, kidneys, muscle, lungs, eyes and brain.

To isolate the aortic sinus, the heart is cut transversely across the base of the left and right atrium and the ascending aorta is cut from the rest of the aorta before the innominate artery. This superior aspect of the heart is then processed and set in paraffin blocks for sectioning. Other organs, such as the kidneys, liver and lungs were also processed and put into paraffin blocks.

The paraffin blocks containing the aortic sinus and ascending aorta are cut transversely into thin slices (4.5 μm for mice 5 to 15 weeks of age, and 5 μm for mice 25 to 40 weeks of age) using a microtome (Leica RM2265). The heart is rotated to find the three valve leaflets to allow for more consistent orientation of the aortic sinus before serial sections are collected onto microscope slides for subsequent staining.

3.3.2 Human Samples

Left anterior descending coronary arteries from deceased diabetic and non-diabetic patients were collected from Hamilton General Hospital and sectioned in paraffin for future immunofluorescent staining. Researchers were blinded to HbA1C levels of the patients during analysis. The McMaster Research Ethics Board pre-approved the collection and analyses of these tissues.

3.4 HISTOLOGY AND IMMUNOFLUORESCENCE

Prior to any histochemical and immunofluorescent staining, all slides were processed by first heat fixing the samples. To remove the paraffin, samples were placed in xylene then rehydrated in serial concentrations of ethanol.

Immunofluorescent staining of all aortic samples was conducted using antigen unmasking solution (H-3300; Vector Laboratories) and goat serum (Vector Laboratories) to block prior to incubation with primary antibodies overnight at 4°C. Secondary antibodies for goat anti-rabbit IgG and goat anti-mouse IgG were tagged with AlexaFluor 488 or AlexaFluor 594 (Invitrogen) and nuclei were visualized with a DAPI stain (Invitrogen). To control for non-specific staining, IgG controls were used for all fluorescent staining.

3.5 AORTIC LESION ANALYSIS

To analyze atherosclerotic lesions in the aortic sinus and ascending aorta, samples were stained with Harris Hematoxylin and Eosin (H & E) stain (Sigma-Aldrich), according to manufacturer's instructions. Stained slides were analyzed under a light microscope (Olympus BX41) and images captured by an Olympus DP71 camera. The cross-sectional area of the lesion was measured at the aortic sinus every 45 µm in 5 to 15 week old mice and every 50 µm in 25 to 40 week old mice until lesions were no longer present. Measurements were conducted using ImageJ software. This data was put into a graph to see any differences in lesion size along the length of the aorta. An approximate volume was calculated by

using the area under the curve. Necrotic core content was calculated by measuring acellular area.

The atherosclerotic lesions of 25 to 40 weeks old ApoE^{-/-} and ApoE^{-/-} STZ-injected mice were also stained with Masson's Trichrome stain (Sigma-Aldrich), according to manufacturer's instructions. This allowed for some morphological qualification of the lesions as cell nuclei are stained black, collagen is stained blue and muscle and cytoplasm are stained a pinkish-red. The lesion area, volume and necrotic content can then be quantified with the same techniques used previously.

3.6 VASA VASORUM QUANTIFICATION

To visualize the vasa vasorum, samples were stained with primary antibodies for polyclonal rabbit anti-human von Willebrand Factor (vWF) (DAKO), secondary antibodies for goat anti-rabbit IgG with AlexaFluor 488 and counterstained with DAPI. A fluorescent microscope (Olympus BX41) was used and images were captured by an Olympus DP72 camera.

Quantification of vasa vasorum vessels occurred at 40 times magnification. To be considered for quantification of vasa vasorum density, vessels had to 1) have the presence of the vWF stain around the entire vessel, 2) have the presence of the DAPI stain around the vessel, 3) have a luminal opening, and 4) be less than 50 µm in diameter.

Human coronary arteries were also stained with vWF antibodies and imaged using a fluorescent microscope (Nikon Eclipse Ti). The number of vasa vasorum microvessels was analyzed using NIS element software. The criteria for inclusion of microvessels to be counted as vasa vasorum was 1) have the presence of the vWF stain around the entire vessel, 2) have a luminal opening, 3) be less than 200 μm in diameter and 4) vessels were in the intima, media or adventitial layers.

3.7 ANALYSIS OF HYPOXIA AND ANGIOGENESIS

To assess the amount of hypoxia in the lesion at the aortic sinus, samples were stained with primary antibodies for monoclonal mouse anti-mouse HIF-1 α (Novus Biologicals), secondary antibodies for goat anti-mouse IgG with AlexaFluor 488 and counterstained with DAPI. To analyze angiogenesis in lesions at the aortic sinus, samples were stained with either polyclonal rabbit anti-mouse VEGF-A (Santa Cruz Biotechnology), secondary antibodies for goat anti-rabbit IgG with AlexaFluor 594, counterstained with DAPI or monoclonal rabbit anti-rabbit VEGFR-2 (Cell Signaling), secondary antibodies for goat anti-mouse IgG with AlexaFluor 488 and counterstained with DAPI. A fluorescent microscope (Olympus BX41) was used and images were captured by an Olympus DP72 camera.

Fluorescent images of HIF-1 α , VEGF-A and VEGFR-2 were analyzed using ImageJ software. To quantify the stained area, non-specific staining was

subtracted from the picture using an IgG control slide for each type of stain, stained area was measured and normalized to total lesion area of that section.

3.8 CELL CULTURE PROCEDURES

Human THP-1 monocytes from American Type Culture Collection were cultured in RPMI 1640 media (Life Technologies) supplemented with 10% fetal bovine serum and antibiotics, and containing 11.1 mM glucose. To differentiate THP-1 monocytes into macrophages, cells were cultured for 72 hours with 100nM PMA. Human aortic smooth muscle cells (HASMCs) (Cascade Biologicals Inc.) were grown in 231 media (Life Technologies) supplemented with smooth muscle cell growth supplement and antibiotics, and containing 4.6 mM glucose. Both THP-1 macrophages and HASMCs were either treated with an additional 30 mM glucose or untreated for 20 hours at 37°C under normoxic conditions (5% carbon dioxide, 95% atmospheric air). The media was then removed and cells either treated with 30mM glucose or untreated and cultured at 37°C under hypoxic (1% oxygen, 5% carbon dioxide, 94% nitrogen) conditions using a hypoxic chamber (Coy Laboratory Products) and specialized gas tank ordered to the previous percentages, or normoxic conditions for 24 hours. Cells, proteins, RNA, DNA and media were then collected for analysis.

3.8.1 Cell Survival

To measure viability, cells were trypsinized and combined with Trypan Blue Stain (Invitrogen). The number of live and dead cells was then measured using the Countess (Invitrogen).

3.8.2 Western blot analysis

Total protein lysates (25µg) were separated using SDS-PAGE on an 8% gel and transferred to a nitrocellulose membrane. Proteins were detected with primary antibodies against HIF-1α and β-actin (Sigma-Aldrich). The blots were then incubated with a secondary antibody conjugated to horseradish-peroxidase (HRP) (Life Technologies) and proteins imaged with a chemiluminescence detection system.

3.8.3 Real-time Polymerase Chain Reaction (PCR)

Total RNA was extracted from cells using an RNeasy Mini Kit (Qiaagen) and reverse transcribed into cDNA using a High Capacity cDNA Reverse Transcription Kit (Applied Biosystems) according to manufacturer's instructions. Expression of mRNA levels was quantified by real-time PCR using Sybr green Master Mix (Invitrogen) with the ABI 7300 System and software (Applied Biosystems). Samples were run in triplicate and expression levels were normalized to a β-actin control. Primers utilized in this study are listed in Table 1.

Table 1- Primers Utilized for PCR

Both forward and reverse primers for real-time quantitative PCR of VEGF-A, VEGF-A_{165a} and VEGF-A_{165b} are listed from 5'- 3'. β -actin was used as a control.

Primer	Forward (5' - 3')	Reverse (5' - 3')
VEGF-A	CACTGCCTGGAAGATTCA	TGGTTTCAATGGTGTGAGGA
VEGF-A _{165a}	GAGCAAGACAAGAAAATCCC	CCTCGGCTTGTACATCTG
VEGF-A _{165b}	GAGCAAGACAAGAAAATCCC	GTGAGAGATCTGCAAGTACG
β -actin	ACCGAGCGCGGCTACAG	CTTAATGTGACGCACGATTTCC

3.8.4 Enzyme-linked immunosorbent assay (ELISA)

To determine the concentration of secreted VEGF-A from the cells, media was collected and stored at -80°C until analyzed with an ELISA kit (Invitrogen) according to manufacturer's instructions.

3.9 STATISTICS

Results are expressed as means \pm SEM and statistically analyzed by two-ANOVA or Student's T-Tests. A p value of less than 0.05 was determined to be statistically significant for all experiments.

4.0 RESULTS

4.1 METABOLIC CHARACTERISTICS OF FEMALE APOE^{-/-} STZ-INJECTED MICE

To determine glucose status in both the female ApoE^{-/-} and ApoE^{-/-}STZ-injected mice, FBG levels were measured starting at 4 weeks of age. The ApoE^{-/-}STZ-injected mice had significantly elevated FPG levels by 8 weeks of age and were chronically hyperglycemic throughout the remainder of the study (Figure 5A). The observed glucose levels are consistent with results obtained previously in this mouse strain used in the lab⁸.

Plasma lipid concentrations of female ApoE^{-/-} and ApoE^{-/-}STZ-injected mice were determined by measuring fasting plasma triglyceride and total cholesterol levels at 25, 30 and 40 weeks of age (Figure 5B & C). From 25 to 40 weeks of age, the triglyceride and cholesterol levels of the ApoE^{-/-} mice were similar across time points. In contrast, the triglyceride levels of the ApoE^{-/-}STZ-injected mice increased at 25 weeks of age and remained elevated. The cholesterol levels of the ApoE^{-/-}STZ-injected mice were also significantly increased compared to controls at 25 weeks of age and continued to increase with age. Previous results from our lab demonstrated that there were no significant differences in fasting plasma triglyceride or cholesterol levels until 20 weeks of age in ApoE^{-/-}STZ-injected mice compared to normoglycemic ApoE^{-/-} mice (Figure 5D & E)⁸.

Total body weights of female ApoE^{-/-} and ApoE^{-/-}STZ-injected mice were measured beginning at 4 weeks of age. From 16 weeks of age until the mice were scarified, ApoE^{-/-}STZ-injected mice had significantly less body weight than ApoE^{-/-} mice (Figure 6A). This correlated with decreased mesenteric adipose tissue and increased liver weight in the ApoE^{-/-}STZ-injected mice from 25 to 40 weeks of age (Figure 6B & C). These hyperglycemic mice likely have decreased mesenteric adipose tissue weight due to impaired glucose utilization in tissues dependent on insulin for glucose uptake causing increased reliance on fatty acid oxidation for energy production. Liver weights may be increased after 25 weeks of age in the hyperglycemic mice since these mice appear to develop fatty livers. This effect correlates with the increased plasma triglyceride and cholesterol levels seen previously.

Figure 5- Metabolic profile of ApoE^{-/-} and ApoE^{-/-}STZ-injected mice

Measurement of **A.** fasting blood glucose in normoglycemic and hyperglycemic mice from 8 to 40 weeks of age. Colorimetric measurement of fasting blood **B.** triglyceride and **C.** cholesterol in normoglycemic and hyperglycemic mice at 25, 30 and 40 weeks of age. Measurement of fasting blood **D.** triglyceride and **E.** cholesterol in control and hyperglycemic mice from 5 to 40 weeks of age (Veerman et al., 2013)⁸. n= 5-8 mice per group; mean ± SEM. *p<0.05, **p<0.01, ***p<0.001 relative to age-matched ApoE^{-/-} controls.

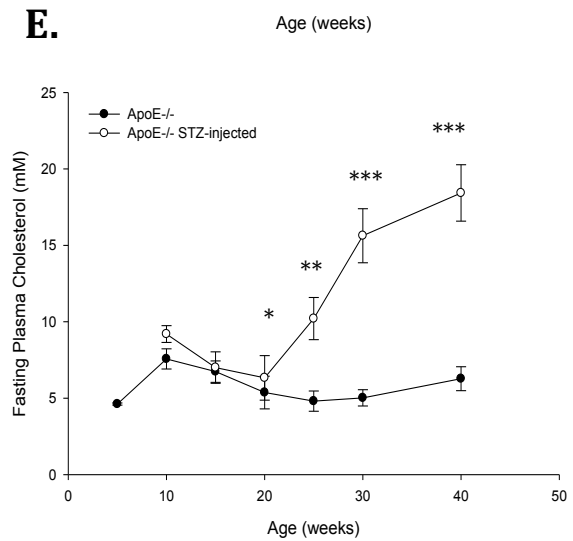
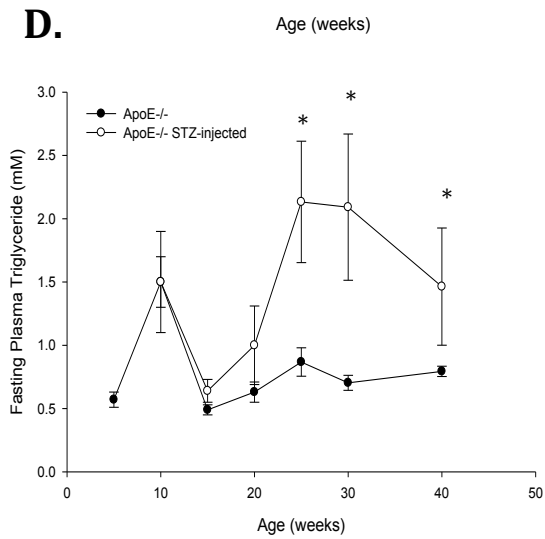
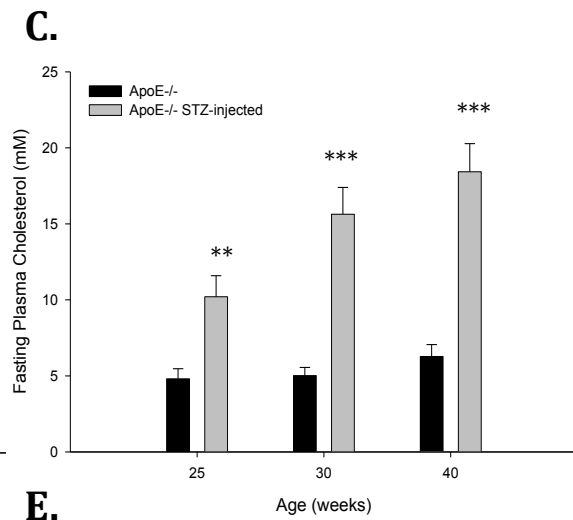
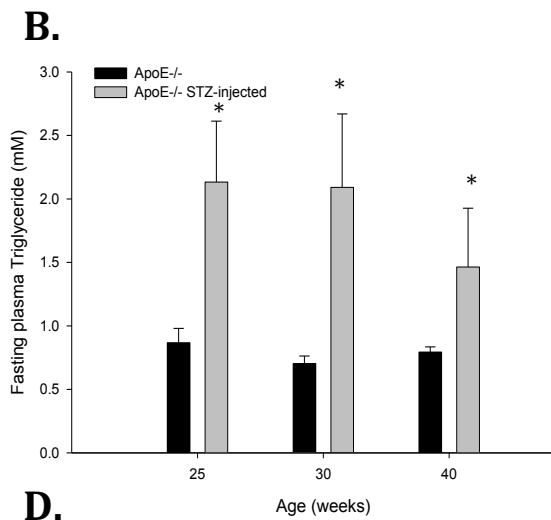
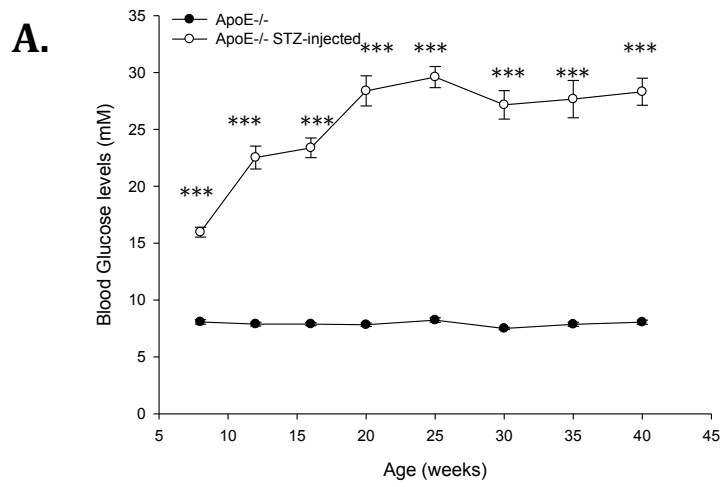
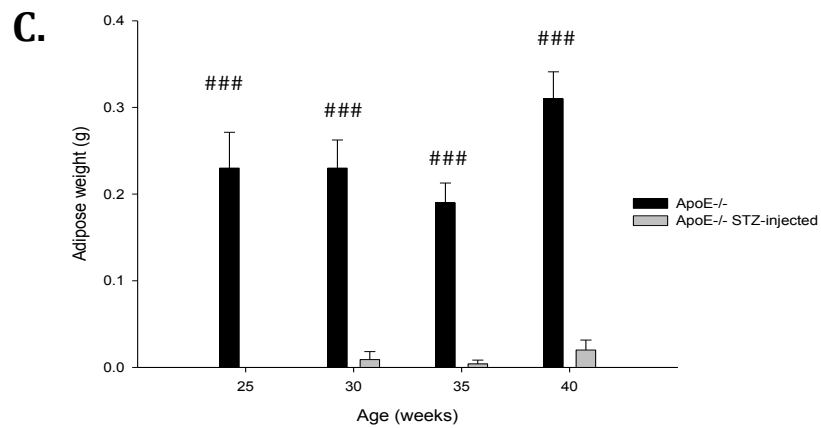
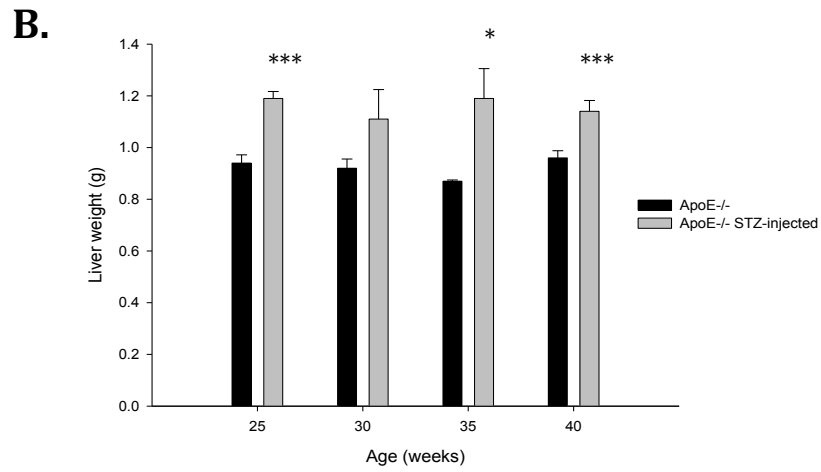
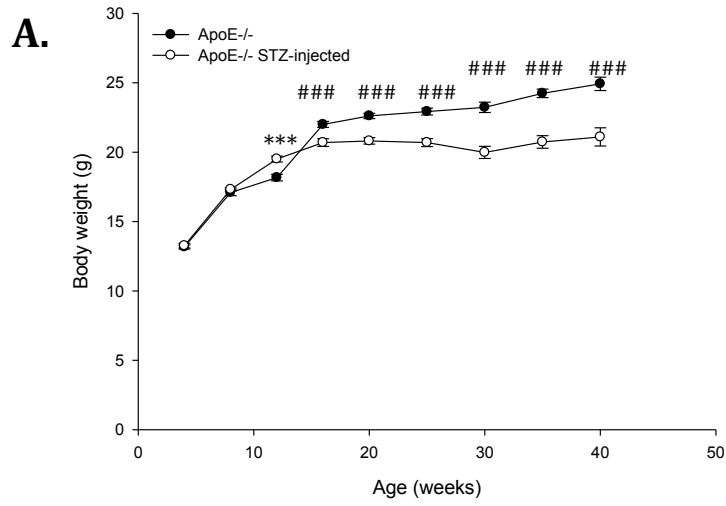


Figure 6- Tissue weights of ApoE^{-/-} and ApoE^{-/-} STZ-injected mice

Measurement of **A.** body weight in control and hyperglycemic mice from 4 to 40 weeks of age. n= 54-75 mice per group; mean ± SEM. Tissue weights of **B.** mesenteric adipose tissue and **C.** liver in normoglycemic and hyperglycemic ApoE^{-/-} mice at 25, 30, 35 and 40 weeks of age. n= 7-9 mice per group; mean ± SEM. *p<0.05, ***p<0.001 relative to age-matched ApoE^{-/-} controls; ###p<0.001 relative to age-matched ApoE^{-/-} STZ-injected.



4.2 ATHEROSCLEROTIC PLAQUE SIZES INCREASE IN FEMALE APOE^{-/-} STZ-INJECTED MICE FROM 25 TO 40 WEEKS OF AGE

Previously published results from our lab to showed that hyperglycemic mice have significantly larger atherosclerotic plaque volumes at 15 weeks of age, relative to normoglycemic controls (Figure 7A)⁸. To investigate the longer term effects of hyperglycemia, female ApoE^{-/-} and ApoE^{-/-} STZ-injected mice were sacrificed at 25, 30 and 40 weeks of age and analyzed for lesion cross-sectional area, volume and necrotic core content. At these ages, there were no significant differences in the cross-sectional area, volume or necrotic core content between normoglycemic and hyperglycemic mice at any time point (Figure 8A). The cross-sectional area of the lesions appeared to increase in each group with increases in age (Figure 8B). There was a trend towards increased total volume of atherosclerotic plaque in the 30 week old ApoE^{-/-} and ApoE^{-/-} STZ-injected mice compared to their 25 week old counterparts, but no statistically significant differences were seen (Figure 8C). ApoE^{-/-} and ApoE^{-/-} STZ-injected mice at 40 weeks of age had significantly more plaque volume than both 25 week and 30 week old normoglycemic and hyperglycemic mice. A two-way ANOVA analysis of differences with age between ApoE^{-/-} and ApoE^{-/-} STZ-injected mice also demonstrated significantly more plaque size with increases in age ($p < 0.0001$), but no significant differences in genotype ($p = 0.31$) or interaction ($p = 0.64$).

The atherosclerotic necrotic core sizes also appeared to increase in each group with increases in age. There was a trend towards increased necrotic core

volume in the 30 week old ApoE^{-/-} and ApoE^{-/-} STZ-injected mice compared to their 25 week old counterparts, but these differences were not statistically significant (Figure 8D). There also appeared to be increased necrotic core volumes in the 40 week old ApoE^{-/-} and ApoE^{-/-} STZ-injected mice compared to the 30 week old mice, but this was not statistically significant. The 40 week old ApoE^{-/-} and ApoE^{-/-} STZ-injected mice had significantly more plaque volume than the 25 week old normoglycemic and hyperglycemic mice. To analysis differences between ApoE^{-/-} and ApoE^{-/-} STZ-injected mice with age, a two-way ANOVA was conducted. The results showed that there was significantly more necrotic core volume with increases in age ($p < 0.0005$), but no significant differences between genotypes ($p = 0.11$) or interaction ($p = 0.60$).

Data about atherosclerotic volume was then combined with previous published results from our lab to demonstrate increases in atherosclerotic plaque volume from 5 to 40 weeks of age in female ApoE^{-/-} and ApoE^{-/-} STZ-injected mice (Figure 7B).

Figure 7- Atherosclerotic lesion volumes in female ApoE^{-/-} and ApoE^{-/-} STZ-injected mice from 5 to 40 weeks of age

Quantification of atherosclerotic lesion volume in **A.** 5 to 20 week old (Veerman et al., 2013)⁸ and **B.** 5 to 40 week old normoglycemic and hyperglycemic mice (Veerman et al., 2013)⁸. n= 7-9 mice per group; mean ± SEM. **p<0.01 relative to age-matched ApoE^{-/-} controls

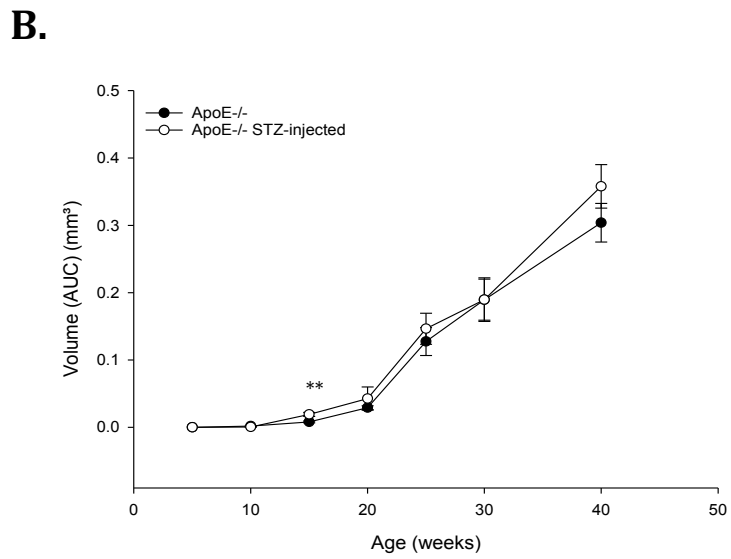
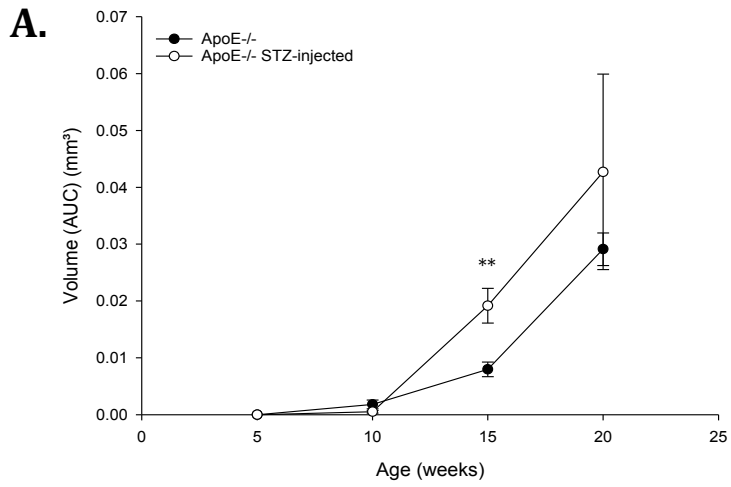
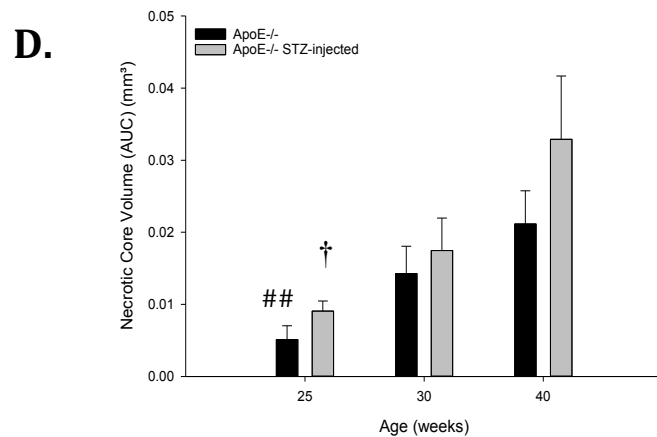
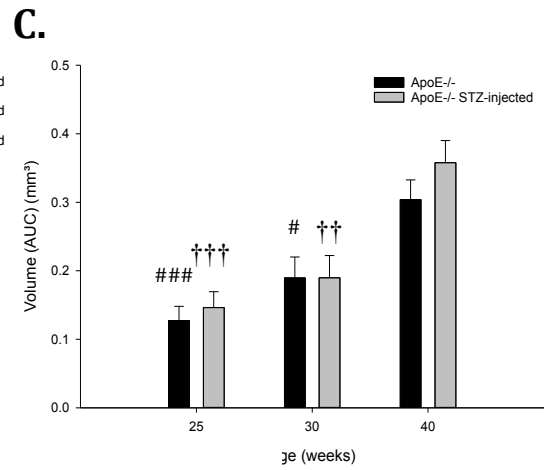
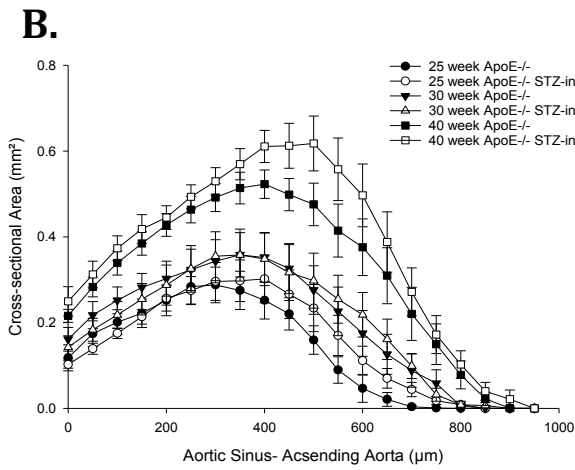
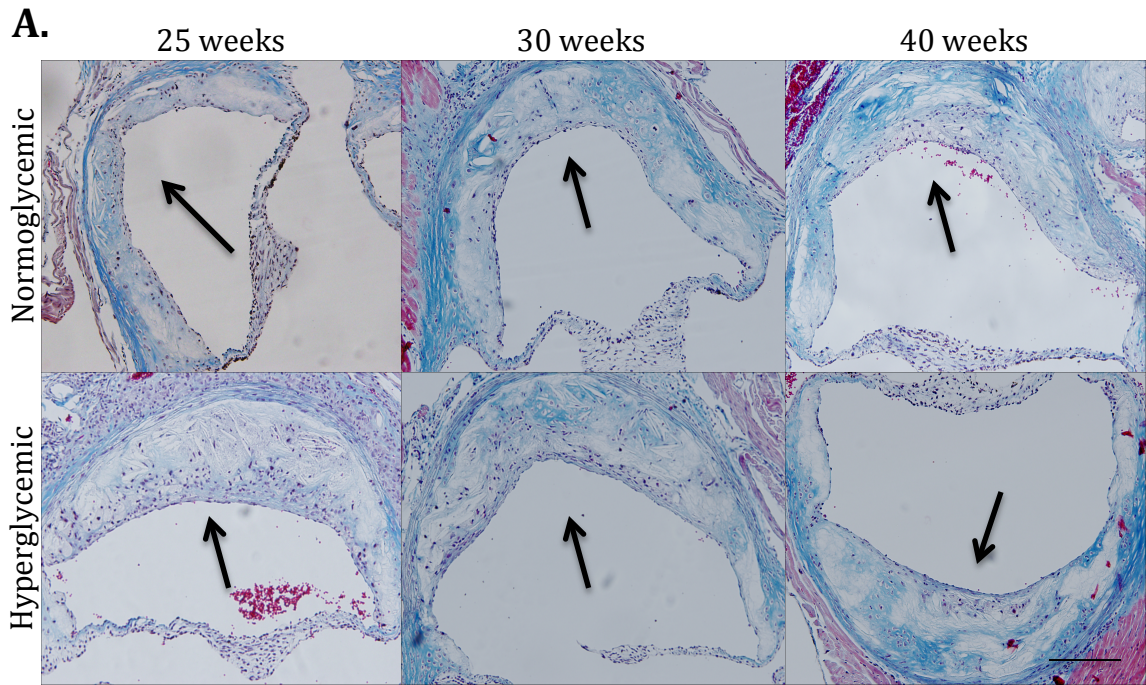


Figure 8- Atherosclerotic lesions in female ApoE^{-/-} and ApoE^{-/-} STZ-injected mice

A. Cross-sections of aortic root from normoglycemic (top) and hyperglycemic (bottom) mice were stained with Masson's trichrome. Atherosclerotic lesions are indicated by arrows. Quantification of **B.** cross-sectional area, **C.** total volume of atherosclerotic lesions, and **D.** necrotic core volume in 25, 30 and 40 week old female ApoE^{-/-} and ApoE^{-/-} STZ-injected mice. n= 7-9 mice per group; mean ± SEM. #p<0.05, p<0.01, ###p<0.001 relative to 40 week old ApoE^{-/-} controls; †<0.05, ††p<0.01, †††p<0.001 relative to 40 week old ApoE^{-/-} STZ-injected mice. Scale= 200µm



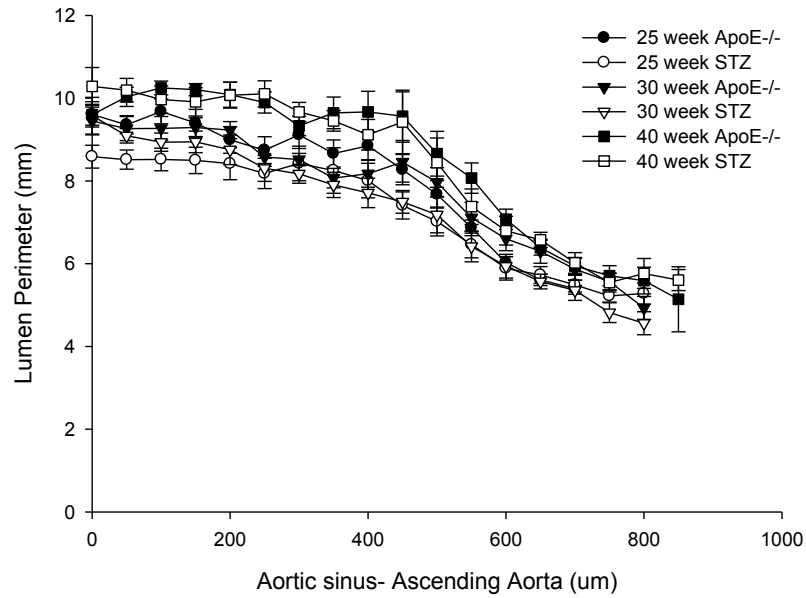
4.3 THE AORTIC LUMINAL AREA DOES NOT CHANGE WITH INCREASES IN ATHEROSCLEROSIS

Since the plaque volumes continued to increase with age in both normoglycemic and hyperglycemic mice, we wanted to examine if the plaques were growing into the lumen or into the arterial wall. We examined this effect by measuring lumen perimeter and area in 25, 30 and 40 week old mice (Figure 9 A &B). The lumen perimeter and area were similar between ApoE^{-/-} and ApoE^{-/-} STZ-injected mice as well as across time points suggesting that the lesions do not intrude into the lumen, but instead the aorta may expand to maintain the lumen area. This explains how the aorta can remain function despite continued plaque growth.

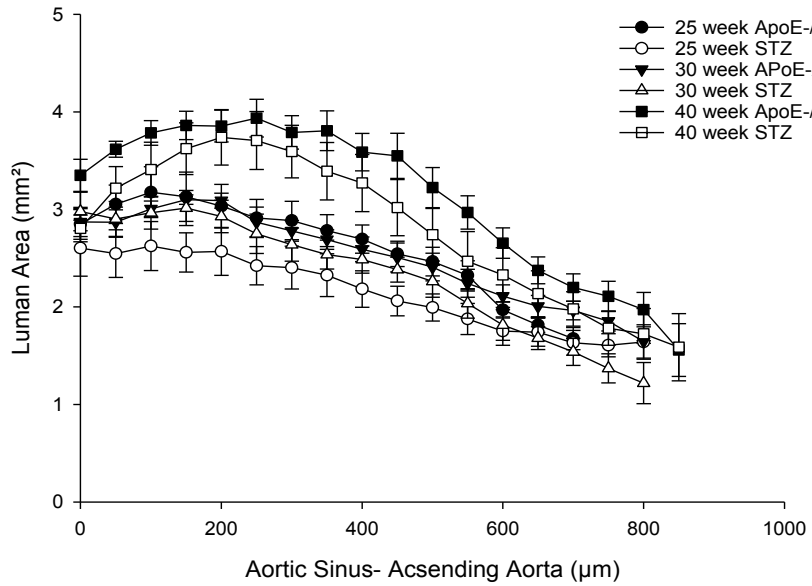
Figure 9- Lumen dimensions at the aortic sinus in female ApoE^{-/-} and ApoE^{-/-} STZ-injected mice

Quantification of A. lumen perimeter and B. lumen cross-sectional area. n= 7-9 mice per group; mean \pm SEM.

A.



B.



4.4 FEMALE APOE^{-/-} STZ-INJECTED MICE HAVE IMPAIRED ANGIOGENESIS FOLLOWED BY ENHANCED NEOVASCULARIZATION

Data previously collected from our lab from female ApoE^{-/-} and ApoE^{-/-} STZ-injected mice at 5, 10, 15 and 20 weeks of age showed impaired vasa vasorum density in the hyperglycemic mice⁸. To determine the effects in older mice, the vasa vasorum was stained using an antibody against vWF in 25, 30 and 40 week old female ApoE^{-/-} and ApoE^{-/-} STZ-injected mice (Figure 10A). At 25 and 30 weeks of age, the ApoE^{-/-} STZ-injected mice had significantly fewer vasa vasorum microvessels than the ApoE^{-/-} mice controls at the aortic sinus (Figure 10B). At 40 weeks of age, however, the ApoE^{-/-} STZ-injected mice had significantly more vessels at the aortic sinus. At the proximal and distal ascending aorta, there were no differences in vasa vasorum density at 25 and 30 weeks of age (Figure 10C & D). At the proximal ascending aorta there were more microvessels in the 40 week old ApoE^{-/-} STZ-injected mice, but no differences at the distal ascending aorta. The combined results from 5 to 40 weeks of age show the initial deficiency in vasa vasorum density starting at 10 weeks of age in ApoE^{-/-} STZ-injected mice, before having increased vessel neovascularization at 40 weeks of age (Figure 11A)⁸. The female ApoE^{-/-} mice showed a plateau in the amount of neovascularization after 20 weeks of age, while the female ApoE^{-/-} STZ-injected mice continued to show microvessel expansion throughout each time point. The trend towards decreased

angiogenesis followed by enhanced neovascularization appears analogous observed effects on the microvasculature in diabetic retinopathy.

Figure 10- Vasa vasorum density in female ApoE^{-/-} and ApoE^{-/-} STZ-injected mice

Immunofluorescent stain, using an antibody against vWF, of aortic adventitia in normoglycemic (top) and hyperglycemic (bottom) mice at 25, 30 and 40 weeks of age. Microvessels are indicated by arrows. Quantification of vasa vasorum density at the **B.** aortic sinus, **C.** proximal ascending aorta and **D.** distal ascending aorta in female ApoE^{-/-} and ApoE^{-/-} STZ-injected mice. n= 7-9 mice per group; mean ± SEM. *p<0.05, **p<0.01. Scale= 100µm

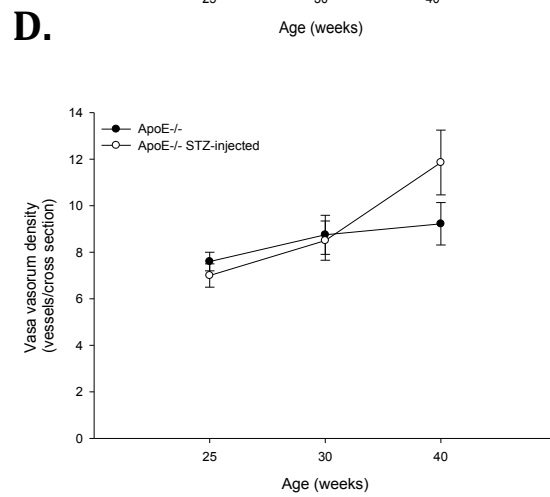
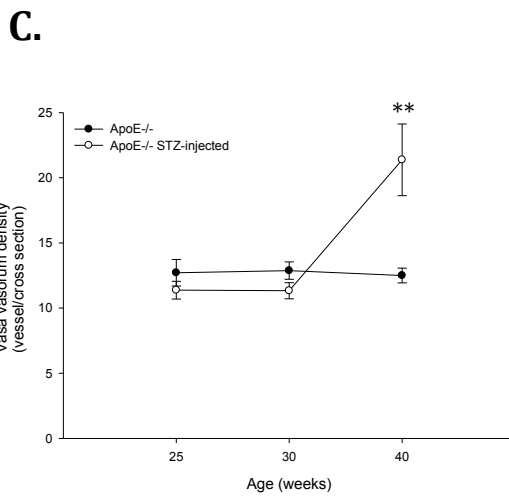
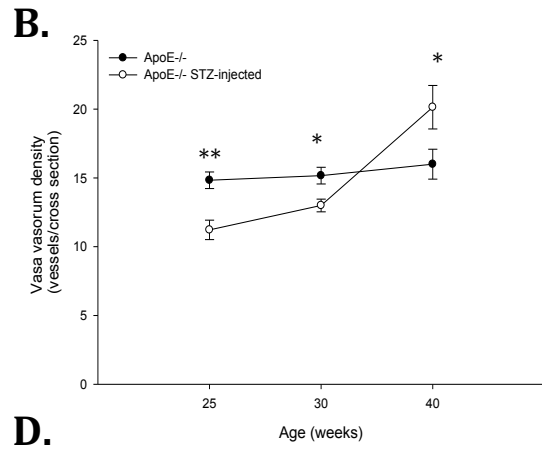
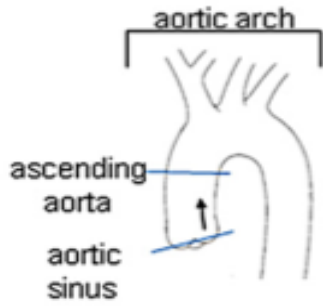
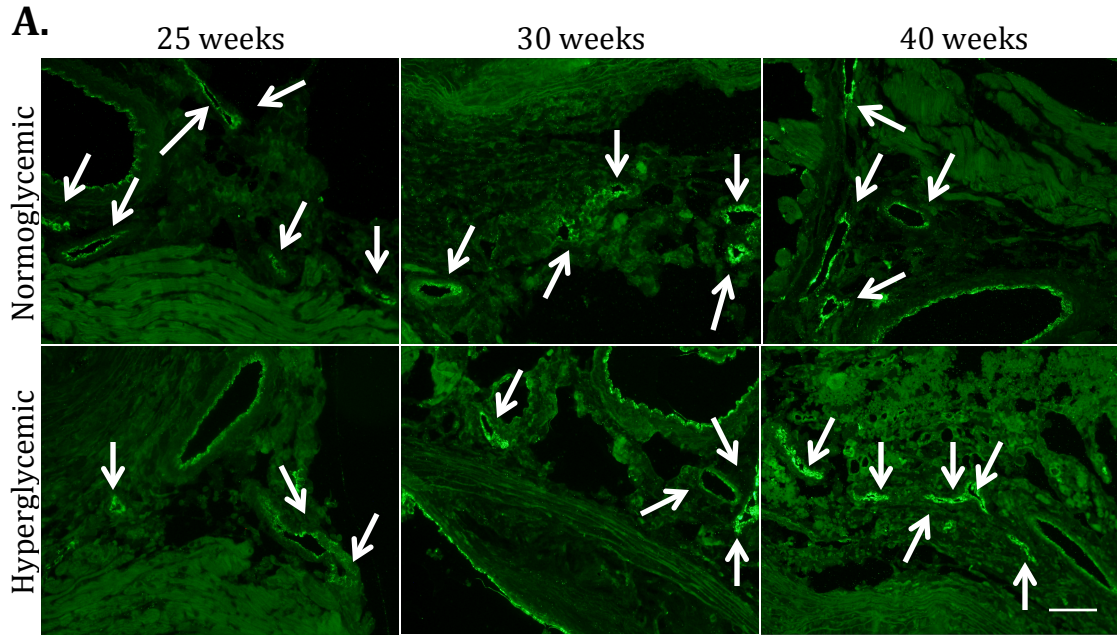
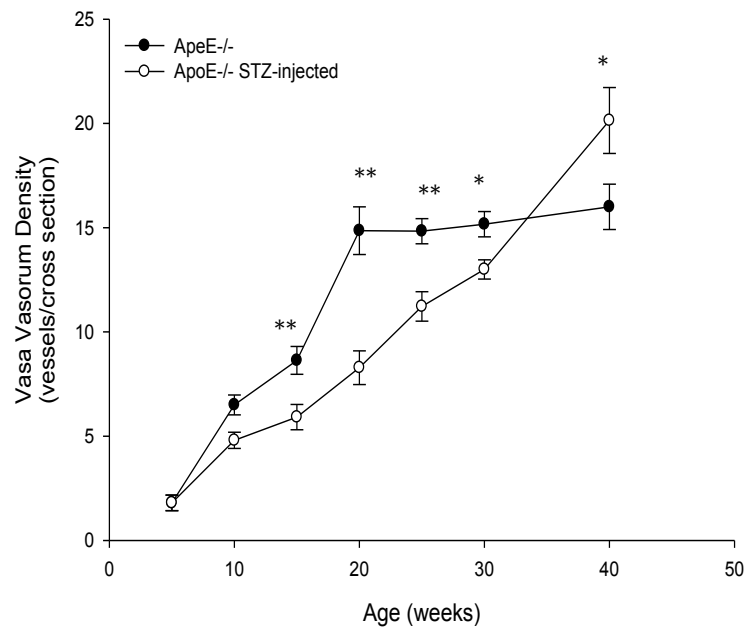


Figure 11- Vasa vasorum density at the aortic sinus

Quantification of vasa vasorum density in 5 to 40 week old normoglycemic and hyperglycemic mice (Veerman et al., 2013)⁸. n= 7-9 mice per group; mean ± SEM. *p<0.05, **p<0.01



4.5 METABOLIC CHARACTERISTICS OF FEMALE APOE^{-/-} INS2^{+/AKITA} MICE

FBG levels were measured in female ApoE^{-/-} and ApoE^{-/-} Ins2^{+/Akita} mice at 5, 10 and 15 weeks of age. Glucose concentrations were significantly higher in ApoE^{-/-} Ins2^{+/Akita} mice at 5 and 10 weeks of age compared to age-matched ApoE^{-/-} mice (Table 2). At 15 weeks of age, however, there was no significant difference in the FBG levels (p= 0.063). The normalization of glucose levels in female ApoE^{-/-} Ins2^{+/Akita} mice is consistent with previous results from our lab¹¹². Previous research from our lab has also shown that female ApoE^{-/-} Ins2^{+/Akita} mice have similar cholesterol and triglyceride levels to ApoE^{-/-} mice from 5 to 15 weeks of age¹¹².

Table 2- Metabolic characteristics of female ApoE^{-/-} Ins2^{+Akita} mice

Fasting plasma glucose levels and body weights of female ApoE^{-/-} and ApoE^{-/-} Ins2^{+Akita} mice from 5 to 10 weeks of age. n= 7-10 mice per group; mean ± SEM.

**p<0.01 relative to age-matched ApoE^{-/-} controls

	5 weeks		10 weeks		15 weeks	
	ApoE ^{-/-}	ApoE ^{-/-} Ins2 ^{+/Akita}	ApoE ^{-/-}	ApoE ^{-/-} Ins2 ^{+/Akita}	ApoE ^{-/-}	ApoE ^{-/-} Ins2 ^{+/Akita}
Glucose (mM)	8.26 ±0.33	17.43 ±1.86 **	8.53 ±0.30	13.51 ±1.35 **	8.46 ±0.84	10.65 ±0.49
Body weight (g)	14.56 ±0.74	13.67 ±0.87	18.16 ±0.18	18.93 ±0.47	22.76 ±0.73	21.45 ±0.26
n	7	9	10	9	7	7

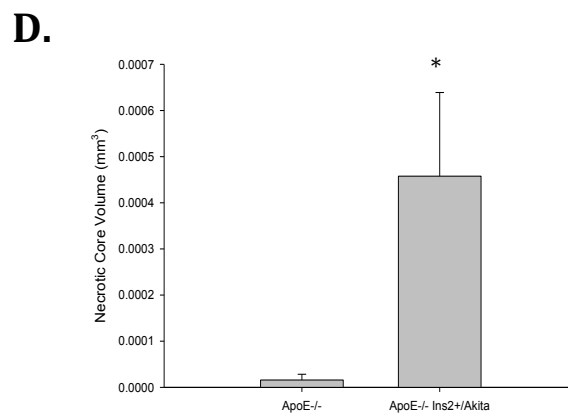
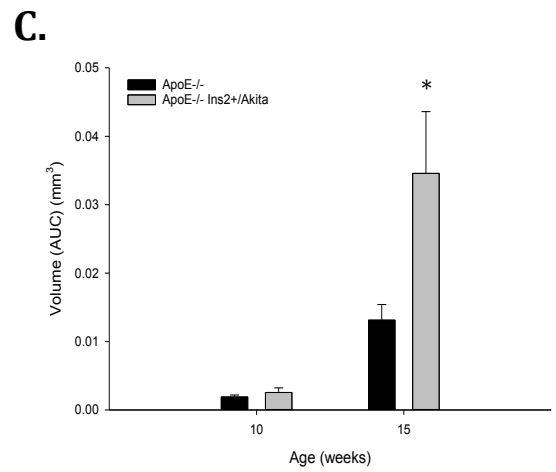
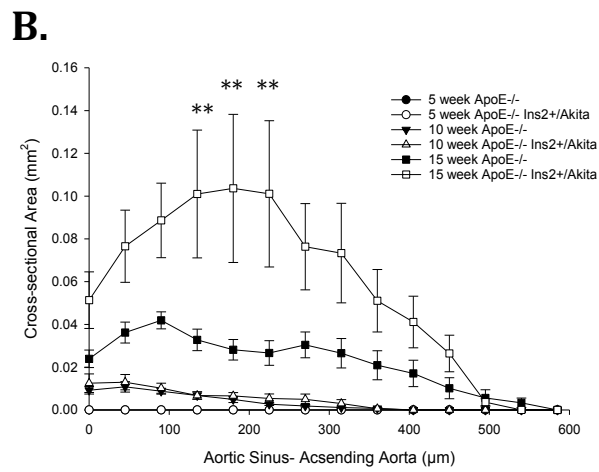
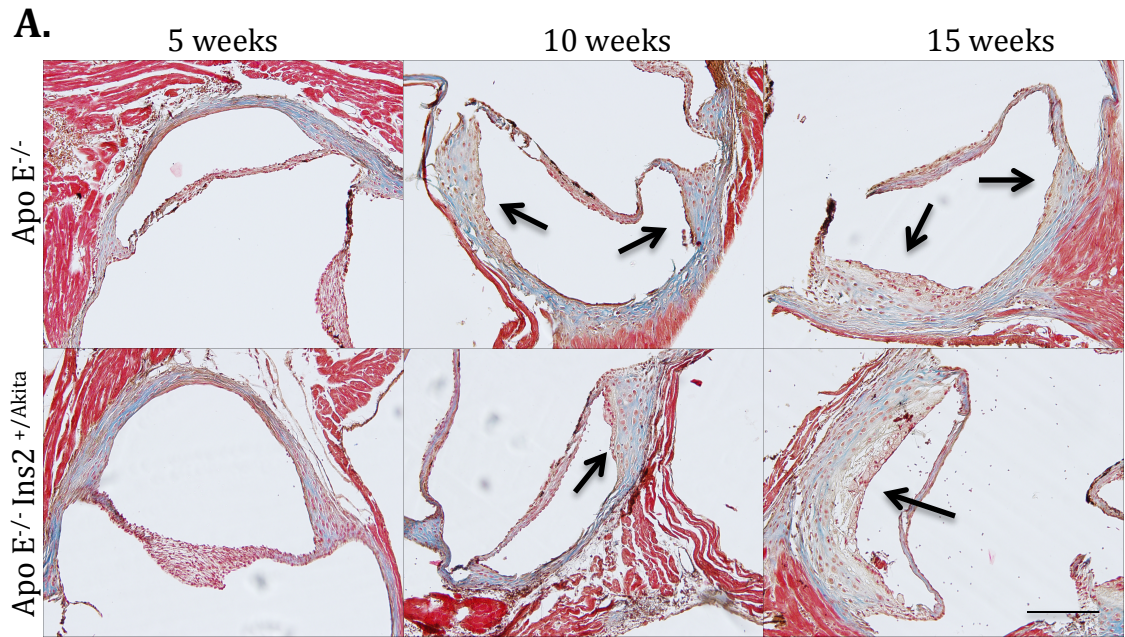
4.6 FEMALE APOE^{-/-} INS2^{+AKITA} MICE HAVE LARGER LESIONS AT 15 WEEKS OF AGE

Female ApoE^{-/-} Ins2^{+Akita} and ApoE^{-/-} mice were harvested at 5, 10 and 15 weeks of age and analyzed for lesion area and volume. At 5 weeks of age, there were no visible atherosclerotic lesions in any mice. Both ApoE^{-/-} Ins2^{+Akita} and ApoE^{-/-} mice had detectable atherosclerosis by 10 weeks of age and had significantly larger plaque sizes at 15 weeks of age (Figure 12A).

While the female ApoE^{-/-} Ins2^{+Akita} and ApoE^{-/-} mice have similar lesion sizes and volumes at 10 weeks of age, there was a significant difference in size between these groups at 15 weeks of age. The 15 week old female ApoE^{-/-} Ins2^{+Akita} mice have significantly more atherosclerotic plaque at the aortic sinus (Figure 12B), increased total lesion volume (Figure 12C) and more necrotic content (Figure 12D) when compared to controls. This data is consistent with findings from female ApoE^{-/-} and ApoE^{-/-} STZ-injected mice also done in our lab⁸.

Figure 12- Atherosclerotic lesions in female ApoE^{-/-} and ApoE^{-/-} Ins2^{+Akita} mice

Hyperglycemia is associated with accelerated atherosclerosis at the aortic sinus in 15 week old ApoE^{-/-} Ins2^{+Akita} mice. **A.** Cross-sections of the aortic root in normoglycemic (top) and hyperglycemic (bottom) mice were stained with H&E. Atherosclerotic lesions are indicated by arrows. Quantification of **B.** cross-sectional area from the aortic sinus to ascending aorta, **C.** total volume of atherosclerotic lesions and **D.** total necrotic core content in 5, 10 and 15 week old female ApoE^{-/-} and ApoE^{-/-} Ins2^{+Akita} mice. n= 7-10 mice per group; mean ± SEM. *p<0.05, **p<0.01 relative to age-matched ApoE^{-/-} controls. Scale= 200µm



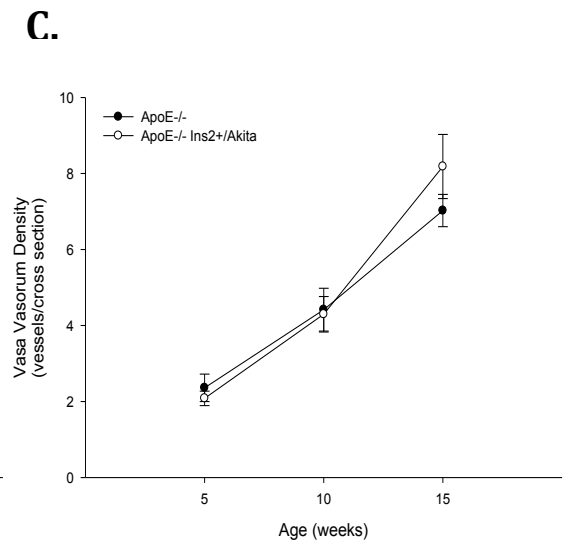
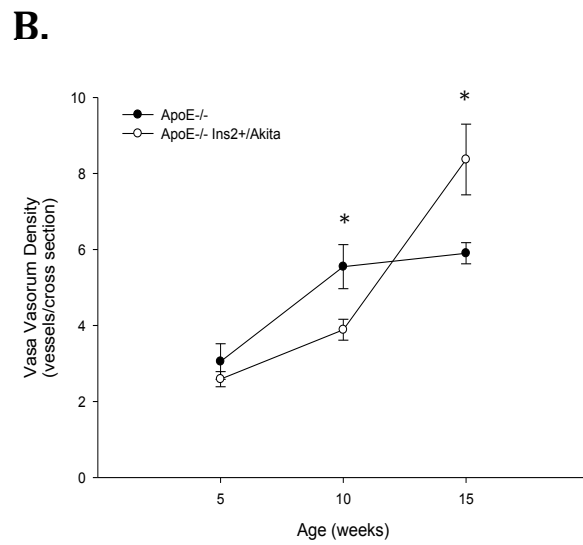
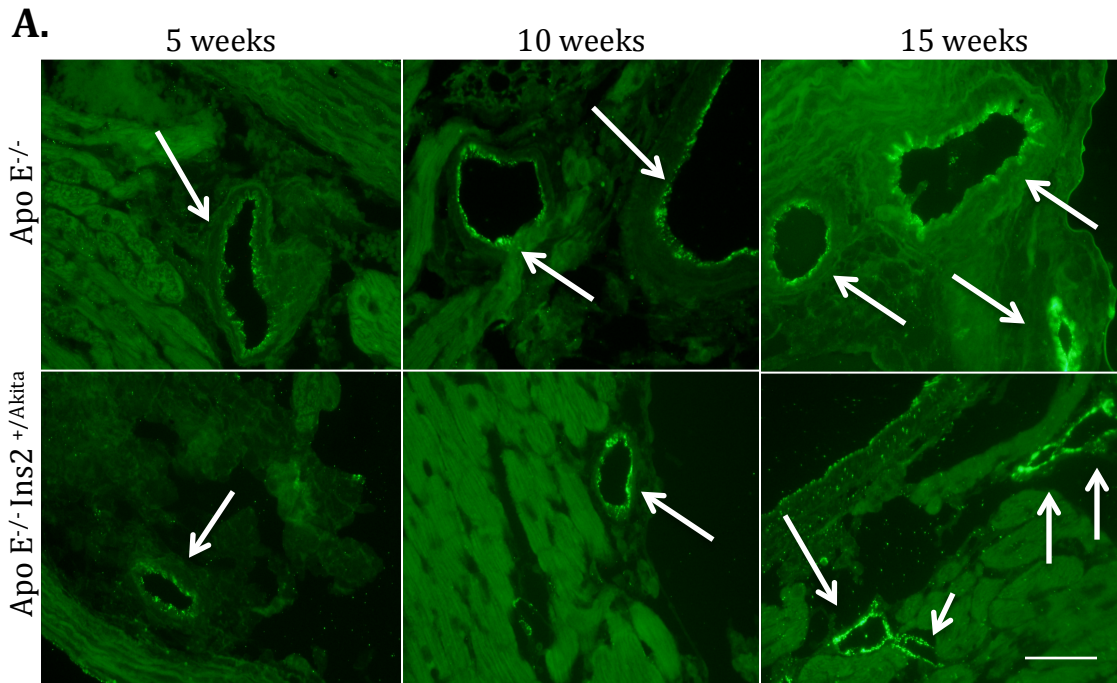
4.7 FEMALE APOE^{-/-} INS2^{+/AKITA} MICE HAVE IMPAIRED NEOVASCULARIZATION AT 10 WEEKS OF AGE AND ENHANCED NEOVASCULARIZATION AT 15 WEEKS OF AGE AT THE AORTIC SINUS

The vasa vasorum was imaged and quantified in 5, 10 and 15 week old female ApoE^{-/-} Ins2^{+/Akita} and ApoE^{-/-} mice (Figure 13A). Results showed that the number of vessels is similar at 5 weeks of age at both the aortic sinus and ascending aorta. At 10 weeks of age, however, the female ApoE^{-/-} Ins2^{+/Akita} mice have significantly fewer vasa vasorum vessels at the aortic sinus (Figure 13B). Interestingly, the number of vessels at the ascending aorta is similar between the ApoE^{-/-} Ins2^{+/Akita} and ApoE^{-/-} mice (Figure 13C).

The 15 week old female ApoE^{-/-} Ins2^{+/Akita} mice have a greater number of vasa vasorum vessels at the aortic sinus than 15 week old ApoE^{-/-} mice. Similarly to the 10 week old ApoE^{-/-} Ins2^{+/Akita} and ApoE^{-/-} mice, there were no observable differences at the ascending aorta. It is possible that the enhanced neovascularization observed in 15 week old female ApoE^{-/-} Ins2^{+/Akita} mice represents a proliferative response to hyperglycemia or is a result of the normalization of blood glucose levels.

Figure 13- Vasa vasorum neovascularization in female ApoE^{-/-} and ApoE^{-/-} Ins2^{+/-Akita} mice

Hyperglycemia is associated with aberrant angiogenesis at the aortic sinus. **A.** Immunofluorescent stain, using an antibody against vWF, of aortic adventitia in normoglycemic (top) and hyperglycemic (bottom) mice at 5, 10 and 15 weeks of age. There are fewer vasa vasorum vessels in hyperglycemic mice at 10 weeks of age, but significantly more microvessels at 15 weeks of age. Microvessels are indicated by arrows. Quantification of vasa vasorum density at the **B.** aortic sinus and **C.** ascending aorta in female ApoE^{-/-} and ApoE^{-/-} Ins2^{+/-Akita} mice. n= 7-10 mice per group; mean ± SEM. *p<0.05. Scale= 100µm



4.8 FEMALE APOE^{-/-} INS2^{+AKITA} MICE HAVE INCREASED HYPOXIA AND INSUFFICIENT ANGIOGENESIS

4.8.1 Increased Hypoxia

Cross-sections of aorta from ApoE^{-/-} Ins2^{+Akita} and ApoE^{-/-} mice at 10 and 15 weeks of age were stained with an antibody for HIF-1 α to determine levels of hypoxia at the aortic root (Figure 14A). At 10 and 15 weeks of age, the ApoE^{-/-} Ins2^{+Akita} mice showed increased levels of HIF-1 α suggesting there may be increased levels of hypoxia at the aortic sinus even when HIF-1 α levels were normalized to lesion area (Figure 14B).

4.8.2 Insufficient Angiogenesis

Cross-sections of aortic sinus from ApoE^{-/-} Ins2^{+Akita} and ApoE^{-/-} mice at 10 and 15 weeks of age were also stained with an antibody for VEGF-A (Figure 15A). Levels of VEGF-A were used as a marker of angiogenic potential in the tissue. Results showed decreased levels of VEGF-A in the atherosclerotic plaques of 10 week old ApoE^{-/-} Ins2^{+Akita} mice compared to controls (Figure 15B) despite the observed increase in HIF-1 α levels. This decrease in a marker of angiogenesis corresponds to the decrease vasa vasorum density seen at this time point. While 15 week old ApoE^{-/-} Ins2^{+Akita} mice had a trend towards higher VEGF-A levels, there were no significant differences seen between groups. This finding is interesting since 15 week old ApoE^{-/-} Ins2^{+Akita} have elevated levels of

HIF-1 α and increased vasa vasorum density and may be expected to have significantly higher levels of VEGF-A. These results may indicate that the new microvessels in the ApoE^{-/-} Ins2^{+Akita} mice are dysfunctional and/or that there is not a sufficient number of vessels present. The number of vessels in the ApoE^{-/-} Ins2^{+Akita} and ApoE^{-/-} mice were compared to lesion cross-sectional area. There were significantly fewer vasa vasorum microvessels per plaque lesion area in the 15 week old ApoE^{-/-} Ins2^{+Akita} mice suggesting that there was an insufficient quantity of microvessels being formed (Figure 16).

To examine if impaired angiogenesis may be a consequence of VEGF resistance, sections from ApoE^{-/-} Ins2^{+Akita} and ApoE^{-/-} mice at 10 and 15 weeks of age were stained at the aortic sinus with an antibody for VEGFR-2 (Figure 17A). At 10 and 15 weeks of age, there were no significant differences in VEGFR-2 expression normalized to lesion area between ApoE^{-/-} Ins2^{+Akita} mice and ApoE^{-/-} mice (Figure 17B). This suggests that “VEGF resistance” may not be a factor in the aortic sinus of ApoE^{-/-} Ins2^{+Akita} mice. It is also possible that “VEGF resistance” is not detectable using this particular technique.

Figure 14- HIF-1 α levels in female ApoE^{-/-} and ApoE^{-/-} Ins2^{+Akita} mice

Hyperglycemia is associated with increased HIF-1 α levels at the aortic sinus. **A.** Immunofluorescent stain with an antibody against HIF-1 α (green) and counterstained with DAPI (blue) in normoglycemic (left) and hyperglycemic (middle) mice at 10 and 15 weeks of age. HIF-1 α staining is indicated by arrows. A control (pre-immune) IgG stain (right) is also shown. **B.** Quantification of HIF-1 α fluorescence in atherosclerotic lesions at 10 and 15 weeks of age. n= 5 mice per group; mean \pm SEM. *p<0.05 relative to ApoE^{-/-} controls. Scale= 100 μ m

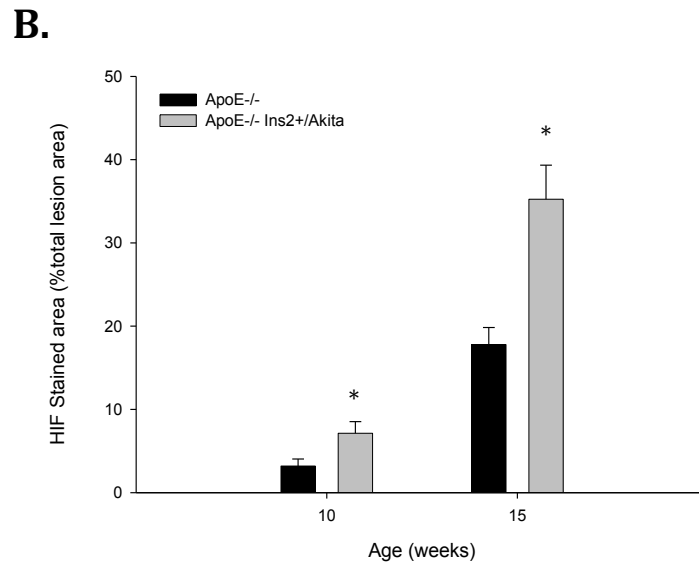
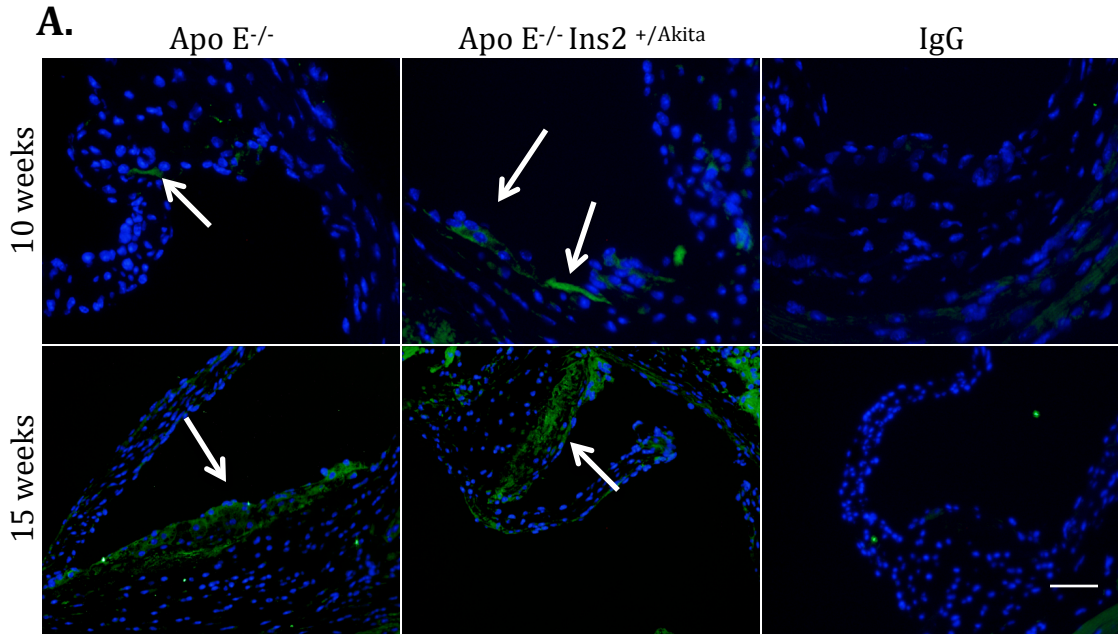
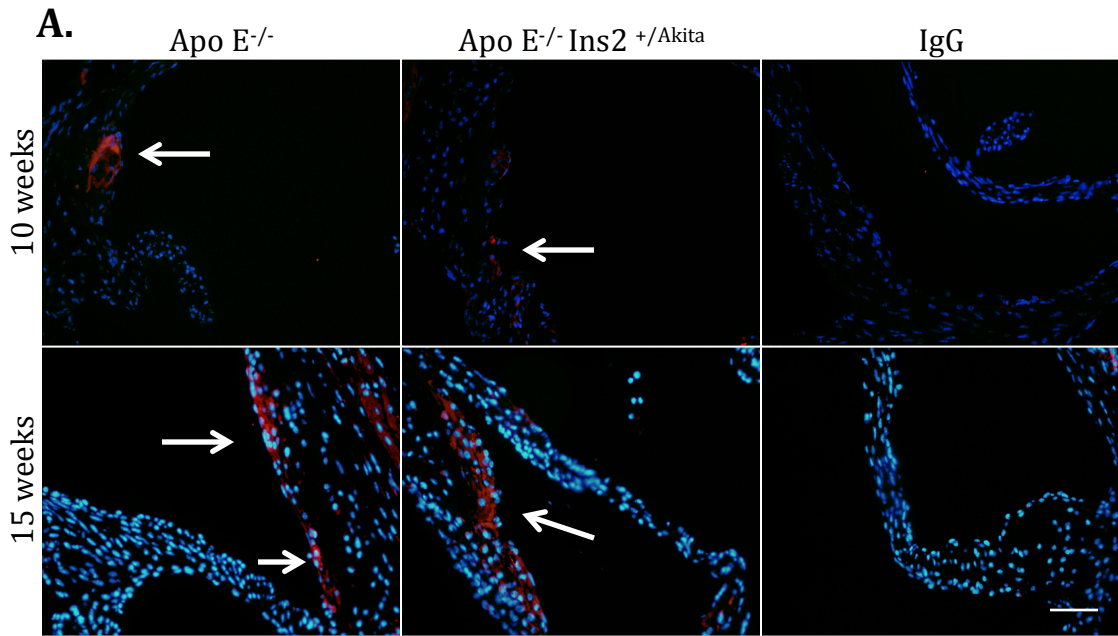


Figure 15- Angiogenesis in female ApoE^{-/-} and ApoE^{-/-} Ins2^{+Akita} mice

Hyperglycemia is associated with insufficient angiogenesis at the aortic sinus. **A.** Immunofluorescent stain with an antibody against VEGF-A (red) and counterstained with DAPI (blue) in normoglycemic (left) and hyperglycemic (middle) mice at 10 and 15 weeks of age. A control (pre-immune) IgG stain (right) is also shown. VEGF-A staining is indicated by arrows. **B.** Quantification of VEGF-A fluorescence in atherosclerotic lesions at 10 and 15 weeks of age. n= 4-5 mice per group; mean \pm SEM. *p<0.05 relative to ApoE^{-/-} controls. Scale= 100 μ m



B.

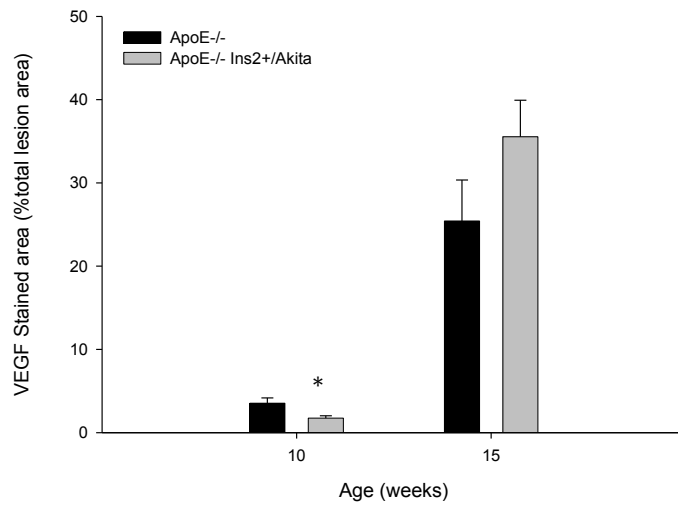


Figure 16- Number of vasa vasorum per plaque area in 15 week old female ApoE^{-/-} and ApoE^{-/-} Ins2^{+Akita} mice

Quantification of number of vasa vasorum microvessels per atherosclerotic lesion area at 15 weeks of age. n= 7 mice per group; mean ± SEM. *p<0.05 relative to ApoE^{-/-} controls.

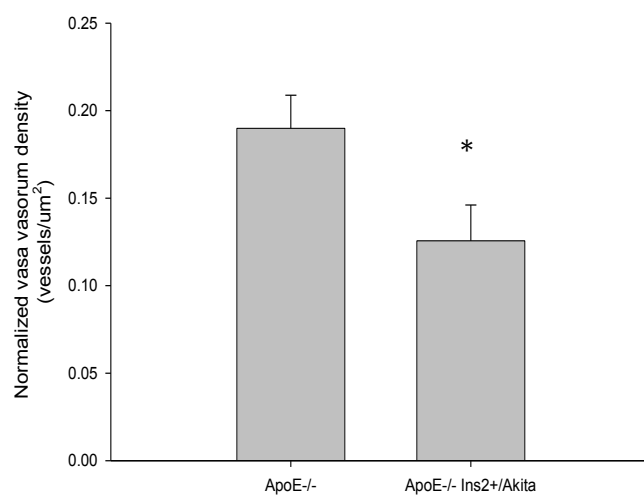
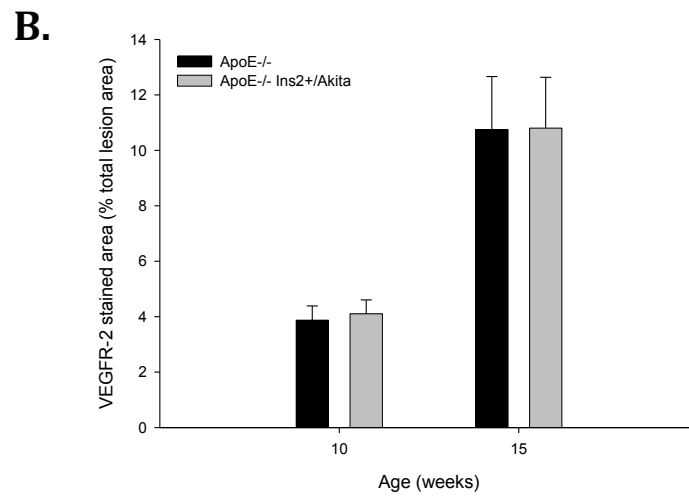
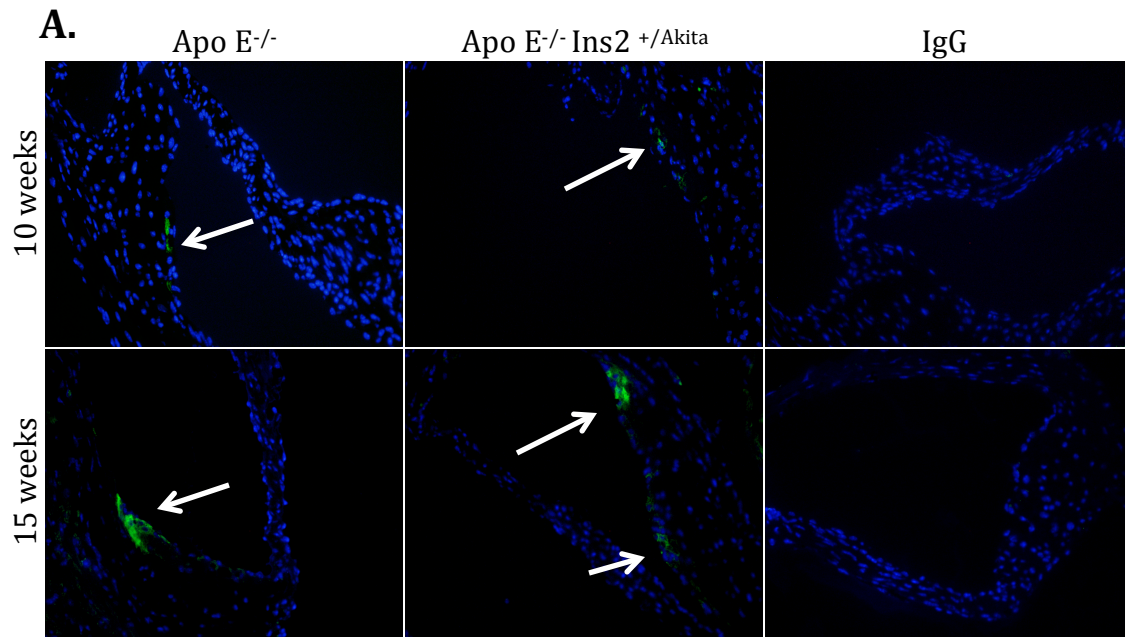


Figure 17- Receptor for VEGF-A in female ApoE^{-/-} and ApoE^{-/-} Ins2^{+/-Akita} mice

There are no observable differences in staining for VEGFR-2 between hyperglycemic and normoglycemic mice at the aortic sinus. **A.**

Immunofluorescent stain with an antibody against VEGFR-2 (green) and counterstained with DAPI (blue) in normoglycemic (left) and hyperglycemic (middle) mice at 10 and 15 weeks of age. VEGFR-2 staining is indicated by arrows A control (preimmune) IgG stain (right) is shown. **B.** Quantification of VEGFR-2 fluorescence in atherosclerotic lesions. n= 4-5 mice per group; mean ± SEM. Scale= 100µm



4.9 EXPRESSION OF ANTI-ANGIOGENIC VEGF-A₁₆₅B MRNA IS ENHANCED IN THP-1 MACROPHAGES TREATED WITH GLUCOSE

4.9.1 Cell Survival

To further explore the mechanism(s) by which hyperglycemia may influence hypoxia-mediated angiogenesis, THP-1 macrophages and HASMCs were cultured in the presence or absent of an additional 30 mM glucose since the media for THP-1 macrophages contains 11.1 mM glucose and the HASMCs contain 4.6 mM glucose. This was done under normoxic conditions for 20 hours then the media was changed with and without additional glucose, and cells were then placed under hypoxic and normoxic conditions for another 24 hours. Both THP-1 macrophages and HASMC showed similar cell survival following each treatment condition (Figure 18A &B), signifying that glucose treatment and changes in the partial pressure of oxygen did not significantly affect cell viability.

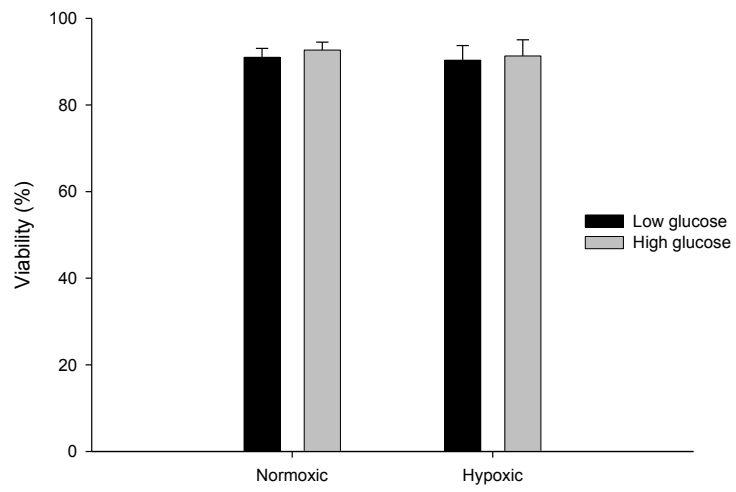
4.9.2 HIF-1 α Stabilization

Total protein lysates were collected and utilized to determine if HIF-1 α was stabilized by hypoxic conditions. There was significantly more HIF-1 α in both THP-1 macrophages and HASMCs when they were cultured in hypoxic conditions compared to normoxic conditions, regardless of glucose concentration (Figure 19A &B). This finding suggests that HIF-1 α was stabilized under hypoxic conditions and available as a transcription factor in these cells.

Figure 18- Cell viability in THP-1 macrophages and HASMCs

Cell survival following changes in partial pressure of oxygen and glucose treatment in **A.** THP-1 macrophages and **B.** HASMCs. n= 3 per group; mean \pm SEM.

A.



B.

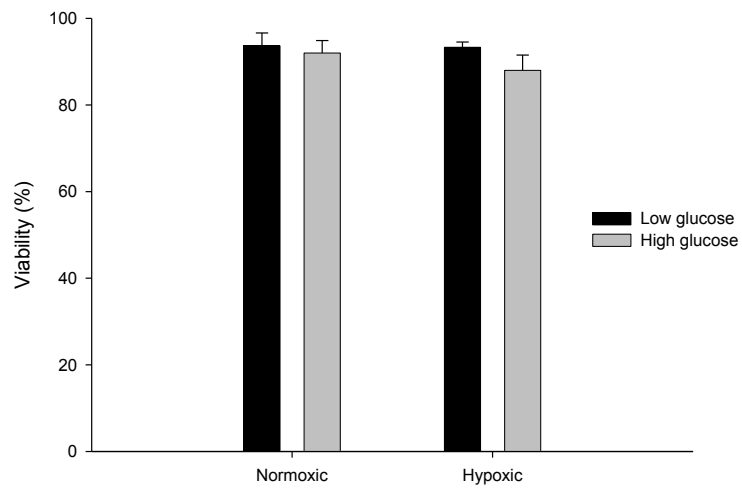
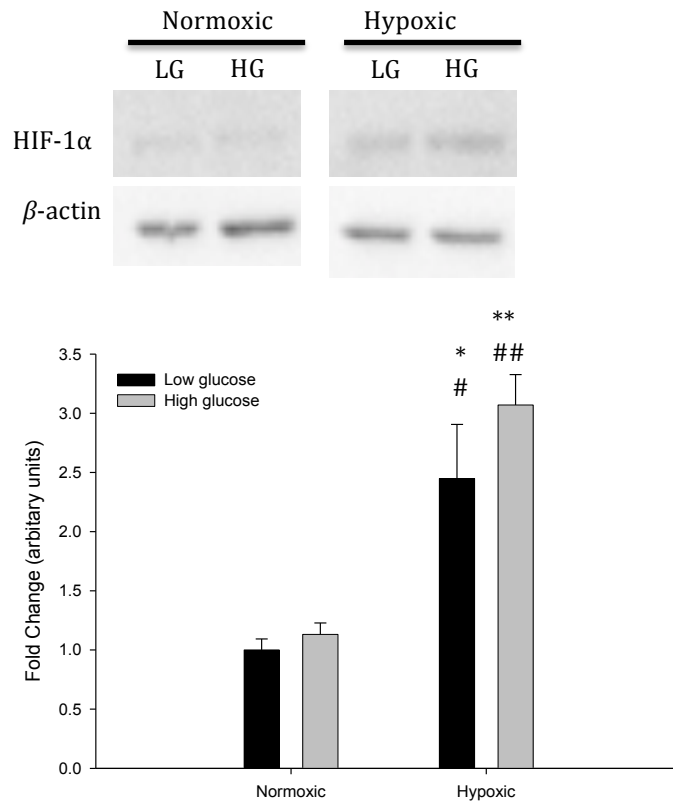


Figure 19- HIF-1 α stability in THP-1 macrophages and HASMCs

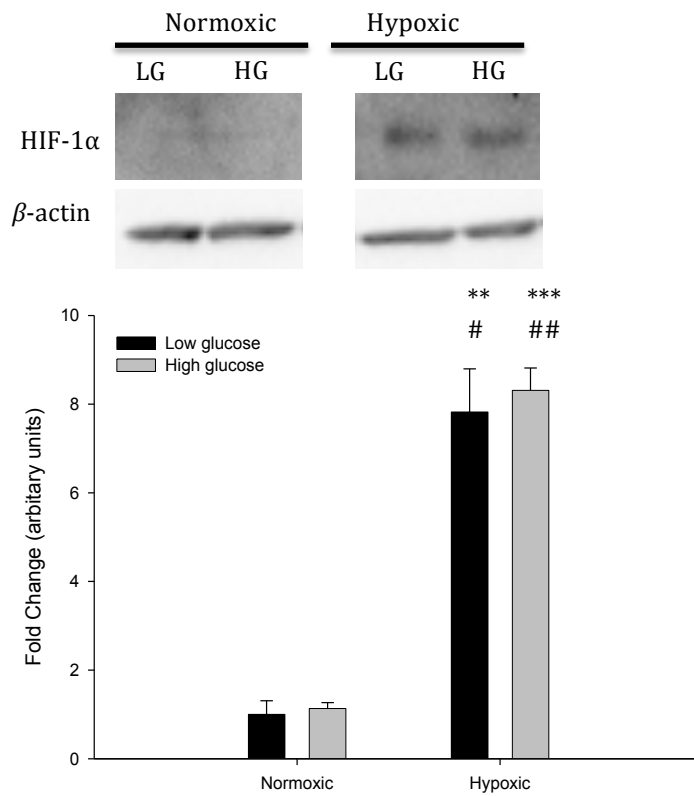
Immunoblots indicate that hypoxic conditions stabilize HIF-1 α in **A.** THP-1 macrophages and **B.** HASMCs. Data normalized to β -actin. n= 3 per group; mean \pm SEM. *p<0.05, **p<0.01, ***p<0.001 relative to the normoxic HG group; #p<0.05, ##p<0.01 relative to the normoxic LG group.

LG indicates cells cultured in low glucose conditions; HG indicates cells cultured in high glucose conditions.

A.



B.



4.9.3 mRNA Expression

To determine the effects of hyperglycemia and/or hypoxia on the VEGF expression, mRNA levels of VEGF-A in THP-1 macrophages and HASMCs were quantified using real-time PCR. To determine if there were post-transcriptional changes occurring through alternative splicing, we specifically quantified VEGF-A_{165a} and VEGF-A_{165b} mRNA levels. Results from the THP-1 macrophages showed that total VEGF-A mRNA was significantly increased in the cells placed under hypoxic conditions regardless of glucose status (Figure 20A). These results are consistent with increases in HIF-1 α leading to increases in transcription of VEGF-A. Expression of VEGF-A_{165a} and VEGF-A_{165b} mRNA levels were also elevated in the THP-1 macrophages in hypoxic conditions and treated with glucose (Figure 20B & C). To evaluate the relative amounts of VEGF-A_{165a} and VEGF-A_{165b} being alternatively spliced, a ratio between the two values was calculated. Findings showed that the ratio of VEGF-A_{165a} mRNA to VEGF-A_{165b} mRNA was significantly lower in glucose-treated cells compared with the untreated cells, both under hypoxic conditions (Figure 20D).

Expression levels of VEGF-A mRNA in HASMCs were significantly lower in glucose-treated cells in hypoxic conditions than untreated cells in both hypoxic and normoxic conditions (Figure 21A). Previous studies have suggested that a glycolytic metabolite associated with diabetes, methylglyoxal, may cause modification of HIF-1 α and/or the cofactor p300 that would reduce transcription of proteins such as VEGF-A. This mechanism may explain the decreased

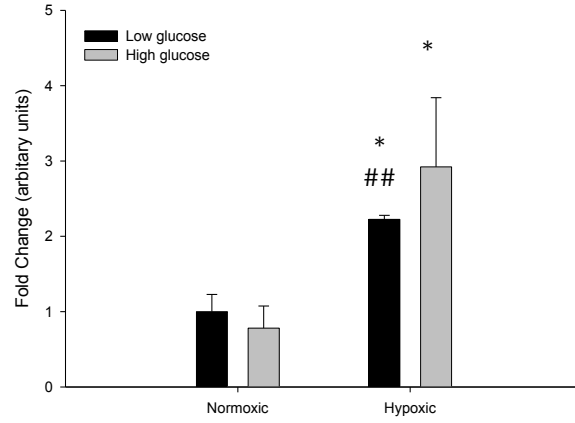
expression of VEGF-A mRNA in hypoxic glucose-treated cells, however, it is perplexing that there were no decreases in glucose-treated cells in normoxic conditions. Alternative splicing of VEGF-A was also evaluated in HASMCs and results showed that there were no significant differences in VEGF-A_{165a} mRNA expression (Figure 21B). There was significantly less VEGF-A_{165b} mRNA in the glucose-treated cells placed in normoxic conditions than the untreated cells under hypoxic conditions, but no other differences were observed (Figure 21C). A ratio of VEGF-A_{165a} mRNA to VEGF-A_{165b} mRNA also showed no significant differences between any of the groups (Figure 21D). From these findings, it appears that alternative splicing of VEGF-A mRNA in HASMCs may not significantly alter the expression of angiogenic VEGF-A under acute hyperglycemic conditions.

Figure 20- Expression of VEGF-A, VEGF-A_{165a} and VEGF-A_{165b} in THP-1 macrophages

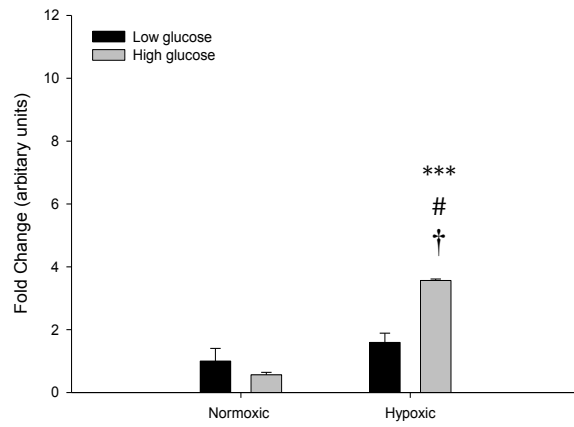
Expression of **A.** VEGF-A, **B.** VEGF-A_{165a}, and **C.** VEGF-A_{165b} mRNA in THP-1 macrophages. **D.** Ratio of VEGF-A_{165a} to VEGF-A_{165b} THP-1 macrophages.

Data normalized to β -actin. n= 3 per group; mean \pm SEM. *p<0.05, ***p<0.001 relative to the normoxic HG group; #p<0.05, ##p<0.01 relative to the normoxic LG group; †p<0.05 relative to hypoxic LG group.

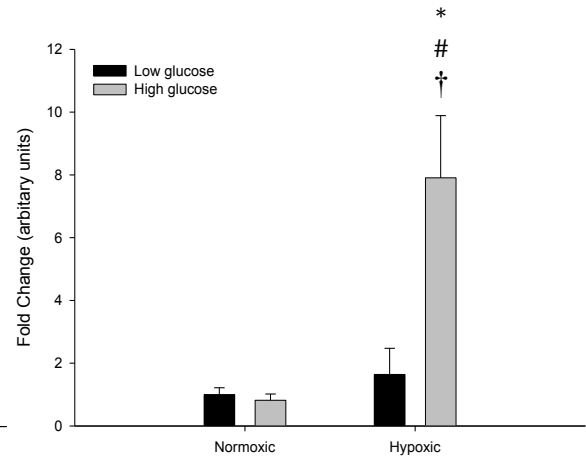
A. VEGF-A



B. VEGF-A_{165a}



C. VEGF-A_{165b}



D. VEGF-A_{165a}/VEGF-A_{165b}

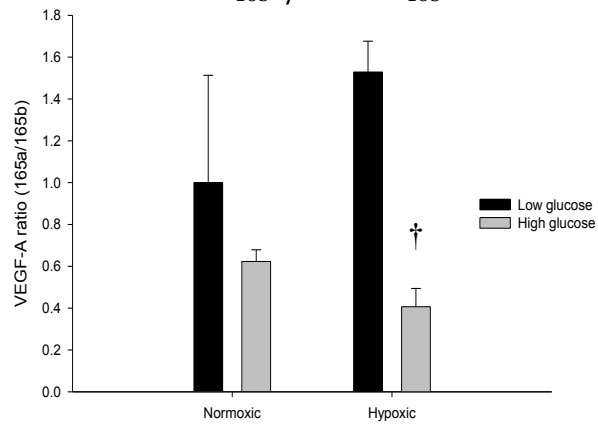
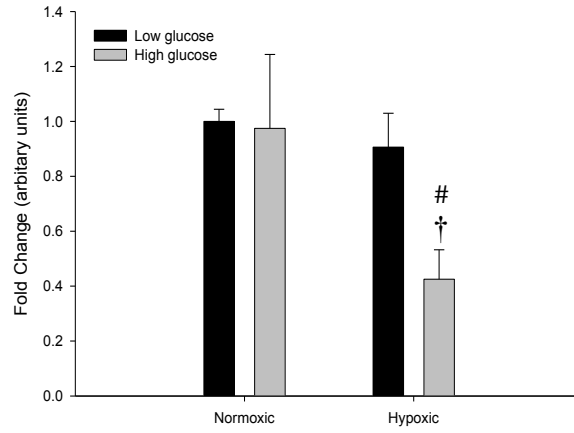


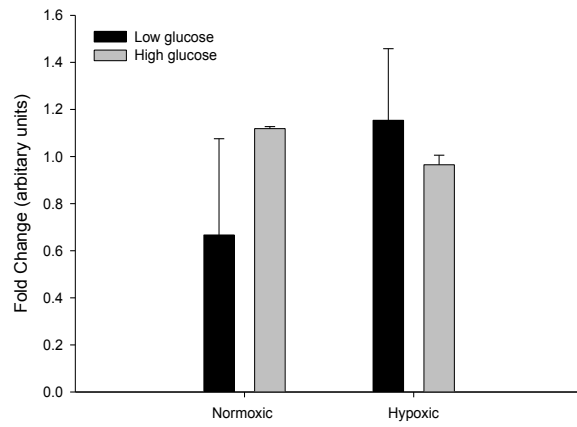
Figure 21- Expression of VEGF-A, VEGF-A_{165a} and VEGF-A_{165b} in HASMCs

Expression of **A.** VEGF-A, **B.** VEGF-A_{165a}, and **C.** VEGF-A_{165b} mRNA in HASMCs. **D.** Ratio of VEGF-A_{165a} to VEGF-A_{165b} in HASMCs. Data normalized to β -actin. n= 3 per group; mean \pm SEM. *p<0.05, ***p<0.001 relative to the normoxic HG group; #p<0.05, ##p<0.01 relative to the normoxic LG group; †p<0.05 relative to hypoxic LG group.

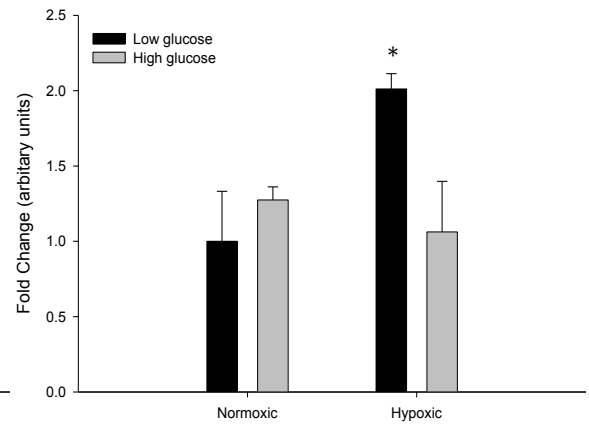
A. VEGF-A



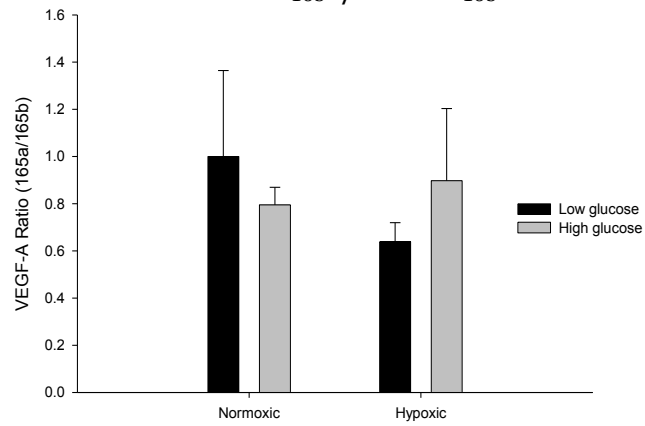
B. VEGF-A_{165a}



C. VEGF-A_{165b}



D. VEGF-A_{165a}/VEGF-A_{165b}



4.10 SECRETED VEGF-A LEVELS ARE DECREASED IN THP-1

MACROPHAGES AND HASMC TREATED WITH GLUCOSE

Media from both THP-1 macrophages and HASMCs was collected to examine the amount of VEGF-A secreted by the cells. An ELISA for VEGF-A showed that both glucose-treated and untreated THP-1 macrophages had elevated VEGF-A levels in the hypoxic conditions compared to the respective glucose-treated and untreated cells in normoxic conditions (Figure 22A). This finding is consistent with the knowledge that stabilized HIF-1 α acts as a transcription factor for VEGF-A. There were also significantly lower levels of VEGF-A present in cells treated with additional 30 mM glucose than cells that were not treated in both the normoxic and hypoxic conditions. This finding when combined with results seen previously suggests that additional post-transcriptional or post-translational modifications may be occurring in hyperglycemic conditions that inhibit the secretion of VEGF-A in THP-1 macrophages.

The amount of VEGF-A released by HASMCs was significantly elevated in the untreated cells placed under hypoxic conditions (Figure 22B). No significant differences were detected between glucose-treated cells under hypoxic and normoxic conditions or in the untreated HASMCs in normoxic conditions. This data, while not as robust as the results observed in the THP-1 macrophages, also demonstrates the potential for upstream changes in glucose-treated cells that results in impaired VEGF-A availability. Reduced transcription of VEGF-A mRNA

may explain the reduced secretion seen and may be the result of changes occurring in the amount of transcription.

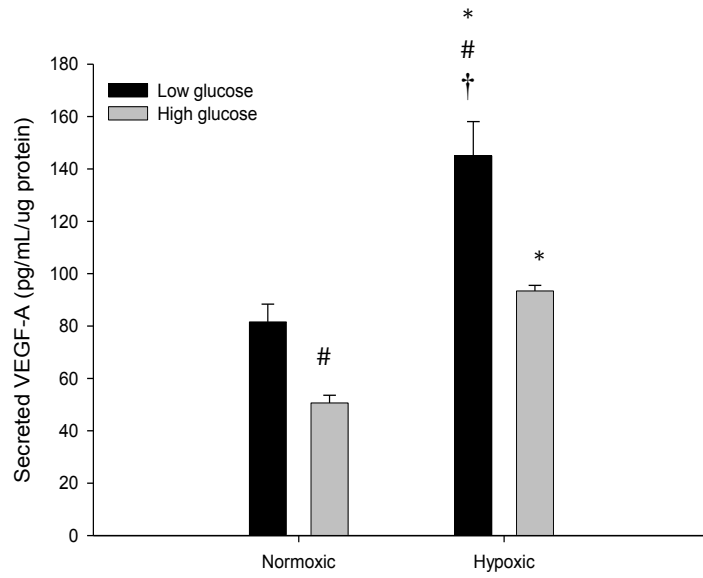
Figure 22- Secretion of VEGF-A in THP-1 macrophages and HASMCs

Secretion of VEGF-A in the media from **A.** THP-1 macrophages and **B.** HASMCs.

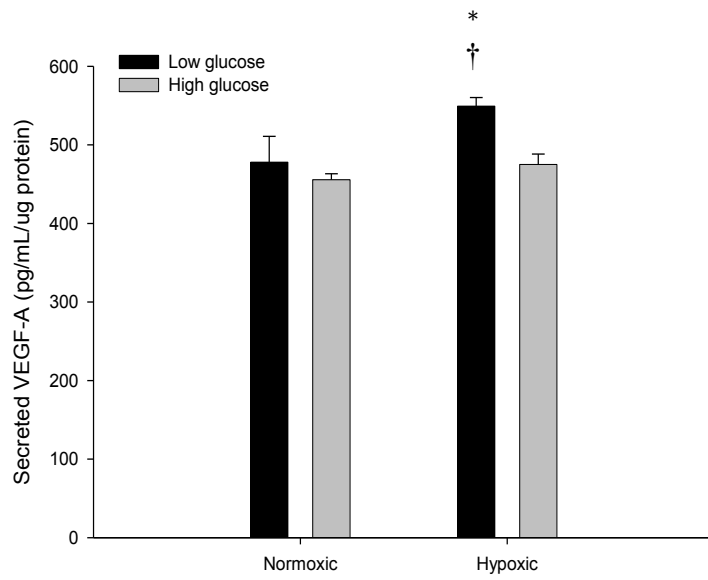
n= 3 per group; mean \pm SEM. *p<0.05 relative to the normoxic HG group;

#p<0.05 relative to the normoxic LG group; †p<0.05 relative to hypoxic HG group.

A.



B.



4.11 VASA VASORUM IN HUMAN CORONARY ARTERIES

To begin to investigate the potential effects of hyperglycemia on the vasa vasorum in humans, tissue samples were obtained from autopsies performed on patients with and without diabetes. Vasa vasorum was imaged and quantified in cross sections of the left anterior descending coronary artery (Figure 23A). The vasa vasorum was quantified in the adventitia, the intimal-medial layer and as total number of microvessels in the arterial wall. All measurements were normalized to the adventitial area, intimal-medial area or total area, respectively. Individuals were classified as diabetic, prediabetic or not diabetic if HbA1C levels exceeded 6.5%, were between 6.0-6.5% or were less than 6.0%, respectively⁴.

There were significantly fewer vasa vasorum microvessels in the adventitial area of the coronary arteries from diabetic patients compared to non-diabetic patients (Figure 23B). The intimal-medial vasa vasorum appeared to increase in density in the diabetic group, but this was not statistically significant (Figure 23C). There were also no significant differences observed in total vasa vasorum microvessels between the diabetic and non-diabetic groups (Figure 23D).

To further assess changes in microvessel density with changes in hyperglycemia, the vasa vasorum density was plotted versus HbA1C levels and a line of best fit generated. The adventitial vasa vasorum microvessels showed a trend towards decreased microvessels with increased HbA1C levels and an R^2

value of 0.21403 (Figure 24A). The intimal-medial vasa vasorum, on the other hand, demonstrated a trend towards increased number of microvessels with increased hyperglycemia with an R^2 value of 0.24146 (Figure 24B). Finally, the total vasa vasorum density was graphed and showed no differences in the microvessel number with changes in hyperglycemia, as the R^2 value was 0.01051 (Figure 24C).

Figure 23- Vasa vasorum in diabetic, prediabetic and non-diabetic human coronary arteries

A. An immunofluorescent stain, using an antibody against vWF, allowed for visualization of vasa vasorum microvessels in the intimal-medial layer (inset left) and adventitial layer (inset right). Representative microvessels are indicated by arrows. Quantification of **B.** adventitial, **C.** Intimal-medial and **D.** total vasa vasorum microvessels at the left anterior descending coronary artery of non-diabetic and diabetic patients. n=13 non-diabetic samples, n= 4 diabetic samples; mean \pm SEM. *p<0.05 relative to non-diabetic samples.

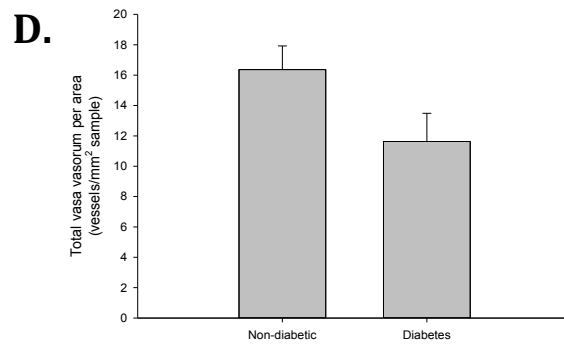
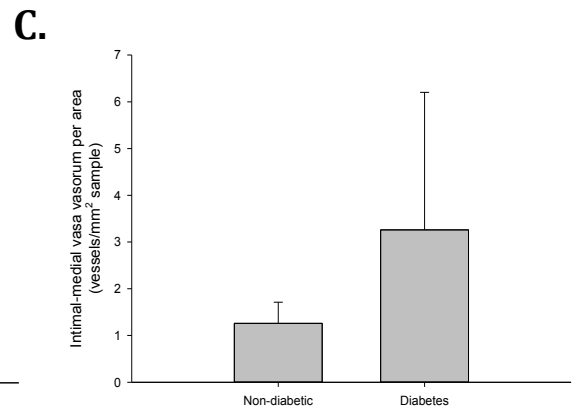
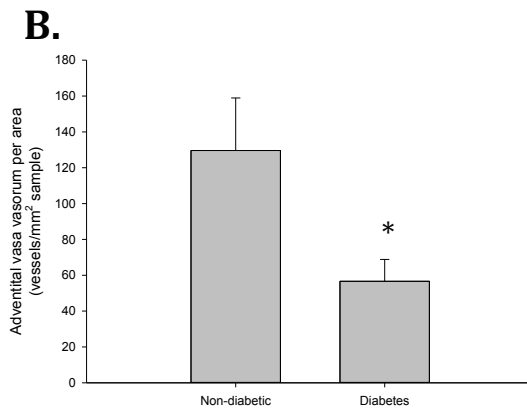
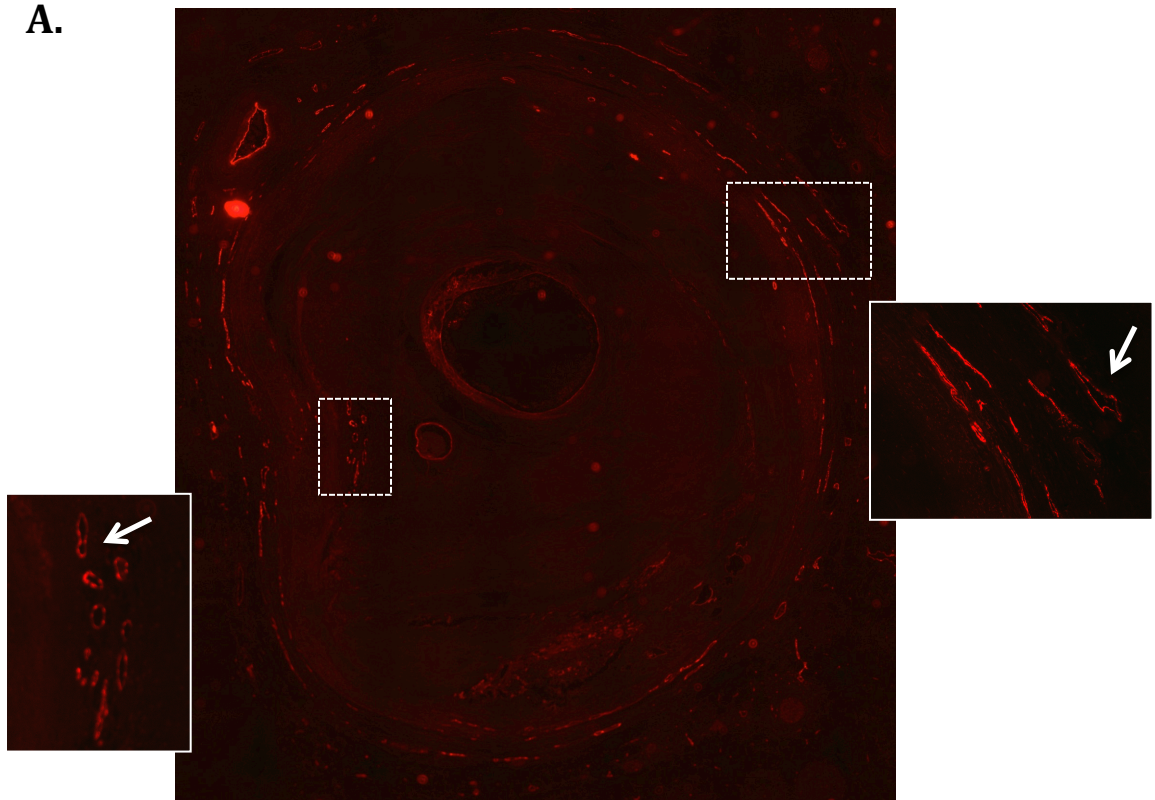
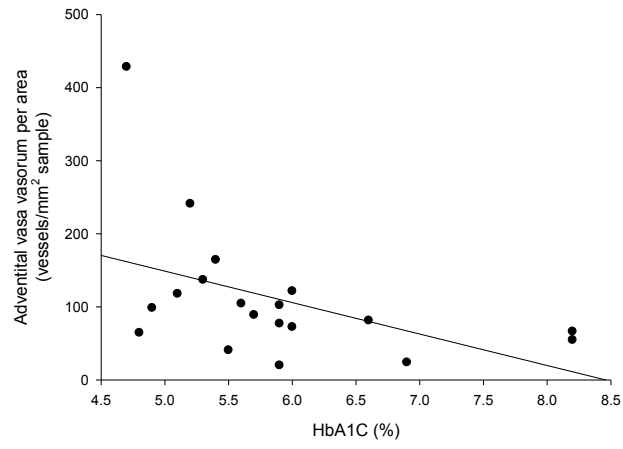


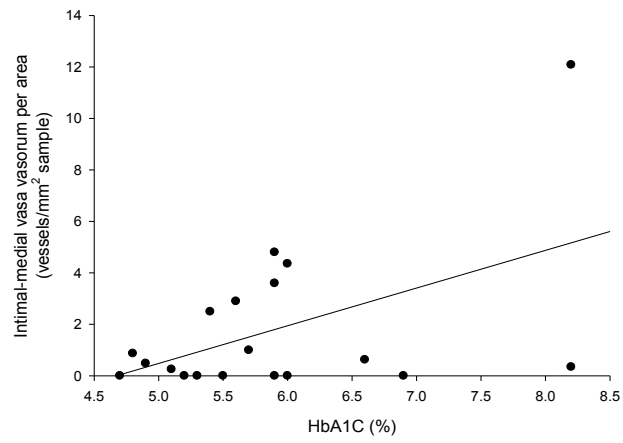
Figure 24- Vasa vasorum density relative to HbA1C levels

Quantification of **A.** adventitial, **B.** Intimal-medial and **C.** total vasa vasorum microvessels relative to HbA1C levels obtained. n= 19 samples

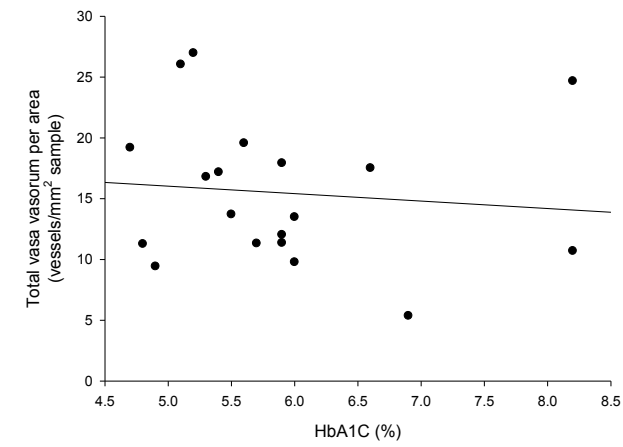
A.



B.



C.



5.0 DISCUSSION

5.1 VASA VASORUM NEOVASCULARIZATION IN APOE^{-/-} STZ-INJECTED MICE

Chronic hyperglycemia is associated with the development of both microangiopathies and macrovascular complications⁸. To assess these complications, we examined atherosclerotic lesions and markers of angiogenesis in hyperglycemic and normoglycemic ApoE^{-/-} mice at 25, 30 and 40 weeks of age. Previous findings from our lab have shown accelerated atherosclerotic lesion area, volume and necrotic core size in 15 week old mice, however, no significant differences in these parameters were seen at later time points. This effect has been previously observed and likely is a result of the genetic predisposition of ApoE^{-/-} mice to spontaneously develop atherosclerosis that overwhelms the effects of hyperglycemia¹¹³.

At 25 and 30 weeks of age, the hyperglycemic mice had impaired neovascularization at the aortic sinus. By 40 weeks of age, however, the diabetic mice had enhanced neovascularization. By combining this information with previous data from hyperglycemic and normoglycemic mice at 5, 10, 15 and 20 weeks of age, the effect of hyperglycemia on the vasa vasorum angiogenesis appears to be analogous to diabetic retinopathy, since there is an initial decrease (pre-proliferative stage) followed by a period of proliferation. Researchers have previously suggested that this “angiogenic switch” may be due to increased

inflammation from hypercholesterolemia that may trigger the angiogenic phenotype^{90, 91}. We observed that female ApoE^{-/-} mice showed a plateau in the amount of neovascularization after 20 weeks of age while microvessel expansion continued to occur in the female ApoE^{-/-} STZ-injected mice. These changes in angiogenesis correlate with increases in total fasting plasma cholesterol levels in the ApoE^{-/-} STZ-injected mice while cholesterol levels in the control ApoE^{-/-} mice remain relatively stable after 20 weeks of age.

5.2 HYPERGLYCEMIA IN APOE^{-/-} INS2^{+AKITA} MICE IS ASSOCIATED WITH ACCELERATED ATHEROSCLEROSIS, INCREASED HYPOXIA AND ABERRANT ANGIOGENESIS OF THE VASA VASORUM

In addition to investigating microangiopathies and macrovascular complications in ApoE^{-/-} STZ-injected mice, we also examined genetically modified hyperglycemic female ApoE^{-/-} Ins2^{+Akita} mice at 5, 10 and 15 weeks of age. Similarly to the previous mouse model there was increased atherosclerotic plaque cross sectional area, total volume and necrotic core content in the 15 week old ApoE^{-/-} Ins2^{+Akita} mice compared to age-matched normoglycemic controls. Aberrant angiogenesis in hyperglycemic mice was observed with decreases in vasa vasorum neovascularization at 10 weeks of age and microvessel expansion at 15 weeks of age. The decreased vasa vasorum density at 10 weeks of age corresponded to increased staining of HIF-1 α , decreased staining for the angiogenic marker VEGF-A and no differences in

VEGFR-2 staining. These results suggest that there may be dysfunction in the pathway that regulates hypoxia-mediated angiogenesis and appears less likely that VEGF resistance is occurring.

From the results obtained in both hyperglycemic mouse models, we are interested in examining if the decreases in microvascular angiogenesis at 10 weeks of age have an influence on accelerated atherosclerosis seen at 15 weeks of age. Previous studies have suggested that angiogenesis must be tightly regulated and that impaired or enhanced neovascularization can cause potential disruptions in endothelial function^{90, 114, 115}. In rabbits with atherosclerotic lesions, areas of hypoxia were co-localized with infiltration of macrophages, increased fat deposition and larger necrotic cores^{105, 114}. Studies using the drug Bevacizumab to bind to VEGF and inhibit its activity have seen increases in CVD risk and thromboembolic events¹¹⁵. It has been suggested that these increased events may be due to the large influence VEGF has on vascular homeostasis and endothelial survival.

The ApoE^{-/-} Ins2^{+Akita} mice at 15 weeks of age had increased vasa vasorum neovascularization, but we are not able to distinguish if this change is from previous hyperglycemic conditions or a restoration of angiogenic function since the glucose levels are similar to normoglycemic controls at this age. It is interesting to note that the ApoE^{-/-} Ins2^{+Akita} mice at 15 weeks of age have increased HIF-1 α levels at the aortic sinus even with increased microvascular density. The increases in hypoxia may be due to an insufficient number of

microvessels present and/or dysfunction of the blood vessels despite no longer being hyperglycemic. Analysis of the number of vessels per area of the lesion revealed that there may not be enough microvessels for the substantial increases in lesion area.

These results suggest that hyperglycemia in mice is associated with increased hypoxia and insufficient angiogenesis of the vasa vasorum. Irregular angiogenesis of the vasa vasorum corresponds to and may influence the development of atherosclerosis in the aortic sinus of hyperglycemic mice. Many studies have observed a correlation between plaque development and the vasa vasorum, but these reports do not support a causative role of angiogenesis in the progression of atherosclerosis^{96, 98, 102, 103, 107}. One of the future aims of this project is to determine if changes in neovascularization have a reactive or causative role in atherosclerosis. Compiling the information from multiple studies demonstrating that vasa vasorum inhibition and expansion may have an influence on atherogenesis suggests that the role of vasa vasorum angiogenesis may be dynamic and differ depending on the stage of atherosclerosis progression.

5.3 POST-TRANSLATIONAL MODIFICATIONS AND ALTERNATIVE SPLICING MAY BE RESPONSIBLE FOR ACUTE CHANGES SEEN IN GLUCOSE-TREATED MACROPHAGES

As previously mentioned, there are multiple theories that may explain impaired angiogenesis seen in diabetes including methylglyoxal modifications,

increased splicing of the anti-angiogenic VEGF-A_{165b} and VEGF resistance. Since levels of VEGFR-2 are unaltered in the aortic sinus of hyperglycemic mice, we concluded that the changes in vasa vasorum angiogenesis are less likely to be due to VEGF resistance. To further examine the potential mechanism by which hyperglycemia may impair vasa vasorum neovascularization, THP-1 macrophages and HASMCs were cultured in the presence or absence of additional 30 mM glucose for 44 hours and under hypoxic or normoxic conditions for 24 of those hours. Both cell lines had increases in HIF-1 α when placed in hypoxic conditions.

The expression levels of VEGF-A mRNA were elevated in both glucose-treated and untreated THP-1 macrophages placed in hypoxic conditions. This is consistent with increases in HIF-1 α contributing to increases in transcription of VEGF-A. Since there were no significant differences between VEGF-A mRNA expression in glucose-treated and untreated macrophages, there is likely no effect on transcription. This may suggest that methylglyoxal modification of HIF-1 α and/or p300 is not responsible for the observed alterations in hypoxia-mediated angiogenesis in macrophages in this system, or that the time point examined was too short to generate sufficient amounts of methylglyoxal required to alter transcription. Interestingly, expression levels of VEGF-A_{165a} and VEGF-A_{165b} were found to be elevated in the glucose-treated hypoxic macrophages. A calculation of VEGF-A_{165a} mRNA to VEGF-A_{165b} mRNA found that there was a significantly higher ratio of the angiogenic isoform of VEGF-A in untreated cells

compared with the glucose-treated cells when under hypoxic conditions. The increased amount of VEGF-A_{165b} splicing in glucose-treated cells suggests that decreases in angiogenesis may result from a mechanisms involving alternative splicing.

In addition to alternative splicing of VEGF-A, there appears to be other post-transcriptional modifications occurring in THP-1 macrophages. VEGF-A may be regulated at the level of transcription, post-transcriptional modifications, translation, protein stability, post-translational modifications and/or intracellular trafficking/secretion⁸⁰. A study published in 2014 noted that the biological effects and transcriptional regulation of VEGF-A have been characterized extensively yet there is relatively little known about VEGF-A processing and secretion¹¹⁶.

Previous studies had shown that a signal sequence on VEGF-A meant that the protein was likely translocated to the ER lumen before being directed to the Golgi apparatus for glycosylation and post-translational modifications then constitutively secreted from the cell¹¹⁷⁻¹¹⁹. To further investigate intracellular trafficking and secretion, researchers used protein tags that were fused to the C-terminus of VEGF-A₁₆₅. Results showed that trafficking proteins, Sar1 and Arf1, were likely responsible for trafficking of VEGF-A₁₆₅ from the ER to Golgi apparatus as mutation of these proteins localized VEGF-A to the ER and inhibited secretion. Glycosylation of VEGF-A₁₆₅ in the Golgi apparatus appeared to be important for protein secretion, but not biological activity, which is consistent with previous studies^{117,120}. A plasma membrane phospholipid PtdIns(4,5)P₂ also appears to

be essential for docking and priming of VEGF-A₁₆₅ containing vesicles, whereas PKC activation and elevations in calcium appeared to only slightly enhance VEGF-A₁₆₅ secretion. The knowledge of these post-translational modifications, intracellular trafficking and protein secretion could be used to investigate the reductions in VEGF-A seen in this study. The gamma interferon (IFN- γ)-activated inhibitor of translation (GAIT) complex may also be responsible for these effects as it is able to bind inflammatory mRNAs, including VEGF-A, and regulate protein synthesis through transcript-selective translation inhibition^{80, 81}. The GAIT complex inhibits the small ribosomal subunit recruitment by binding the 3' untranslated region (UTR) on mRNA and interacting with a eukaryotic translation initiation factor, eIF4G, to block translation initiation. To our knowledge, these targets of VEGF-A regulation have not been examined in a diabetic model.

Our data show that the reaction of HASMCs to hyperglycemia and hypoxia is quite different than that of the THP-1 macrophages. The mRNA expression levels were significantly decreased in glucose-treated cells in hypoxic conditions compared to untreated cells, and may suggest a role for methylglyoxal modification causing decreases in VEGF transcription. These levels, however, also appeared to be lower than glucose-treated cells under normoxic conditions ($p= 0.1$). As noted previously, levels of HIF-1 α were elevated in the HASMCs under hypoxic conditions, so VEGF-A transcription is expected to be higher in these cells than respective normoxic controls. What was observed, however, was similar or potentially even decreased expression of VEGF-A mRNA and there is

currently no explanation for these findings. Examination of VEGF-A alternative splicing resulted in no significant differences between any of the groups, unlike results seen in THP-1 macrophages. Lastly, the concentration of secreted VEGF-A was significantly higher in the untreated cells placed under hypoxic conditions. These decreases in VEGF-A may be due to reduced mRNA levels observed in the glucose-treated hypoxic cells or due to other post-transcriptional and/or post-transcriptional regulations occurring that have yet to be determined.

The results obtained suggest that hyperglycemia may disrupt angiogenesis by multiple, different, cell-specific mechanisms.

5.4 HUMAN CORONARY ARTERIES REQUIRE FURTHER INVESTIGATION

To assess if hyperglycemia potentially had an influence on vasa vasorum neovascularization in a human population, coronary arteries were collected from autopsies performed on diabetic, prediabetic and non-diabetic patients. Similar to the hyperglycemic mouse models utilized in this study, there was a significant reduction in the number of adventitial vasa vasorum microvessels in the diabetic patients compared to non-diabetic individuals. When analyzing intimal-medial and total microvessel density, however, there were no significant differences observed between the groups. It is important to note that this is preliminary data as the sample size is quite small for the diabetic and prediabetic groups with 4 and 2 samples, respectively. Collection and analysis of additional samples may provide more definitive information about trends in vasa vasorum density.

Another limitation of this study is that limited data was provided regarding the metabolic profile of these individuals. It is impossible, at this point, to determine if any effects observed are solely due to changes in glucose levels or if there are potential effects of other metabolites, such as cholesterol, on vasa vasorum neovascularization. Additional information may provide more insight into the effects of hyperglycemia and the complex relationship it may have with other metabolites on vasa vasorum angiogenesis.

5.5 FUTURE DIRECTIONS

In addition to gathering more samples to analyze the human coronary artery data, there are a number of other tests that can be conducted to further our knowledge of hyperglycemic effects on the vasa vasorum.

5.5.1 Chromatin Immunoprecipitation (ChIP) assay

To further assess the potential influence of hyperglycemia on transcription of VEGF-A, a ChIP assay for p300 can be utilized. In this experiment, transcription factors and cofactors such as HIF-1 α and p300 are cross-linked to DNA¹²¹. The chromosomes are fragmented into smaller pieces (~1000bp) through sonication. Samples can then be immunoprecipitated for p300 which will also pull down any crossed DNA from promoter elements to which the p300 was bound. VEGF-A specific promoter DNA can be quantified by real-time PCR using a promoter-specific primers¹²². In order to complete this experiment, the

procedure must be optimized for each cell type, as there may be differences in cross-linking time, sonication and immunoprecipitation. This experiment may offer increased understanding of the DNA-protein interactions occurring under hyperglycemic conditions.

5.5.2 Explore molecular mechanisms of diabetes-associated aberrant angiogenesis

While some potential mechanisms of hyperglycemia induced aberrant angiogenesis at the aortic sinus have been explored in this study, the exact mechanism still remains to be understood. The results from this study implied that THP-1 macrophages have increased expression of an antiangiogenic form of VEGF-A known as VEGF-A_{165b}. While this may explain some of the decreases in angiogenesis observed, there were also decreases in VEGF-A secretion that may suggest post-translational modifications of VEGF-A that, to the best of our knowledge, have yet to be explored in diabetic models.

While we have observed changes in THP-1 macrophages when treated with glucose, there are some limitations of utilizing cell lines that could be overcome with additional experimentation. THP-1 macrophages are a commonly used cell line in atherosclerosis, diabetes and inflammatory research due to their homogeneous genotype that reduces phenotype variability, long storage life and ability to mimic both monocytes and macrophages^{123, 124}. While this is considered a reasonable model to study macrophage function in the vasculature,

observations made should still be verified using primary cells. One way that different cells such as macrophages, smooth muscle cells and endothelial cells could be studied is with laser capture microdissection. This technique would allow isolation of individual cells types from atherosclerotic plaques followed by DNA, RNA or protein analysis¹²⁵. An additional benefit of this technique is that it could aid in determining the relative contribution of each cell type to promoting or inhibiting angiogenesis.

Another limitation of this study was the short time period in which cells were treated with glucose. Methylglyoxal modification has been suggested as a potential mechanism of impaired angiogenesis in diabetic retinopathy and impaired wound healing^{74, 75}. This modification may also contribute to decreases in vasa vasorum angiogenesis, but the time periods utilized in this study may have been too short to produce sufficient amounts of methylglyoxal and observe any differences. Cell culture experiments with prolonged exposure to glucose or treatment with methylglyoxal may allow for investigation of transcriptional changes of VEGF-A from chronic hyperglycemia^{126, 127}.

5.5.3 Explore effects of cholesterol on vasa vasorum angiogenesis

Finally, our results have shown that there are increases in vasa vasorum angiogenesis in ApoE^{-/-} STZ-injected mice that correlate to increases in cholesterol levels. These results are consistent with previous findings that cholesterol may promote angiogenesis, but the possible mechanism(s) for this

increase are not fully understood⁹⁰⁻⁹³. Experiments on mice that express high levels of cholesterol, such as ApoE^{-/-} mice and LDLR^{-/-} mice fed a high fat diet, could be utilized to compare with wild type controls and a subset treated with lipid lowering statins to examine vasa vasorum angiogenesis¹²⁸⁻¹³⁰.

5.6 LIMITATIONS

It is important to note that the focus of this research was on the effects of hyperglycemia on the vasa vasorum angiogenesis and to correlate this data to atherosclerotic plaque progression. The diabetic mouse models utilized in this research had chronically elevated glucose levels in the case of the ApoE^{-/-} STZ-injected mice and transiently elevated glucose levels in the case of the ApoE^{-/-} Ins2^{+/Akita} mice to reflect this emphasis on hyperglycemia. Both these models of diabetes also have a common characteristic in that these mice have hypoinsulinemia. So a limitation of this study is that the potential effects of decreased insulin levels on vasa vasorum angiogenesis were not explored.

Previous studies have observed that insulin can stimulate angiogenesis to induce microvessel development¹³¹⁻¹³⁴. Insulin appears to promote endothelial cell migration, tube formation and vessel maturation. Interestingly, the effects of insulin on angiogenesis appear to be dependent on signalling through the insulin receptor leading to Rac1 activation¹³¹. Since the mice utilized in this study have decreased insulin levels, there may be inhibitory effects on vasa vasorum angiogenesis from hypoinsulemina that we have yet to explore.

In addition to not observing the effects of insulin, the effects of growth factors such as insulin-like growth factor and proteins such as plasminogen activator inhibitor-1 have not been considered^{132, 135}. While hyperglycemia and hypoinsulinemia are characteristics of the mouse models utilized in this study, other growth factors and proteins may be influenced by diabetes and have an effect on the results observed.

6.0 CONCLUSIONS

The microvascular and macrovascular complications of diabetes appear to be related and some research has suggested that microvascular dysfunction may promote cardiovascular outcomes. Utilizing two mouse models of diabetes, our results have shown that chronically hyperglycemic mice have accelerated atherosclerosis that correlates to initial decreases in vasa vasorum density at the aortic sinus. Examination of these samples have suggested that there may be disruption of hypoxia-mediated angiogenesis as there is increased staining for the transcription factor HIF-1 α yet decreased levels of the angiogenic marker VEGF-A. Cell culture experiments conducted have implicated a potential role for increased splicing of antiangiogenic VEGF-A_{165b} as well as additional post-transcriptional and/or post-translational modifications that reduce VEGF-A secretion in macrophages. Experiments on ApoE^{-/-} STZ-injected mice also demonstrated increased vasa vasorum density at later time points that correlated with increases in fasting plasma cholesterol levels. Further research is needed to determine if the correlations between plaque development and the vasa vasorum angiogenesis are causative and/or reactive as well as exploration of potential molecular mechanisms that may alter vasa vasorum angiogenesis.

Evidence supporting a role of diabetic microvascular disease in the accelerated development of atherosclerosis would represent a paradigm shift in our understanding of how diabetes predisposes individuals to CVD. A better

understanding of the mechanisms by which diabetes promotes CVD will facilitate the development of new and more effective treatments.

7.0 REFERENCES

- 1 Alberti, K.G.M.M, Zimmet, P.Z. (1998). Definition, diagnosis and classification of diabetes mellitus and its complications. Part 1: diagnosis and classification of diabetes mellitus. Provisional report of a WHO consultation. *Diabetic Medicine*, 15(7), 539-553. doi: 10.1002/(SICI)1096-9136(199807)15:7<539::AID-DIA668>3.0.CO;2-S
- 2 Canadian Diabetes Association Clinical Practice Guidelines Expert Committee (2008). Definition, classification and diagnosis of diabetes and other dysglycemic categories. *Canadian Journal of Diabetes*, 32(1), S10-S13.
- 3 American Diabetes Association. (2010). Diagnosis and classification of diabetes mellitus. *Diabetes Care*, 33(1), S62-S69. doi: 10.2337/dc10-S062
- 4 The International Expert Committee. (2009). International Expert Committee Report on the Role of the A1C assay in the diagnosis of diabetes. *Diabetes Care*, 32(7), 1327-1334. doi: 10.2337/dc09-9033
- 5 Guariguata, L., Whitling, D.R., Hambleton, I., Beagley, J., Linnenkamp, U., Shaw, J.E. (2013). Global estimates for 2013 and projections for 2035 for the IDF Diabetes Atlas. *Diabetes Research and clinical practice*, 11. doi: 10.1016/j.diabres.2013.11.002
- 6 Beagley, J., Guariguata, L., Weil, C. Motala, A.A. (2013). Global estimates of undiagnosed diabetes in adults for 2013 for IDF Diabetes Atlas. *Diabetes Research and clinical practice*, 11. doi: 10.1016/j.diabres.2013.11.001
- 7 International Diabetes Federation. (2014). IDF Diabetes Atlas (6th ed.): 2014 Update. Retrieved from <http://www.idf.org/diabetesatlas/update-2014>
- 8 Veerman, K.J. Venegas-Pino, D.E., Shi, Y., Khan, M.I., Gerstein, H.C., Werstuck, G.H. (2013). Hyperglycaemia is associated with impaired vasa vasorum neovascularization and accelerated atherosclerosis in apolipoprotein-E deficient mice. *Atherosclerosis*, 227, 250-258. doi: 10.1016/j.atherosclerosis.2013.01.018
- 9 Heinonen, S.E. et al. (2015). Animal models of Diabetic Macrovascular Complications: Key players in the Development of New Therapeutic Approaches. *J Diabetes Res*, 2015, 1-14. doi:10.1155/2015/404085

- 10 Paneni, F., Beckman, J.A., Creager, M.A., Cosentino, F. (2013). Diabetes and vascular disease: Pathophysiology, clinical consequences and medical therapy: part I. *European Heart Journal*, 34(31). doi: 10.1093/eurheartj/eh149
- 11 Malandrino, N., Wu, W.C., Taveira, T.H., Whitlatch, H.B., Smith, R.J. (2012). Association between red blood cell distribution width and macrovascular and microvascular complications in diabetes. *Diabetologia*, 55, 226-234. doi: 10.1008/s00125-011-2331-1
- 12 Warren, C.M., Ziyad, S., Briot, A., Der, A., Iruela-Arispe, M.L. (2014). A ligand-independent VEGFR2 signaling pathway limits angiogenic responses in diabetes. *Science Signalling*, 7(307), ra1, 1-12. doi: 10.1126/scisignal.2004235
- 13 Haffner, S.M., Lehto, S., Ronnema, T., Pyorala, K., Laakso, M. (1998). Mortality from coronary heart disease in subjects with Type 2 diabetes and in nondiabetic subjects with and without prior myocardial infarction. *N Engl J Med*, 339(4), 229-234.
- 14 Howangyin, K.Y., Silvestre, J. (2014). Diabetes Mellitus and Ischemic Disease: Molecular Mechanisms of Vascular Repair Dysfunction. *Arterioscler Thromb Vasc Biol*, 34(6), 1126-1135. doi: 10.1161/ATVBAHA.114.303090
- 15 Werstuck, G.H. (2006). Molecular and cellular mechanisms by which diabetes mellitus promotes the development of atherosclerosis. *Biochemistry of atherosclerosis*, 1, 284-304.
- 16 Targher, G. et al. (2008). Diabetic retinopathy is associated with an increased incidence of cardiovascular events in Type 2 diabetic patients. *Diabet Med*, 25(1), 45-50. doi: 10.1111/j.1464-5491.2007.02327.x.
- 17 Gimeno-Orna, J.A., Molinero-Herguedas, E., Sanchez-Vano, R., Lou-Arnal, L.M., Boned-Juliani, B., Castro-Alonso, F.J. (2006). Microalbuminuria presents the same vascular risk as overt CVD in type 2 diabetes. *Diabetes Res Clin Pract*, 74(1), 103-109.
- 18 Vigili de Kreutzenberg, S. et al. (2011). Microangiopathy is independently associated with presence, severity and composition of carotid atherosclerosis in type 2 diabetes. *Nutrition, Metabolism & Cardiovascular Diseases*, 21, 286-293. doi:10.1016/j.numecd.2009.10.003

- 19 Rosenson, R.S., Fioretto, P., Dodson, P.M. (2011). Does microvascular disease predict macrovascular events in type 2 diabetes? *Atherosclerosis*, 218(1), 13-18. doi: 10.1016/j.atherosclerosis.2011.06.029
- 20 Jax, T.W. (2010). Metabolic memory: a vascular perspective. *Cardiovasc Diabetol*, 9, 1-8. doi: 10.1186/1475-2840-9-51
- 21 Zeiher, A.M., Drexler, H., Wollschlager, H., Just, H. (1991) Endothelial dysfunction of the coronary microvasculature is associated with coronary blood flow regulation in patients with early atherosclerosis. *Circulation*, 84(5), 1984-1992.
- 22 D'Souza, A., Hussain, M., Howarth, F.C., Woods, N.M., Bidasee, K., Singh, J. (2009). Pathogenesis and pathophysiology of accelerated atherosclerosis in the diabetic heart. *Mol Cell Biochem*, 331, 89-116. doi: 10.1007/s11010-009-0148-8
- 23 Brownlee, M. (2004). The pathobiology of diabetic complications: a unifying mechanism. *Diabetes*, 54, 1615-1625.
- 24 Giacco, F., Brownlee, M. (2010). Oxidative stress and diabetic complications. *Circ Res*, 107(9), 1058-1070. doi: 10.1161/CIRCRESAHA.110.223545
- 25 Li, H., Forstermann, U. (2013). Uncoupling of endothelial NO synthase in atherosclerosis and vascular disease. *Curr Opin Pharmacol*, 13(2), 161-167. doi: 10.1016/j.coph.2013.01.006
- 26 Kris-Etherton, P.M, Liechtenstein, A.H., Howard, B.V., Steinberg, D., Witztum, J.L., Nutrition Committee of the American Heart Association Council on Nutrition, Physical Activity and Metabolism. (2004). Antioxidant vitamin supplements and cardiovascular disease. *Circulation*, 110, 637-641. doi: 10.1161/01.CIR.0000137822.39831.F1
- 27 Schiffrin, E.L. (2014). Reactive Oxygen Species in Hypertension and Atherosclerosis. *Systems Biology of Free Radicals and Antioxidants*, 1239-1254. doi: 10.1007/978-3-642-30018-9_58
- 28 Roy, S., Trudeau, K., Roy, S., Behl, Y., Dhar, S., Chronopoulos, A. (2010). New insights into hyperglycemia-induced molecular changes in microvascular cells. *JDR*, 89(2), 116-127. doi: 10.1177/0022034509355765

- 29 Boussageon, R. et al. (2011). Effect of intensive glucose lowering treatment on all cause mortality, cardiovascular death and microvascular events in type 2 diabetes: meta-analysis of randomized controlled trials. *BMJ*, 343, 1-12. doi: 10.1136/bmj.d4169
- 30 Fullerton, B., Jeitler, K., Seitz, M., Horvath, K., Berghold, A. Siebenhofer, A. (2014). Intensive glucose control versus conventional glucose control for type 1 diabetes mellitus. *Cochrane Database Syst Rev*, 14(2), 1-156. doi: 10.1002/14651858.CD009122.pub2
- 31 The Action to Control Cardiovascular Risk in Diabetes Study Group. (2008). Effects of intensive glucose lowering in type 2 diabetes. *N Engl J Med*, 358, 2545-2559. doi: 10.1056/NEJMoa0802743
- 32 Reichard, P., Nilsson, B.Y., Rosenqvist, U. (1993). The effect of long-term intensified insulin treatment on the development of microvascular complications of diabetes mellitus. *N Engl J Med*, 329(5), 304-309. doi: 10.1056/NEJM199307293290502
- 33 The ADVANCE Collaborative Group. (2008). Intensive blood glucose control and vascular outcomes in patients with Type 2 diabetes. *N Engl J Med*, 358, 2560-2572. doi: 10.1056/NEJMoa0802987
- 34 Schulman, I.H., Zhou, M.S. (2009). Vascular insulin resistance: a potential link between cardiovascular and metabolic disease. *Curr Hypertens Rep*, 11(1), 48-55.
- 35 Jiang, Z.Y. et al. (1999). Characterization of selective resistance to insulin signaling in the vasculature of obese Zucker (*fa/fa*) rats. *J Clin Invest*, 104(4), 447-457.
- 36 Paneni, F., Volpe, M., Luscher, T.F., Cosentino, F. (2013). SIRT1, p66^{Shc} and Set7/9 in Vascular Hyperglycemic Memory: Bringing all the strands together. *Diabetes*, 62, 1800-1807. doi: 10.2337/db12-1648
- 37 Ihnat, M.A. et al. (2007). Reactive oxygen species mediate a cellular 'memory' of high glucose stress signalling. *Diabetologia*, 50(7), 1523-1531.
- 38 Orasanu, G., Plutzky, J. (2009). The pathologic continuum of diabetic vascular disease. *J Am Coll Cardiol*, 53(5), 35-42. doi: 10.1016/j.jacc.2008.09.055

- 39 Libby, P., Ridker, P.M. Hansson, G.K. (2011). Progress and challenges in translating the biology of atherosclerosis. *Nature*, 473(7347), 317-325. doi: 10.1038/nature10146
- 40 Stary, H.C. et al. (1992). A definition of the intima of human arteries and of its atherosclerosis-prone regions. A report from the Committee on Vascular Lesions of the Council on Arteriosclerosis, American Heart Association. *Arterioscler Thromb Vasc Biol*, 12(1), 120-134.
- 41 Majesky, M.W., Dong, X. R., Høglund, V., Mahoney Jr., W.M., Daum, G. (2011). The adventitia: A dynamic interface containing resident progenitor cells. *Arterioscler Thromb Vasc Biol*, 31, 1530-1539. doi: 10.1161/ATVBAHA.110.221549
- 42 Carmeliet, P. (2003). Angiogenesis in health and disease. *Nat Med*, 9(6), 653-660.
- 43 Yonekura, H. et al. (2003). Novel splice variants of the receptor for advanced glycation end-products expressed in human vascular endothelial cells and pericytes, and their putative roles in diabetes-induced vascular injury. *J Biochem*, 370, 1097-1109.
- 44 Ross, R. (1999). Atherosclerosis- An Inflammatory Disease. *N Engl J Med*, 340(2), 115-126.
- 45 Hopkins, P.N. (2013). Molecular Biology of Atherosclerosis. *Physiological Reviews*, 93(3), 1317-1542. doi: 10.1152/physrev.00004.2012
- 46 Li, J.J., Fang, C.H. (2004). Atheroscleritis is a more rational term for the pathological entity currently known as atherosclerosis. *Med Hypotheses*, 63(1), 100-102.
- 47 Pirillo, A., Zhu, W., Roma, P., Galli, G., Caruso, D., Pellegatta, F., Catapano, A.L. (1999). Oxysterols from oxidized LDL are cytotoxic but fail to induce hsp70 expression in endothelial cells. *FEBS Lett*, 462(1-2), 113-116.
- 48 Maiti, R., Agrawal, N.K. (2007). Atherosclerosis in diabetes mellitus: role of inflammation. *Indian J Med Sci*, 61(5), 292-306.
- 49 Kanter, J.E., Bornfeldt, K.E. (2013). Inflammation and diabetes-accelerated atherosclerosis: myeloid cell mediators. *Trends Endocrinol Metab*, 24(3), 137-144. doi: 10.1016/j.tem.2012.10.002

- 50 Hayden, M.R., Tyagi, S.C. (2004). Vasa vasorum in plaque angiogenesis, metabolic syndrome, type 2 diabetes mellitus and atheroscleropathy: a malignant transformation. *Cardiovasc Diabetol*, 3, 1-16.
- 51 Semenza, G.L. (2007). Vasculogenesis, angiogenesis and arteriogenesis: mechanism of blood vessel formation and remodeling. *Journal of cellular biochemistry*, 102, 840-847. doi: 10.1002/jcb.21523
- 52 Laschke, M.W., Giebels, C., Nickels, R.M, Scheuer, C., Menger, M.D. (2011). Endothelial progenitor cells contribute to vascularization of endometriotic lesions. *Am J Pathol*, 178(1), 442-450. doi: 10.1016/j.ajpath.2010.11.037
- 53 Liu, L., Liu, H., Jiao, J., Liu, H., Bergeron, A., Dong, J.F., Zhang, J. (2007). Changes in circulating human endothelial progenitor cells after brain injury. *J Neurotrauma*, 24(6), 936-943.
- 54 Carmeliet, P. (2005). Angiogenesis in life, disease and medicine. *Nature*, 438(7070), 932-936.
- 55 Martin, A., Komada, M.R., Sane, D.C. (2003). Abnormal angiogenesis in diabetes mellitus. *Med Res Rev*, 23(2), 117-145. doi: 10.1002/med.10024
- 56 Pugh, C.W., Ratcliffe, P.J. (2003). Regulation of angiogenesis by hypoxia: Role of the HIF system. *Nat Med*, 9, 677-684.
- 57 Hewitson, K.S., Schofield, C.J. (2004). The HIF pathway as a therapeutic target. *DDT*, 9(16), 704-711.
- 58 Prabhakar, N.R., Semenza, G.L. (2012). Adaptive and maladaptive cardiorespiratory responses to continuous and intermittent hypoxia mediated by hypoxia-inducible factors 1 and 2. *Physiol Rev*, 92(3), 967-1003. doi: 10.1152/physrev.00030.2011
- 59 Eltzschig, H.K., Carmeliet, P. (2011). Hypoxia and Inflammation. *N Engl J Med*, 364, 656-665.
- 60 Shimoda, L.A., Laurie, S.S. (2013). HIF and pulmonary vascular responses to hypoxia. *J Appl Physiol*, 116(7), 867-874. doi: 10.1152/jappphysiol.00643.2013
- 61 Wiesener, M.S. et al (2003). Widespread hypoxia-inducible expression of HIF-2alpha in distinct cell populations of different organs. *FASEB J*, 17(2), 271-273.

- 62 Zagorska, A., Dulak, J. (2004). HIF-1: the knowns and unknowns of hypoxia sensing. *Acta Biochim Pol*, 51(3), 563-585.
- 63 Wang, G.L, Jiang, B.H., Rue, E.A., Semenza, G.L. (1995). Hypoxia-inducible factor 1 is a basic-helix-loop-helix-PAS heterodimer regulated by cellular O₂ tension. *Proc Natl Acad Sci USA*, 92(12), 5510-5514.
- 64 Waltenberger, J. (2009). VEGF resistance as a molecular basis to explain the angiogenesis paradox in diabetes mellitus. *Biochem Soc Trans*, 37(6), 1167-1170. doi: 10.1042/BST0371167
- 65 Ferrara, N., Gerber, H.P., LeCouter, J. (2003). The biology of VEGF and its receptors. *Nat Med*, 9(6), 669-676.
- 66 Uhlmann, D. (2006). Vascular endothelial growth factor: the good, the bad and the ugly. *Transplantation*, 82(4), 450-451.
- 67 Joukov, V. et al. (1997). Vascular endothelial growth factors VEGF-B and VEGF-C. *J Cell Physiol*, 173, 211-215.
- 68 Oliver, G., Alitalo, K. (2005). The lymphatic vasculature: recent progress and paradigms. *Annu Rev Cell Dev Biol*, 21, 457-483.
- 69 Nagy, J.A., Dvorak, A.M., Dvorak, H.F. (2007). VEGF-A and the induction of pathological angiogenesis. *Annu Rev Pathol*, 2, 251-275. doi: 10.1146/annurev.pathol.2.010506.134925
- 70 Carmeliet, P. et al. (2001). Synergism between vascular endothelial growth factor and placental growth factor contributes to angiogenesis and plasma extravasation in pathological conditions. *Nat Med*, 7, 575-583.
- 71 Boucher, J.M., Bautch, V.L. (2014). Antiangiogenic VEGF-A in peripheral artery disease. *Nat Med*, 20, 1383-1385. doi:10.1038/nm.3767
- 72 Kikuchi, R. et al. (2014). An antiangiogenic isoform of VEGF-A contributes to impaired vascularization in peripheral artery disease. *Nat Med*, 20, 1464-1471. doi:10.1038/nm.3703
- 73 Ferrara, N., Kerbel, R.S. (2005). Angiogenesis as a therapeutic target. *Nature*, 438(7070), 967-974.

- 74 Thangarajah, H. et al. (2009). The molecular basis for impaired hypoxia-induced VEGF expression in diabetic tissues. *PNAS*, 106(32), 13505–13510. doi: 10.1073/pnas.090667
- 75 Bento, C.F., Fernandes, R., Matafome, P., Sena, C., Seica, R., Pereira, P. (2010). Methylglyoxal-induced imbalance in the ratio of vascular endothelial growth factor to angiopoietin 2 secreted by retinal pigment epithelial cells leads to endothelial dysfunction. *Exp Physiol*, 95(9), 955-970. doi: 10.1113/expphysiol.2010.053561
- 76 Ceradini, D.J. et al. (2008). Decreasing intracellular superoxide corrects defective ischemia-induced new vessel formation in diabetic mice. *J Biol Chem*, 283(16), 10930-10938. doi: 10.1074/jbc.M707451200
- 77 Ikeda, Y. et al. (2011). Deferoxamine promotes angiogenesis via the activation of vascular endothelial cell function. *Atherosclerosis*, 214(2), 339-347. doi: 10.1016/j.atherosclerosis.2011.01.009
- 78 Moriya, J., Ferrara, N. (2014). Inhibiting the response to VEGF in diabetes. *Science signaling*, 7(307), pe1, 1-2. doi: 10.1126/scisignal.2004996
- 79 Leiter, L., A. (2005). The prevention of diabetic microvascular complications of diabetes: is there a role for lipid lowering? *Diabetes Res Clin Pract*, 68(S2), 3-14. doi: 10.1016/j.diabres.2005.03.015
- 80 Mukhopadhyay, R., Jia, J., Arif, A., Ray, P.S., Fox, P.L. (2009). The GAIT system: a gatekeeper of inflammatory gene expression. *Trends Biochem Sci*, 34(7), 324-331. doi: 10.1016/j.tibs.2009.03.004
- 81 Arif, A., Chatterjee, P., Moodt, R.A., Fox, P.L. (2012). Heterotrimeric GAIT complex drives transcript-selective translation inhibition in murine macrophages. *Mol Cell Biol*, 32(24), 5046-5055. doi: 10.1128/MCB.01168-12
- 82 Schultz, G.S., Grant, M.B. (1991). Neovascular growth factors. *Eye*, 5, 10-180.
- 83 Tomanek, R.J., Schatteman, G.C. (2000). Angiogenesis: New insights and therapeutic potential. *Anat Rec*, 261, 126-135.

- 84 Twigg, S.M. et al. (2001). Advanced glycosylation end products up-regulate connective tissue growth factor (insulin-like growth factor-binding protein-related protein 2) in human fibroblasts: A potential mechanism for expansion of extracellular matrix in diabetes. *Endocrinology*, 142, 1760-1769.
- 85 Stromblad, S., Cheresh, D.A. (1996). Cell adhesion and angiogenesis. *Trends Cell Biol*, 6, 462-467.
- 86 Stark, J. et al. (1998). Basic fibroblast growth factor stimulates angiogenesis in the hindlimb of hyperglycemic rats. *J Surg Res*, 79, 8-12.
- 87 Arello, L.P. et al. (1994). Vascular endothelial growth factor in ocular fluid of patients with diabetic retinopathy and other retinal disorders. *N Engl J Med*, 331, 1480-1487.
- 88 Cooper, M.E. et al. (1999). Increased renal expression of vascular endothelial growth factor (VEGF) and its receptor VEGFR-2 in experimental diabetes. *Diabetes*, 48, 2229-2239.
- 89 Tsuchida, K. et al (1999). Suppression of transforming growth factor beta and vascular endothelial growth factor in diabetic nephropathy in rats by a novel advanced glycation end product inhibitor, OPB-9195. *Diabetologia*, 42, 579-588.
- 90 Kolodgie, F.D., Finn, A.V., Narula, J., Virmani, R. (2011). Atherosclerotic plaque angiogenesis as a mechanism of intraplaque hemorrhage and acute coronary rupture. *Therapeutic Angiogenesis for Vascular Diseases*, Ch. 9, 213-236. doi: 10.1007/978-90-481-9495-7_9
- 91 Moos, M.P.W. et al. (2005). The lamina adventitia is the major site of immune cell accumulation in standard chow-fed Apolipoprotein E-deficient mice. *Arterioscler Thromb Vasc Biol.*, 25, 2386-2391. doi: 10.1161/01.ATV.0000187470.31662.fe
- 92 Kwon, H.M., Sangiorgi, G., Ritman, E.L., McKenna, C., Holmes Jr, D.R., Schwartz, R.S., Lerman, A. (1998). Enhanced coronary vasa vasorum neovascularization in experimental hypercholesterolemia. *J Clin Invest*, 101(8), 1551-1556. doi: 10.1172/JCI1568
- 93 Wilson, S.H., Herrmann, J., Lerman, L.O., Holmes Jr., D.R., Napoli, C., Ritman, E.L., Lerman, A. (2002). Simvastatin preserves the structure of coronary adventitial vasa vasorum in experimental hypercholesterolemia independent of lipid lowering. *Circulation*, 105(4), 415-418.

- 94 Mulligan-Kehoe, M.J. (2010). The vasa vasorum in diseased and nondiseased arteries. *Am J Physiol Heart Circ Physiol*, 298(2), 295-305. doi: 10.1152/ajpheart.00884.2009
- 95 Langheinrich, A.C., Kampschulte, M., Buch, T., Bohle, R.M. (2007). Vasa vasorum and atherosclerosis- Quid novi? *Thromb Haemost*, 97, 873-879. doi:10.1160/TH06-12-0742
- 96 Ritman, E.L., Lerman, A. (2007). Role of vasa vasorum in arterial disease: a re-emerging factor. *Current Cardiology Reviews*, 3(1), 43-55. doi: 10.2174/157240207779939907
- 97 Galis, Z.S., Lessner, S.M. (2009). Will the real plaque vasculature please stand up? Why we need to distinguish the vasa plaquorum from the vasa vasorum. *TCM*, 19(3), 87-94.
- 98 Barger, A.C., Beeuwkes, R., Lainey, L.L., Silverman, K.J. (1984). Hypothesis: vasa vasorum and neovascularization of human coronary arteries. A possible role in the pathophysiology of atherosclerosis. *N Engl J Med*, 310(3), 175-177. doi: 10.1056/NEJM198401193100307
- 99 Langheinrich, A.C., Michniewicz, A., Bohloe, R.M., Ritman, E.L. (2007). Vasa vasorum neovascularization and lesion distribution among different vascular beds in ApoE^{-/-}/LDL^{-/-} double knockout mice. *Atherosclerosis*, 191, 73-81.
- 100 Moulton, K.S., Heller, E., Konerding, M.A., Flynn, E., Palinsi, W., Folkman, J. (1999). Angiogenesis inhibitors endostatin or TNP-470 reduce intimal neovascularization and plaque growth in apolipoprotein E-deficient mice. *Circulation*, 99, 1726-1732.
- 101 Moulton, K.S. et al. (2003). Inhibition of plaque neovascularization reduces macrophage accumulation and progression of advanced atherosclerosis. *PNAS*, 100(8), 4736-4741.
- 102 Ribatti, D., Levi-Schaffer, F., Kovanen, P.T. (2008). Inflammatory angiogenesis in atherogenesis- a double-edged sword. *Ann Med*, 40, 606-621.
- 103 Heistad, D.D., Marcus, M.L. (1979). Role of the vasa vasorum in nourishment of the aorta. *Blood Vessels*, 26, 225-238.

- 104 Chepelenko, G.V. (2015). Atherosclerosis regulation via media lipid-driven VSMC cholesterol efflux switch. *Med Hypotheses*, 84(2), 141-144. doi: 10.1016/j.mehy.2014.12.002
- 105 Leppanen, O., Bjornheden, T., Evaldsson, M., Boren, J., Wiklund, O., Levin, M. (2006). ATP depletion in macrophages in the core of advanced rabbit atherosclerotic plaques in vivo. *Atherosclerosis*, 188(2), 323-330. doi: 10.1016/j.atherosclerosis.2005.11.017
- 106 Doyle, B., Caplice, N. (2007). Plaque neovascularization and antiangiogenic therapy for atherosclerosis. 49(21), 2073-2080.
- 107 Virmani, R. et al. (2005). Atherosclerosis plaque progression and vulnerability to rupture: angiogenesis as a source of intraplaque hemorrhage. *Circulation*, 25, 2054-2061.
- 108 Felmeden, D.C., Blann, A.D., Lip, G.Y. (2003). Angiogenesis: basic pathophysiology and implications for heart disease. *Eur Heart J*, 24(7), 586-603. doi: 10.1016/S0195-668X(02)00635-8
- 109 Magnoni, M., Ammirati, E., Camici, P.G. (2015). Non-invasive molecular imaging of vulnerable atherosclerotic plaques. *J Cardiol*, 0914-5087(15), 1-9. doi: 10.1016/j.jjcc.2015.01.004
- 110 Arcidiacono, M.V. et al. (2013). Microangiopathy of large artery wall: A neglected complication of diabetes mellitus. *Atherosclerosis*, 228, 142-147. doi: 10.1016/j.atherosclerosis.2013.02.011
- 111 Arcidiacono, M.V., Rubinat, E., Ortega, E., Betriu, A., Fernandex, E., Mauricio, D. (2013). Pseudo-enhancement does not explain the increased carotid adventitial vasa vasorum signal in diabetic patients. *Atherosclerosis*, 229, 459-461. doi: 10.1016/j.atherosclerosis.2013.06.007
- 112 Venegas-Pino, D.E. et (2015). Gender Specific Differences in a New ApoE^{-/-}:Ins2^{+Akita} Mouse Model of Hyperglycemia-induced Atherosclerosis. Submitted to Journal of Pathology
- 113 Khan, M.I., Picha, B.A., Shi, Y., Bowes, A.J., Werstuck, G.H. (2009). Evidence supporting a role for endoplasmic reticulum stress in the development of atherosclerosis in a hyperglycaemic mouse model. *Antioxidants & Redox signaling*, 11 (9), 2289-2298. doi:10.1089/ars.2009.2569

- 114 Moreno, P.R., Purushothaman, M., Purushothaman, K.R. (2012). Plaque neovascularization: defense mechanisms, betrayal, or a war in progress. *Ann. NY Acad. Sci.*, 1254, 7-17. doi: 10.1111/j.1749-6632.2012.06497.x
- 115 Pant, S., Deshmukh, A., Mehta, J.L. (2013). Angiogenesis in Atherosclerosis: An overview. *Biochemical Basis and Therapeutic Implications of Angiogenesis*, 6, 209-224. doi: 10.1007/978-1-4614-5857-9_12
- 116 Guzman-Hernandez, M.L., Potter, G., Egervari, K., Kiss, J.Z., Balla, T. (2014). Secretion of VEGF-165 has unique characteristics including shedding from the plasma membrane. *Mol Biol Cell*, 25(7), 1061-1072. doi: 10.1091/mbc.E13-07-0418
- 117 Claffey, K.P., Senger, D.R., Spiegelman, B.M. (1995). Structural requirements for dimerization, glycosylation, secretion and biological function of VPF/VEGF. *Biochimica et Biophysica Acta*, 1246(1), 1-9.
- 118 Huez, I., Bornes, S., Bresson, D., Creancier, L., Prats, H. (2001). New vascular endothelial growth factor isoform generated by internal ribosome entry site-driven CUG translation initiation. *Mol Endocrinol*, 15, 2197-2210.
- 119 Meiron, M., Anunu, R., Scheinman, E.J., Hashmueli, S., Levi, B.Z. (2001). New isoforms of VEGF are translated from alternative initiation CUG codons located in its 5'UTR. *Biochem Biophys Res Commun*, 282, 1053-1060.
- 120 Yeo, T.K., Senger, D.R., Dvorak, H.F., Freter, L., Yeo, K.T. (1991). Glycosylation is essential for efficient secretion but not for permeability-enhancing activity of vascular permeability factor (vascular endothelial growth factor). *Biochem Biophys Res Commun*, 179, 1568-1575.
- 121 Das, P.M., Ramachandran, K., vanWert, J., Singal, R. (2004). Chromatin immunoprecipitation assay. *BioTechniques*, 37, 961-969.
- 122 Jung, J.E. et al (2005). STAT3 is a potential modulator of HIF-1-mediated VEGF expression in human renal carcinoma cells. *FASEB J*, 19(10), 1296-1298.
- 123 Qin, Z. (2012). The use of THP-1 cells as a model for mimicking the function and regulation of monocytes and macrophages in vasculature. *Atherosclerosis*, 221(1), 2-11. doi:10.1016/j.atherosclerosis.2011.09.003

- 124 Auwerx, J. (1991). The human leukemia cell line, THP-1: A multifaceted model for the study of monocyte-macrophage differentiation. *Experientia*, 47(1), 22-31.
- 125 Calvert, V.S., Coukos, G., Espina, V., Geho, D.H., Liotta, L.A., Petricoin, E.F. (2006). Laser capture microdissection. *Nature Protocols*, 1(2), 586-603. doi:10.1038/nprot.2006.85
- 126 Abordo, E.A., Thornalley, P.J. (1997). Synthesis and secretion of tumour necrosis factor- α by human monocytic THP-1 cells and chemotaxis induced by human serum albumin derivatives modified with methylglyoxal and glucose-derived advanced glycation endproducts. *Immunology Letters*, 58(3), 139-147. doi:10.1016/S0165-2478(97)00080-1
- 127 Mathys, K.C., Ponnampalam, S.N., Padival, S., Nagaraj, R.H. (2002). Semicarbazide-sensitive amine oxidase in aortic smooth muscle cells mediates synthesis of a methylglyoxal-AGE: implications for vascular complications in diabetes. *Biochemical and Biophysical Research Communications*, 297(4). doi:10.1016/S0006-291X(02)02293-3
- 128 Ishibashi, S., Goldstein, J.L., Brown, M.S., Herz, J., Burns, D.K. (1994). Massive xanthomatosis and atherosclerosis in cholesterol-fed low density lipoprotein receptor-negative mice. *J Clin Invest*, 93(5), 1885-1893.
- 129 Veniant, M.M, Withycombe, S., Young, S.G. (2001). Lipoprotein size and atherosclerosis susceptibility in Apoe^{-/-} and Idr^{-/-} Mice. *Arterioscler Thromb Vasc Biol*, 21, 1567-1570. doi: 10.1161/hq1001.097780
- 130 Ishibashi, S., Herz, J., Maeda, N., Goldstein, J.L., Brown, M.S. (1994). The two-receptor model of lipoprotein clearance: tests of the hypothesis in "knockout" mice lacking the low density lipoprotein receptor, apolipoprotein E, or both proteins. *PNAS*, 91(10), 4431-4435.
- 131 Liu, Y., Petreaca, M., Martins-Green, M. (2009). Cell and molecular mechanisms of insulin-induced angiogenesis. *J Cell Mol Med*, 13(11-12), 4492-4504. doi: 10.1111/j.1582-4934.2008.00555.x
- 132 Nakao-Hayashi, J., Ito, H., Kanayasu, T., Morita, I., Murota, S. (1992). Simultaneous effects of insulin and insulin-like growth factor I on migration and tube formation by vascular endothelial cells. *Atherosclerosis*, 92(2-3), 141-149.

- 133 Lassance, L., Miedl, H., Absenger, M., Diaz-Perez, F., Lang, U., Desoye, G., Hiden, U. (2013). Hyperinsulinemia Stimulates Angiogenesis of Human Fetoplacental Endothelial Cells: A possible role of Insulin in Placental Hypervascularization in Diabetes Mellitus. *J Clin Endocrinol Metab*, 98(9), 1438-1447. doi: 10.1210/jc.2013-1210
- 134 Meng, D., Mei, A., Liu, J., Kang, X., Shi, X., Qian, R., Chen, S. (2012). NADPH Oxidase 4 mediates insulin-stimulated HIF-1 α and VEGF expression, and angiogenesis In Vitro. *PLoS One*, 7(10), 1-9. doi: 10.1371/journal.pone.0048393
- 135 Wu, J. et al. (2015). Plasminogen Activator Inhibitor-1 Inhibits Angiogenic Signaling by Uncoupling Vascular Endothelial Growth Factor Receptor-2- α V β 3 Integrin Cross Talk. *Atheroscler Thromb Vasc Biol*, 35(1), 111-120. doi: 10.1161/ATVBAHA.114.304554